

INTEGRATION OF OFFSHORE WIND FARMS INTO THE LOCAL DISTRIBUTION NETWORK

K/EL/00272/REP

URN 03/1641

Contractor
IPSA Power Ltd

Prepared by
Rida D Youssef

(With Contributions by Mr Paul Bernat, Mr Steve Elliott, Dr John B Heath, Dr Charles A Lynch,
Dr Simon Todd)

The work described in this report was carried out under contract as part of the DTI New and Renewable Energy Programme, which is managed by Future Energy Solutions. The views and judgements expressed in this report are those of the contractor and do not necessarily reflect those of the DTI or Future Energy Solutions.

First Published 2003
© Crown Copyright 2003

The logo for the Department of Trade and Industry (DTI), consisting of the lowercase letters 'dti' in a bold, sans-serif font. The 'd' and 't' are connected, and the 'i' has a small dot.

EXECUTIVE SUMMARY

The project has four main activities:

a) Model Development: this phase includes the development of steady state and dynamic models of the doubly-fed induction machine and incorporates these into the IPSA computer program. IPSA is a commercially available power system analysis program and one of the most widely used in the UK. The model development consists of two parts. The first deals with developing the equations for the doubly-fed machine in a form that is suitable for steady state modeling at a general system. The second handles the transfer functions and other equations for the doubly-fed machine in a form that is suitable for dynamic modeling at a system wide level.

b) Connection Studies: three types of wind generation technology namely, fixed speed, variable speed and doubly fed induction machines are used for these studies. The studies are done by simulating a real-life situation.

c) Optimal Power Flow Development: for the evaluation of alternative voltage control strategies and their optimisation an active distribution network oriented Optimal Power Flow (OPF) tool is required. Therefore a fixed speed and doubly-fed induction machine models are incorporated into an existing OPF code. The OPF module is then integrated into the IPSA power system analysis package.

d) Voltage Control Studies: the Voltage Control Studies, based on the developed OPF under Activity (c) above, consists of the following: Firstly, contrast the network voltage performance associated with the application of (1) fixed speed (2) variable speed and (3) doubly fed induction machines under various loading conditions for various levels of penetration of off-shore wind generation. The next step determines the optimal control strategy of doubly-fed induction generators to maximise penetration of wind generation on the existing 132kV network, considering full spectrum of network loading conditions. Then, the benefits of the application of on-shore reactive compensation in conjunction with fixed speed induction machine and variable speed based off-shore wind generation and contrast it with the previous step are determined. Finally, finding an optimal strategy of coordinated area based voltage control using OLTCs in the local network and controlling active and reactive outputs of doubly-fed induction machines.

Results Summary

Steady state and dynamic models for the Doubly-fed Induction Generators have been developed for the widely used IPSA software. The models were used for the studies carried out in this project and the results are presented in this report.

From the load flow and fault level analysis the impact of the variable speed synchronous generator connected via back-to-back static converters is not creating a major thermal overload or fault level problem with the simplified modelling of the converter contributions. Transient analysis calculations are needed to simulate the behaviour of the converter controllers and its effects on the converter contribution. However the cost and operational complexity of the converters controllers of this size for delivering a special operating conditions often prohibits the developers of using this configuration.

The advantages and disadvantages of the fixed speed offshore induction generator are clear. In the positive side it is simple, reliable and will known technology. However, it presents the worst reactive power consumption, it is also lack smooth voltage and power control. As a result of the increased reactive power compensation and flows in the local network, switchgear upgrading and protection current and time resetting are needed in the local 132 kV substations. Fixed speed generation has mechanical problems from the wind turbine side with extraction of power of

variable wind speed. Various schemes usually used to overcome this problem such as multiples gearbox ratios but they add extra cost and complexities and they are outside the scope of this work.

From the transient stability results the fault contribution from doubly fed induction machine proved to be slower to decay and has a higher initial value than a fixed speed induction generator.

Section 7 of G75/1 discusses the importance of maintaining system stability of generation within limits of Generating Plant capability during network disturbances and the need to disconnect reliably for true “loss of mains” situations. Some forms of loss of mains protection may not achieve the required level of discrimination.

Governor and turbine controller characteristics and their time delay play a significant part in the stability of the system and the controllers need to react to change the power input to the turbine with a maximum time delay of 200ms to keep the doubly fed induction generators relatively stable on reconnection to the system. This is more critical in DFIGs, as they may operate at super synchronous speed at a typical –12% slip.

More work needed to put modelling of AVRs, governors and turbines for induction generators and DFIGs of windfarm in the full dynamic analysis of the distribution network.

The Optimal Power Flow software has been successfully integrated into the IPSA power system analysis program. The same final answers were obtained from the software running under IPSA as when the software was run under console mode. The same intermediary results were obtained while the calculations were in progress.

Facilities for adding Static VAR compensator OPF data will be added to IPSA. This information is currently within the program but it is not yet visible to the user. The conversion of IPSA induction generators to OPF induction generators will be improved. The IPSA user interface will be extended to display OPF data on individual item property pages, and to provide HTML reports on the results of OPF analysis.

Testing needs to be carried out on more complicated networks to ensure the same results are obtained between the OPF in console mode and in IPSA. It is not anticipated that this will pose any significant problems.

Summary of the Conclusions

The doubly fed induction generators technology provides solution for two major shortfalls in the induction generators. The first is the reactive power consumption by controlling power factor of these generators. Setting the power factor to unity provide better alternative compared with capacitive VAR compensation. It also can provide active speed/power control through the back-to-back converters in the rotor windings. There is no harmonics source in the stator connection and the expectation that the power quality is not a problematic issue. However, connection of generation increases the connectivity of the network and fault level flows specially for the initial peak values.

From the transient stability analysis the impact of the variable speed synchronous generator connected via back-to-back static converters is not seem to create a major thermal overloads or fault level problem with the dynamic modelling of the converter contributions. Transient simulation of the behaviour of the converter controllers and their effects on the converter contribution shows that the converter protection is able to disconnect the windfarm very fast for high fault current contribution. However, the fault ride through capability is a problem for the network transmission operator. If the wind farm disconnects itself when a fault occurs on the transmission system then

the integrity of the transmission system can be undermined as the lost generation can exceed the amount of spinning reserve.

To continue to comply with P2/5 and G75/1 may need some security and contingency studies with the new system loading conditions, and this may introduce further constraints in the operation or maximum generation of the wind farms under certain operating conditions or configurations. These studies are not included within the scope of this report.

The OPF program has proved highly useful in determining the solution to a whole range of issues when it comes to connecting new generation into an existing network. It permits the user to firstly maximise the generation capacity, and also to compare how different generation technologies compare when trying to maximise this capacity. The study has also highlighted the benefits of using DFIG machines in voltage control mode, as it has the effect of improving the network voltage performance while eliminating the need for a substantial amount of reactive compensation in the 132kV network for similarly rated IG wind farm connections.

Project Collaborators:

IPSA Power Ltd,
EEPS Group at the Department of Electrical Engineering and Electronics, UMIST,
PowerGen UK Plc,
Innogy Plc,

Project Co-operators:

SP Power Systems Ltd,
United Utilities

Table of Contents		Page
1	Introduction	1
2	Doubly-fed Induction Generator (DFIG) Static Model	3
2.1	Equivalent Circuit Model	4
2.1.1	Single wound rotor	4
2.1.2	Double wound rotor	5
2.2	DFIG steady state operating principles:	6
2.3	Implementation of the DFIG Models For IPSA Software:.....	7
2.3.1	The DFIG extra data and symbol	7
2.4	Modelling detail.....	7
2.5	Induction Machines in IPSA.....	8
2.5.1	Implementation of the DFIG for IPSA load flow	9
2.5.2	Implementation of the DFIG for IPSA fault calculations:.....	10
3	DFIG Dynamic Model	13
3.1	Doubly Fed Induction Generator (DFIG).....	13
	List of Symbols	13
3.2	Fifth order model of the DFIG	14
3.3	Third order model of the DFIG	17
4	System and Connection Description:	19
4.1	System Description:.....	19
4.2	System Equipment Ratings:.....	21
4.3	Offshore Connection:	21
5	Connection Policies, Technical Problems and Merits:	25
5.1	Connection Polices:	25
5.2	Technical Problems:	25
5.3	Offshore Windfarm Connection Merits:.....	26
6	Connection Studies:.....	27
6.1	Synchronous Machine based offshore wind farm:	27
6.1.1	Load flow studies:.....	28
6.1.2	Fault Level studies:	30
6.2	Induction generator connection (IG)	31
6.2.1	Load flow studies:.....	32
6.2.2	Fault Level studies:	34
6.3	Doubly-fed induction generator connection (DFIG)	35
6.3.1	Loadflow studies:	36
6.3.2	Fault Level studies:	38
7	Comments on the Steady State Results.....	41
8	Stability Connection Studies for Wind farms with Synchronous Generators:	43
8.1	Synchronous Machine:	43
8.2	Wind Turbine and Governor:	43
8.3	Converters:.....	45
8.4	Transient Analysis of Fault at The Local Network:	46
a)	Transient analysis for a fault at the local 33kV node (busbar 'OFSW33'):	46

	b) Transient analysis for a fault at the local 132kV network (busbar 'HOLY C2'): ...	47
8.5	Comments on the Variable Speed Generator dynamic Results:.....	47
9	Transient Stability Connection Studies for Wind farms with Fixed Speed Induction Generators: 49	
9.1	Fixed Speed Induction Generators:	49
9.2	Transient Analysis of Faults at The Local Network:.....	49
	a) Transient analysis for a fault at the local 33kV node to 'Offshore windfarm 1':	50
	b) Transient analysis for a fault at the local 132kV node (busbar 'HOLY C2'):.....	51
9.3	Comments on the Induction Generator Dynamic Results:	53
10	Transient Stability Connection Studies for Wind farms with Doubly-Fed Induction Generators (DFIGs):	55
10.1	DFIG Connection:	55
10.2	Transient Analysis of Faults at the Local Network:	55
	a) Transient analysis for a fault at the local 33kV node to 'Offshore windfarm 1' (busbar 'OFSW33'):	56
	b) Transient analysis for a fault at the local 132kV node (busbar 'HOLY C2') (DFIGs steady state full load slip =0):	57
	c) Transient analysis for a fault at the local 132kV node (busbar 'HOLY C2') (steady state DFIGs full load slip =-12%):.....	59
10.3	Comments on the DFIGs Results:	61
11	Comments on the Dynamic Results	63
12	Optimal Power Flow Development	65
12.1	Capabilities	65
12.2	Further Developments	65
12.3	Development of an Application Programming Interface (API) to the OPF	66
	12.3.1 The structure of the API.....	66
	12.3.2 API Layers	66
	12.3.3 Message and Error handling	67
	12.3.4 Types of API routines	67
	12.3.5 Packaging of the OPF	67
12.4	Addition of OPF Data to IPSA	68
12.5	Separation and Conversion of Data	68
	12.5.1 Busbars.....	69
	12.5.2 Loads	69
	12.5.3 Generators	69
	12.5.4 Induction machines	69
	12.5.5 Branches.....	70
	12.5.6 Shunts.....	70
	12.5.7 Transformers	70
	12.5.8 Static VAr Compensators (SVCs).....	71
	12.5.9 OPF Control	71
12.6	Further Developments	71
13	Addition of OPF Results to IPSA	73
13.1	Stored Results	73
	13.1.1 Busbars.....	73
	13.1.2 Generators	73

13.1.3	Induction generators.....	73
13.1.4	Branches.....	74
13.1.5	Shunts.....	74
13.1.6	Transformers	74
13.1.7	Static VAR compensators	74
13.1.8	Network results	74
14	Integrating the OPF into IPSA	75
14.1	OPF Façade.....	75
14.2	Interface Changes	75
14.3	File Format Changes.....	77
14.4	Further Developments	77
15	Validating the OPF in IPSA	79
15.1	The Test Network	79
15.1.1	Test Network Data	80
15.2	Results from OPF Console	81
15.3	Results from IPSA OPF.....	83
15.3.1	Busbars.....	84
15.3.2	Generators	84
15.3.3	Induction Generators.....	84
15.3.4	Lines.....	84
15.4	Further Developments	84
16	Voltage Control.....	85
16.1	System Models	86
16.1.1	Network Model	86
16.1.2	DFIG and IG data.....	86
16.1.3	Load Data.....	87
16.2	Using The Optimal Power Flow Program	87
16.2.1	Variants of the OPF.....	88
16.2.2	Formulation of the IPSA-OPF	89
16.2.3	Summary	89
16.3	Voltage Control Study – Case 1	90
16.3.1	Network Performance Comparison of IG and DFIG machines.....	90
16.3.2	Study results.....	90
16.3.3	Conclusion	91
16.4	DFIG Optimal Control Strategy (I)	91
16.4.1	Maximum penetration assessment based on LF method	91
16.4.2	Maximum penetration assessment based on OPF method – Study Case 1	92
16.4.3	Maximum penetration assessment based on OPF method – Study Case 2.....	93
16.4.4	Conclusion	93
16.5	On-shore Reactive Compensation vs DFIG	93
16.5.1	Study Results.....	94
16.5.2	Conclusions.....	94
16.6	DFIG Optimal Control Strategy (II)	95
16.6.1	Scenario 1 – Stronger AC network	95
16.6.2	Optimal Control Strategy – Weakened AC system	96

	16.6.3	Conclusions	97
16.7		Conclusions for Voltage Control Analysis Using OPF Program	98
17		Conclusions.....	101

1 Introduction

Presently, the UK Government's Policy is to increase the contribution of electricity supplied from renewable sources in the UK to 10% by 2010. One key element of this is to stimulate the development of new technologies such as offshore wind power. The report by the Royal Commission of Environmental Pollution (*Twenty-second Report. Energy – The Changing Climate*, June 2000) confirms the widely acknowledged fact that the development of wind energy both onshore and offshore will be needed in order to achieve these targets.

In the year 2001 approval was given for the development of at least thirteen offshore wind farm sites. Nine of these sites are for single developments of 30 turbines, three are for two developments (i.e. 60 turbines) and one for three developments (i.e. 90 turbines). Although it is early days, it is likely that each turbine size will be between 2 and 4 MW. This means each set of 30 turbines could have an output of up to 120MW. This is the level of infeed that has to be accommodated by the local distribution network

Three types of wind generation technology are available: fixed speed induction generator; variable speed induction or synchronous generators connected via back-to-back static converters; or doubly fed induction generators.

Before DNOs accept these large blocks of wind generation onto their network, steady state and dynamic studies need to be carried out using validated models. In general, models are available for the first two generation types described above (though there must be a question concerning the use of traditional synchronous machine models over a range of frequencies), but there is no industry standard or even accepted model for the doubly-fed induction generator (DFIG).

The emergence of doubly fed generators as the preferred choice by a number of wind turbine manufacturers offers the possibility of active voltage and /or reactive power control from the wind farms.

IPSA Power Ltd in collaboration with The EEPS Group at UMIST, PowerGen UK plc, and Innogy plc with the co-operation of SP Power Systems Ltd and United Utilities plc were commissioned to carry out this project under the New and Renewable Energy Programme and supported by the Department of Trade and Industry (DTI).

This project is building on existing work to develop robust, validated wind generator models implemented in both conventional power system analysis tools (load flow, fault level analysis, protection co-ordination dynamic simulation and harmonics) and in an optimal power flow solution environment.

The overall aim of the project is to establish the viability of connecting a large offshore wind farm into a 132kV distribution system. To achieve this requires the development of specific modelling capabilities and the study of the voltage and dynamic stability of the potential connection arrangements. SP Power Systems Ltd provided the model of the existing 132kV system to facilitate this project.

Mainly, very large wind turbines with doubly-fed induction generators, such as those being considered for use in off-shore installation, benefit from an increase in efficiency of the prime mover by ensuring it operates at its most efficient speed for a range of input wind speeds. From the network voltage control perspective, the doubly fed induction generators can play a critical role in

enhancing the ability of local networks to absorb a significant amount of offshore wind generation at 132kV rather than 400 kV, and hence considerably reduce overall connection costs.

The scope of this project covers four main activities. First is the development of static and dynamic models of the doubly fed induction generators and incorporation of these into the IPSA computer software suite. In the second activity, studies of the likely scenarios for three types of wind generation technology described above are performed. The third involves the development of an Optimal Power Flow (OPF) to evaluate alternative voltage control strategies and their optimisation. The fourth activity will include voltage control studies using the important characteristic of the operation of the DFIG to control reactive demand and to some extent active power output of the generator independently.

In each salient stage an interim report has been submitted. This report summarises the work of each stage and presents the project conclusions.

2 Doubly-fed Induction Generator (DFIG) Static Model

The DFIG system produces electrical power at constant voltage and frequency to the DNO grid for a wide range of shaft speed variation ($-1 < s < 1$), where s is rotor slip). A schematic diagram of the system is given in Figure 2-1. In this system, a controlled converter cascade is connected between the slip-ring terminals and the three-phase AC supply terminals. Power flow between the rotor circuit and the supply can be controlled by adjustment of the converter controllers. This effectively corresponds to controlling the injected rotor voltage and power [1].

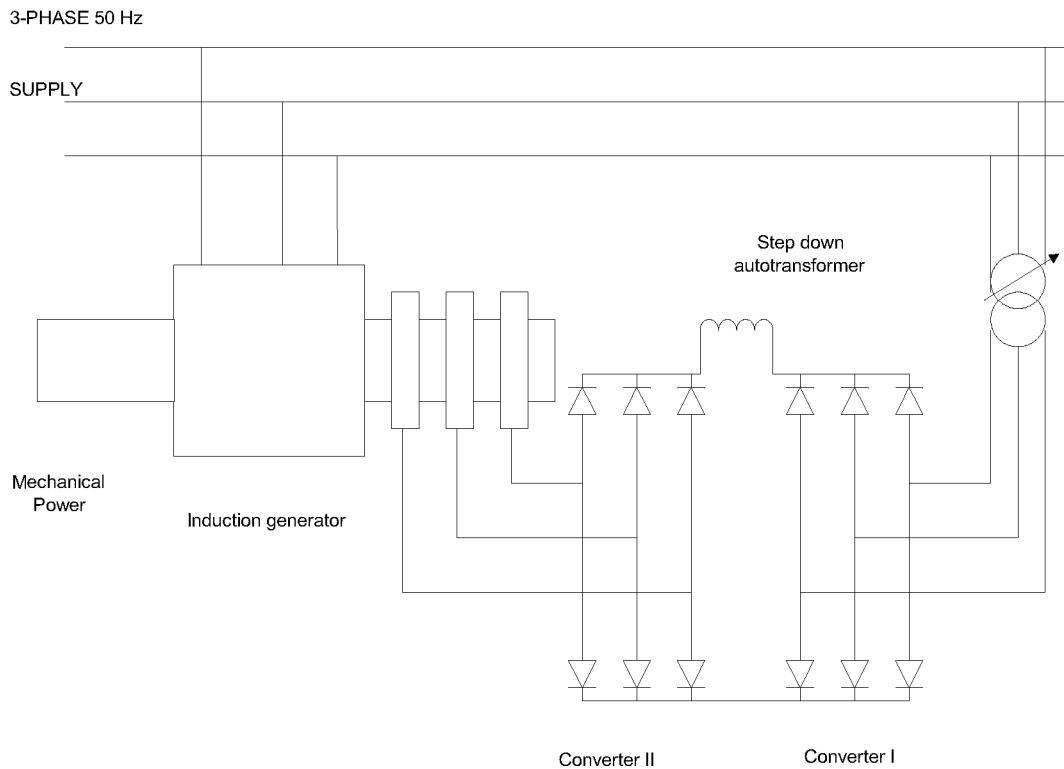


Figure 2-1 Schematic diagram of DFIG

To transfer electrical power from the rotor circuit to the supply, converters I and II should be operated in their inverter and rectifier modes, respectively. On the other hand, when converter II acts as an inverter and converter I acts as a rectifier, the direction of power flow is reversed. While, the rotor side converter may be naturally (with some limitation in the reactive power control) or line commutated, the supply converter is line-commutated (References [5,6,12]).

It must be recognised that the steel rotor contributes to the machine characteristics and, therefore, it is best to model induction machines using two rotor windings, or in term of “equivalent” starting and running winding circuits. Control of the torque-speed characteristics can be achieved either by the injection of a rotor voltage of the same frequency as the rotor current from the slip rings.

Keys

R_1 , X_1 are stator resistance and reactance;

R'_2 , X'_2 are rotor running resistance and reactance;

$S = \text{slip} = (T_o - T) / T_o$;
 $V'_{3/s}$ = the injected voltage per phase referred to the stator
 V_1 = the stator terminal voltage per phase.
 V_g = the air gap voltage.
 X_m = magnetizing reactance.
 I_2' = rotor current referred to the stator side
 I_1 = stator current.
 P_1 = stator power output
 P_2 = rotor injected power
 P_o = total output power
 P_m = mechanical power.
 P_g = Air gap power.

2.1 Equivalent Circuit Model

2.1.1 Single wound rotor

The steady-state analysis of the DFIG is carried out by means of a modified version of the conventional (short circuited) equivalent circuit (References [2,3,5,6]). Variations in the machine torque/speed characteristics are obtained using double wound rotor. The single wound rotor with injected voltage is represented in Figure 2-2.

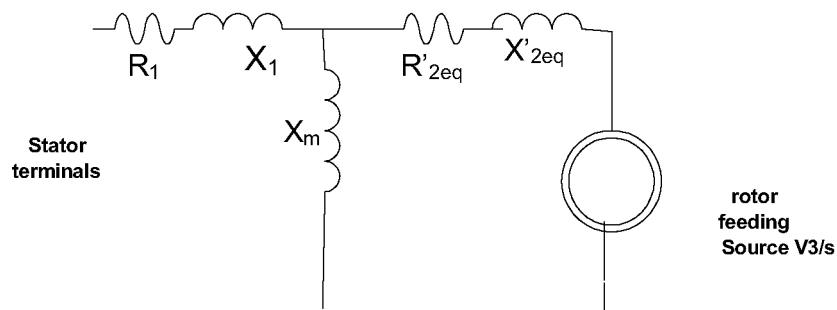


Figure 2-2: Double fed Single rotor

winding IM equivalent circuit

The corresponding set of algebraic equations for single wound rotor doubly fed machine are as follows:

$$\ddot{V}_g = \frac{jX_m}{R_1 + j(X_1 + X_m)} \ddot{V}_1 \dots \dots \dots [2 - 1]$$

$$Z_g = \frac{jX_m(R_1 + jX_1)}{R_1 + j(X_1 + X_m)} = R_g + jX_g \dots \dots \dots [2 - 2]$$

$$\ddot{V}_3 = V_3 \angle \phi \dots \dots \dots [2 - 3]$$

$$\ddot{I}_2' = I_2' \angle \theta = \frac{V_g - V_3' / s}{R_g + R_2' / s + j(X_g + X_2')} \dots \dots \dots [2 - 4]$$

$$\ddot{I}_1 = I_1 \angle \delta = I_2' + I_m \dots \dots \dots [2 - 5]$$

$$P_1 = 3V_1 I_1 \cos \delta \dots \dots \dots [2 - 6]$$

$$P_2 = 3V_3' I_2' \cos(\phi - \theta) \dots \dots \dots [2 - 7]$$

$$P_o = P_1 - P_2 \dots \dots \dots [2 - 8]$$

$$P_g = 3I_2'^2 R_2' / s + 3V_3' I_2' [\cos(\phi - \theta)] / s \dots \dots \dots [2 - 9]$$

$$P_m = (1 - s) P_g \dots \dots \dots [2 - 10]$$

$$\eta = P_o / P_m \dots \dots \dots [2 - 11]$$

Throughout the analysis only fundamental components of voltage and current are taken into account.

2.1.2 Double wound rotor

The equivalent circuit of the double wound rotor of DFIG can be presented as shown in Figure 2-3. The injected power is presented in the running winding.

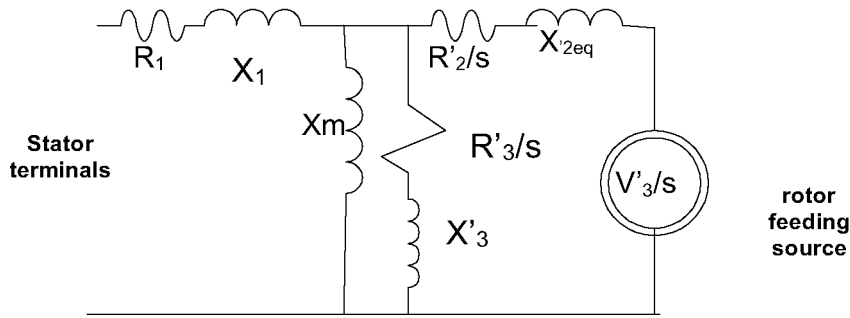


Figure 2-3: Double fed double wound rotor

winding IM equivalent

Where R'_3 , X'_3 are the rotor starting resistance and reactance referred to the stator side.

2.2 DFIG steady state operating principles:

The entire working range of the DFIG system can be divided into two regions, namely sub-synchronous and super-synchronous.

In the sub-synchronous region, the rotor speed is lower than the synchronous speed. The rotor power component sP_g can be made negative by injecting the slip-frequency power P_2 into the rotor circuit. At sub-synchronous speeds, since the slip s is between zero and unity, this will reverse the direction of P_g and P_m , resulting in generator operation. In the conventional use of an induction machine, however, since sP_g is always positive, the machine will never operate as a generator at sub-synchronous speeds. The sub-synchronous operating condition can then be summarised mathematically as:

$$\begin{aligned} 0 < s < 1; \\ sP_g < 0; \\ P_g < 0; \\ P_m < 0; \\ P_2 < 0; \\ sP_g &= P_2 + 3I_2'^2 R_2'; \\ |P_m| &< |P_g|; \end{aligned}$$

In the super-synchronous region, the rotor speed is greater than the synchronous speed. This region can be divided into two sub-regions from the point of the rotor power flow. In sub-region 1, the rotor speed is between the synchronous speed and the rated rotor speed. In sub-region 2, the rotor speed is higher than the rated rotor speed. For the DFIG the rated speed is defined at the rated operating point. The rated operating point for a given machine is defined theoretically by assuming that the stator terminals are connected to an infinite busbar and the slip ring terminals are short circuited. The rated speed, the rated stator power output and the corresponding power factor are calculated for the rated rotor current given in the nameplate. In sub-region 2, corresponding to operation with a mechanical source able to drive the generator beyond the rated speed, the DFIG system needs to be controlled to avoid the excessive machine currents that would otherwise occur, the mechanical power surplus being extracted from the rotor into the converter back-to-back, thus

electrical power output from both stator and rotor present the total power output. This briefly can be presented mathematically as follows:

$$\begin{aligned}
 & -1 < S < S_r \\
 & sP_g > 0; \\
 & P_g < 0; \\
 & P_m < 0; \\
 & P_2 > 0; \\
 & sP_g = P_2 + 3I_2'^2 R_2'; \\
 & |P_m| > |P_g|;
 \end{aligned}$$

2.3 Implementation of the DFIG Models For IPSA Software:

2.3.1 The DFIG extra data and symbol

The doubly fed induction machine is a ‘special’ induction machine. Hence, the well tested existing induction machine model are used and extended to handle the extra parameters needed to model the DFIG in IPSA.

2.4 Modelling detail

The DFIG is treated as an extension of the Induction Machine modelling in IPSA. It is input into the network by drawing an induction machine, and is then identified as being a DFIG by the data that are associated with it. The one significant difference between a conventional or Fixed Speed Induction Generator (FSIG) is that the DFIG can supply power to (or absorb from) the network via both the stator and the rotor windings. A DFIG is therefore connected to the network at two locations, however, it may not be required to represent the DFIG in such a level of detail, and there are three possibilities. These are described below with reference to Figure 2-4.

- 1) In a DFIG the rotor is fed via back-to-back converters (see Figure 2-1), and so the greatest level of detail is to include these converters in the modelling. This is the case for the DFIG at busbar dfig3 in Figure 2-4.
- 2) If it is not required to model the converters, yet it is still necessary to identify the flow separately in the rotor and stator, then the configuration used is as at busbar dfig2 in Figure 2-4. Note, however, that the reactive power input to the rotor is provided by the DFIG side converter and does not come from the main network.

The reactive power provided by (or absorbed by) the network side converter is a function of the control strategy of that converter, and is completely independent of the DFIG rotor reactive power needs. Since a common strategy for this converter is to operate at unity power factor, this is the assumption made in IPSA for this level of modelling. The way this is actually handled in IPSA is as follows: If the rotor bus (dfig2-ro in this example) and the stator bus (dfig2-st in this example) are both in the same AC island, then the reactive power at the rotor bus (dfig2-ro) is set to zero.

- 3) The next, and final, level of simplification is shown at busbar dfig1 in Figure 2-4. Here the stator and rotor windings are shown connected to a common busbar (i.e. dfig1). For the same reasons as given in the previous case, only the stator reactive power requirements are presented

to the network at busbar dfig1, whereas the active power is the sum of the rotor and stator requirements.

In all of the above cases the modelling of the DFIG itself is the same, so details of the rotor and stator winding real and reactive powers are always available.

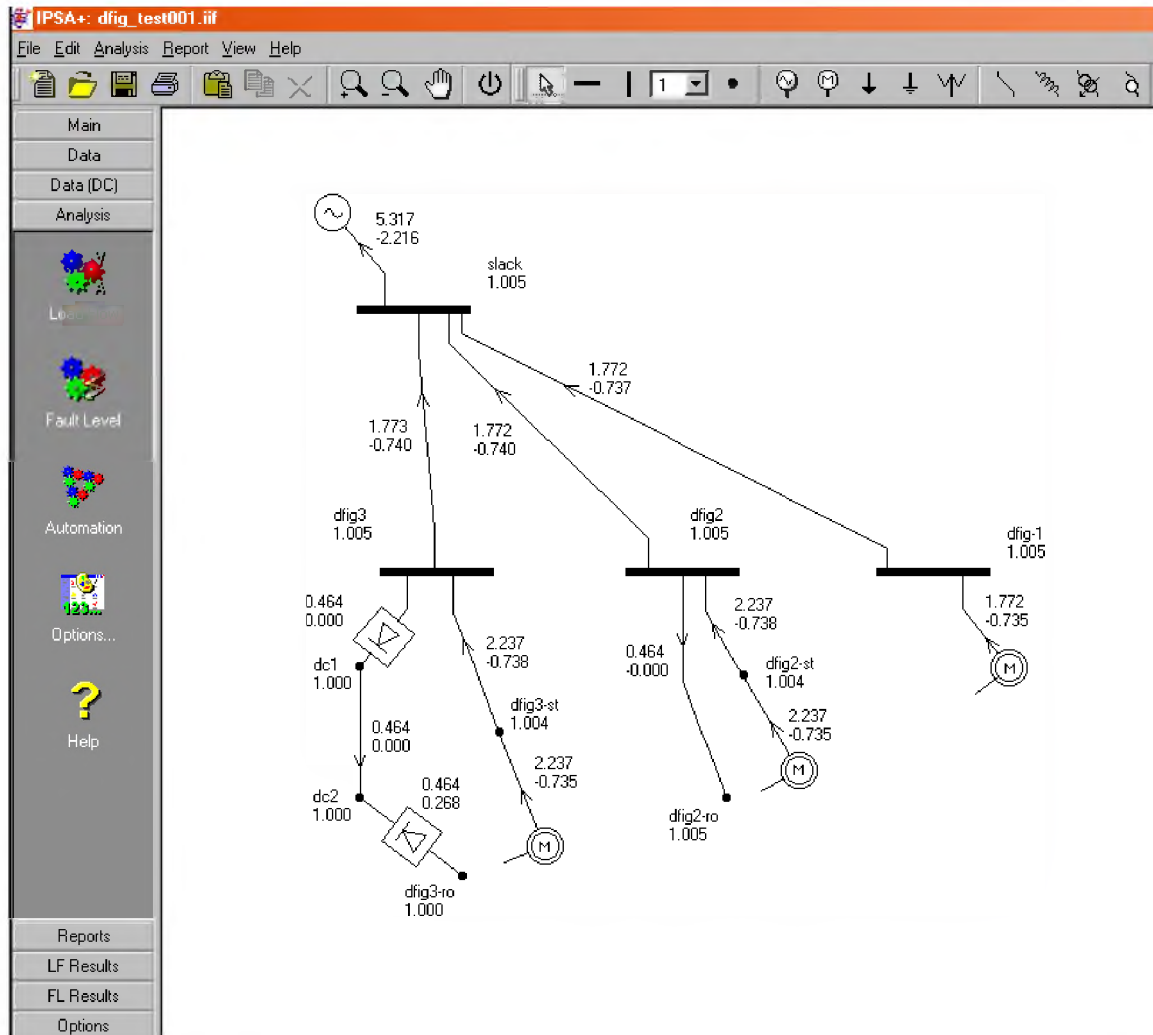


Figure 2-4: Different levels of DFIG modeling detail

2.5 Induction Machines in IPSA

The doubly fed induction machine is an extension of the existing induction machine modelling within IPSA. Additional parameters are needed to identify the DFIG and its mode of operation.

IPSA uses a parameter index to identify the type of induction machine model, and this has been extended to cater for the DFIG modelling. In the following table indices 0 to 3 already existed in IPSA and indices 4-7 have been added to cater for the DFIG model.

IM Parameter Index	Type of Induction Machine modelled
0	IM with single or double cage rotor. Rotor parameters specified as start/run values.
1	IM with single or double cage rotor. Rotor parameters specified as inner/outer values.
2	As index 0, but using an 'old' method of solving the machine equations. Retained for backwards compatibility with earlier IPSA releases.
3	As index 1, but using an 'old' method of solving the machine equations. Retained for backwards compatibility with earlier IPSA releases.
4	DFIG with single or double wound rotor Rotor parameters specified as start/run values. Slip specified.
5	DFIG with single or double wound rotor, rotor parameters specified as inner/outer values. Slip specified.
6	DFIG with single or double wound rotor, rotor parameters specified as start/run values. Both slip and power factor specified.
7	DFIG with single or double wound rotor, rotor parameters specified as inner/outer values. Both slip and power factor specified.

Table 2-1: IM Parameter indices currently implemented in IPSA

IPSA uses a parameter index to identify the type of induction machine model. For instance type '0' presents run and start rotor parameters, type '1' represents inner and outer rotor impedance values. The parameter indices used for DFIG are presented in Table 2-1.

2.5.1 Implementation of the DFIG for IPSA load flow

The load flow section of IPSA incorporates the fast decoupled load flow algorithm [4] and has provisions for diagrammatic and tabular display of the results, outages, load changes and direct entry to load margins, faults and harmonics sections. Busbar voltage magnitudes and angles calculated in any load flow are stored and form starting point for any subsequent calculations.

2.5.2.1 Slip control by rotor power injection/export:

For DFIG models for slip control presented in modes 4 or 5 in Table 2-1, the slip and mechanical power input are set from induction machine data page 1. In this case the angle $(\phi - \theta) = 0$ in equations [2-7] and [2-9] of the previous section

The load flow iterations use the equivalent presented in section 2-2 to calculate and update the injected active and reactive power for both the stator and rotor busbars. IPSA load flow detailed results of induction machines were extended to present the calculated active and reactive power of both busbars.

2.5.1.2 Slip and reactive stator power control by rotor power injection/export:

Under slip and reactive power control on the stator terminals network, the introduction of reactive power control presents the control of the equivalent circuit angle. This introduces a reactive component into the injected/exported power to rotor slip rings, and the angle $(\phi - \theta)$ is not equal to zero. The load flow model calculates the injected active and reactive power to the rotor.

2.5.2 Implementation of the DFIG for IPSA fault calculations:

The fault level module in IPSA is used to simulate the effects of various types of short circuit on AC busbars of system and to display, on the network diagram, the calculated values of fault currents for each busbar in the network [4]. The calculation procedure is divided into the main sections:

- Initial phase
- Fault level calculation and display of fault level for each busbar in the network.
- Fault flow in every branch in the network as a result of a fault in a selected busbar.
- Fault current waveform simulation at any selected busbar.
- Protection coordination and display.

The initial phase is executed when the fault level section is first entered. It performs the necessary data checks and some basic calculations common to all fault types. The other sections are menu driven. The fault level calculation uses the voltage profile of the load flow solution when it is selected after load flow. Alternatively, if it is selected before any load flow calculations it uses 1.0 pu voltage.

Modelling of Induction machines:

Fault level contributions by induction machines in the system are calculated either on a similar basis (by calculating the transient and sub-transient parameters from the winding data) or by considering the running and starting characteristics of the machines. The approach used is determined by the type of rotor impedance entered, for the later:

$$Y_{ac} = \frac{1}{X''} e^{-t/T''} \dots\dots\dots [2 - 12]$$

$$Y_{dc} = \frac{1}{X''} e^{-t/Ta} \dots\dots\dots [2 - 13]$$

where

$$T'' = \frac{X''}{\omega R_r}$$

$$Ta = \frac{X''}{\omega (R_s + R_e)}$$

$$X'' = X_e + X_s + \frac{X_{st}X_m}{X_{st} + X_m}$$

$$Z_e = R_e + jX_e$$

Z_e = the system external impedance between the machine terminals and the fault point.

The external impedance is a function of the fault path and also the operating conditions and is calculated iteratively since this impedance has a significant effect on the decay of the dc components. One iteration is performed for the a. c. component.

The DFIG contribution is considering its pre-fault voltage profile and loading and hence the time constant and the level of contribution are affected. As the converter network injection is usually a small fraction of the stator power and also static converters performance is a function of their controllers and the dc system behind the converter and can be determine only by full transient analysis. Here it is assumed that the a. c. contribution of the converter injection is only limited to its effect on the pre-fault level.

3 DFIG Dynamic Model

3.1 Doubly Fed Induction Generator (DFIG)

DFIG wind turbines utilize a wound rotor induction generator, where the rotor winding is fed through back-to-back variable frequency, voltage source converters. A typical configuration of a DFIG based wind turbine is shown schematically in Figure 3-1. The converter system enables variable speed operation of the wind turbine by decoupling the power system electrical frequency and the rotor mechanical frequency.

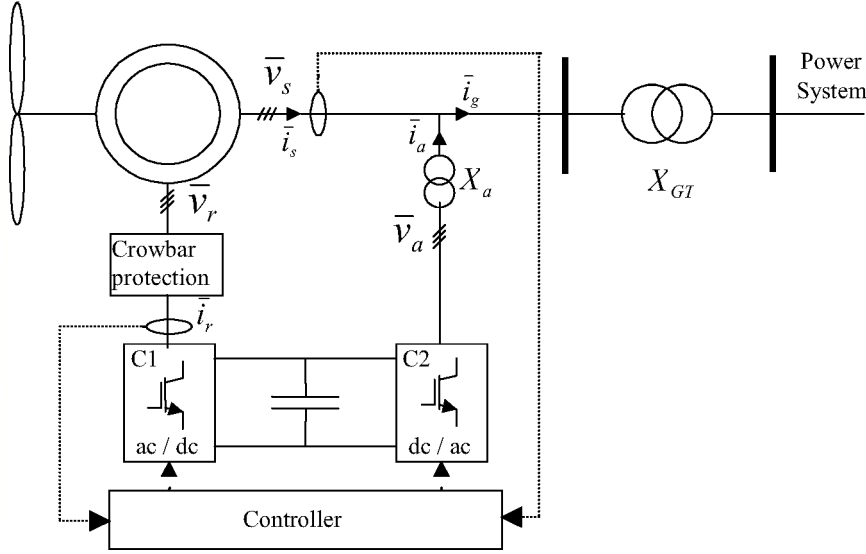


Figure 3-1: Basic configuration of a DFIG wind turbine

List of Symbols

v_s, v_r = Stator ($v_s = v_{ds} + jv_{qs}$) and rotor ($v_r = v_{dr} + jv_{qr}$) voltage

i_s, i_r, i_g = Stator ($i_s = i_{ds} + ji_{qs}$), rotor ($i_r = i_{dr} + ji_{qr}$) and generated current

v_a, i_a = Stator side converter (C2) voltage and current

P_g, Q_g, v_n = Generated active and reactive power, network voltage

X_{GT}, X_a = Transformer reactances

R_s, R_r = Stator and rotor machine resistance

$\omega_s, \omega_{base}, \omega_r$ = Synchronous, base and rotor angular frequency

λ = Flux linkage

L_m = Mutual inductance between the stator and the rotor

L_{ss}, L_{rr} = Stator and rotor self-inductance

s = Rotor slip

X', X = Transient or short circuit reactance and open circuit reactance

e_d, e_q = Voltage behind transient reactance d-q components

T_o = Transient open circuit time constant

J = Inertia constant

T_m, T_e, T_{sp} = Mechanical, electromagnetic, set point torque

T_{opt}, K_{opt} = Optimal torque and optimal constant of wind turbine

— = Superscript indicates a per unit quantity

3.2 Fifth order model of the DFIG

Three-phase stator and rotor windings of an induction machine can be represented by two sets of orthogonal fictitious coils. A generalized fifth order machine model can then developed by considering the following conditions and assumptions [7]:

- The stator current was assumed positive when flowing towards the machine.
- The equations were derived on the synchronous reference.
- The q-axis was assumed to be 90° ahead of the d-axis with respect to the direction of rotation.
- The q component of the stator voltage was selected as the real part of the busbar voltage and d component was selected as the imaginary part.

Machine equations can be represented in terms of the machine variables or in terms of arbitrary reference frame variables. However, for power system studies it is desirable to use a per unit (pu) representation. This enables the conversion of the entire system to per unit quantities on a single power base. Figure 3-2 shows the dq representation of the machine.

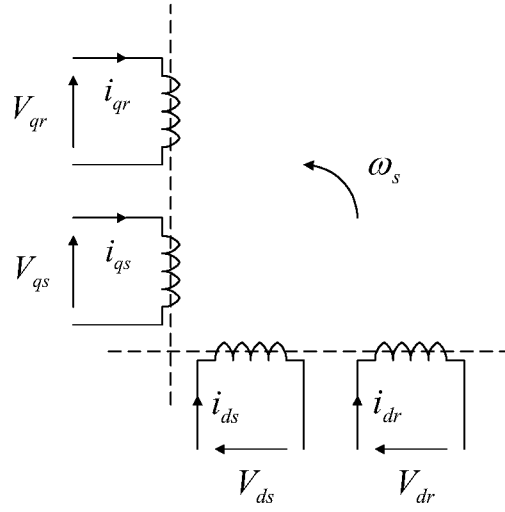


Figure 3-2: Direct (d) and quadrature (q) representation of induction machine

The voltage equations for the induction generator are given below, where all quantities except the synchronous speed are in pu [7]:

$$\begin{cases} \bar{v}_{ds} = \bar{R}_s \times \bar{i}_{ds} - \bar{\lambda}_{qs} + \frac{1}{\omega_s} \frac{d}{dt} \bar{\lambda}_{ds} \\ \bar{v}_{qs} = \bar{R}_s \times \bar{i}_{qs} + \bar{\lambda}_{ds} + \frac{1}{\omega_s} \frac{d}{dt} \bar{\lambda}_{qs} \end{cases} \quad [3-1]$$

$$\begin{cases} \bar{v}_{dr} = \bar{R}_r \times \bar{i}_{dr} - s \times \bar{\lambda}_{qr} + \frac{1}{\omega_s} \frac{d}{dt} \bar{\lambda}_{dr} \\ \bar{v}_{qr} = \bar{R}_r \times \bar{i}_{qr} + s \times \bar{\lambda}_{dr} + \frac{1}{\omega_s} \frac{d}{dt} \bar{\lambda}_{qr} \end{cases} \quad [3-2]$$

Where

$$\begin{cases} \bar{\lambda}_{ds} = \bar{L}_{ss} \times \bar{i}_{ds} + \bar{L}_m \times \bar{i}_{dr} \\ \bar{\lambda}_{qs} = \bar{L}_{ss} \times \bar{i}_{qs} + \bar{L}_m \times \bar{i}_{qr} \end{cases} \quad [3-3]$$

$$\begin{cases} \bar{\lambda}_{dr} = \bar{L}_{rr} \times \bar{i}_{dr} + \bar{L}_m \times \bar{i}_{ds} \\ \bar{\lambda}_{qr} = \bar{L}_{rr} \times \bar{i}_{qr} + \bar{L}_m \times \bar{i}_{qs} \end{cases} \quad [3-4]$$

From equation [3-4]:

$$\bar{i}_{dr} = \left(\frac{\bar{\lambda}_{dr} - \bar{L}_m \times \bar{i}_{ds}}{\bar{L}_{rr}} \right) \text{ and } \bar{i}_{qr} = \left(\frac{\bar{\lambda}_{qr} - \bar{L}_m \times \bar{i}_{qs}}{\bar{L}_{rr}} \right) \quad [3-5]$$

Substituting from [3-5] in to [3-3] and with $\bar{X}_1 = \left[\bar{L}_{ss} - \frac{\bar{L}_m^2}{\bar{L}_{rr}} \right]$:

$$\bar{\lambda}_{ds} = \bar{X}_1 \times \bar{i}_{ds} + \left(\frac{\bar{L}_m}{\bar{L}_{rr}} \right) \times \bar{\lambda}_{dr} \text{ and } \bar{\lambda}_{qs} = \bar{X}_1 \times \bar{i}_{qs} + \left(\frac{\bar{L}_m}{\bar{L}_{rr}} \right) \times \bar{\lambda}_{qr} \quad [3-6]$$

In order to obtain a voltage behind a transient model for the DFIG, the following two voltage components were defined.

$$\bar{e}_d = -\frac{\bar{L}_m}{\bar{L}_{rr}} \bar{\lambda}_{qr} \text{ and } \bar{e}_q = \frac{\bar{L}_m}{\bar{L}_{rr}} \bar{\lambda}_{dr} \quad [3-7]$$

Substituting from equation [3-7] into equation [3-6]:

$$\bar{\lambda}_{ds} = \bar{X}_1 \times \bar{i}_{ds} + \bar{e}_q \text{ and } \bar{\lambda}_{qs} = \bar{X}_1 \times \bar{i}_{qs} - \bar{e}_d \quad [3-8]$$

By substituting from equation [3-8] in to equation [3-1]:

$$\begin{cases} \bar{v}_{ds} = \bar{R}_s \times \bar{i}_{ds} - \bar{X}_1 \times \bar{i}_{qs} + \bar{e}_d + \frac{\bar{X}_1}{\omega_s} \frac{d}{dt} \bar{i}_{ds} + \frac{1}{\omega_s} \frac{d}{dt} \bar{e}_q \\ \bar{v}_{qs} = \bar{R}_s \times \bar{i}_{qs} + \bar{X}_1 \times \bar{i}_{ds} + \bar{e}_q + \frac{\bar{X}_1}{\omega_s} \frac{d}{dt} \bar{i}_{qs} - \frac{1}{\omega_s} \frac{d}{dt} \bar{e}_d \end{cases} \quad [3-9]$$

Substituting from equation [3-5] in to equation [3-2] and then substituting for $\bar{\lambda}_{dr}$ and $\bar{\lambda}_{qr}$ in terms of \bar{e}_d and \bar{e}_q from equation [3-7]:

$$\begin{cases} \frac{d\bar{e}_d}{dt} = -\frac{1}{\bar{T}_o} \left[\bar{e}_d + \frac{\bar{L}_m^2}{\bar{L}_{rr}} \times \bar{i}_{qs} \right] + s \times \omega_s \times \bar{e}_q - \omega_s \times \frac{\bar{L}_m}{\bar{L}_{rr}} \times \bar{v}_{qr} \\ \frac{d\bar{e}_q}{dt} = -\frac{1}{\bar{T}_o} \left[\bar{e}_q - \frac{\bar{L}_m^2}{\bar{L}_{rr}} \times \bar{i}_{ds} \right] - s \times \omega_s \times \bar{e}_d + \omega_s \times \frac{\bar{L}_m}{\bar{L}_{rr}} \times \bar{v}_{dr} \end{cases} \quad [3-10]$$

Where $\bar{T}_o = \frac{\bar{L}_{rr}}{\omega_s \bar{R}_r}$

Substituting from equation [3-7] into equation [3-5]:

$$\begin{cases} \bar{i}_{dr} = \left(\frac{\bar{\lambda}_{dr} - \bar{L}_m \times \bar{i}_{ds}}{\bar{L}_{rr}} \right) = \frac{1}{\bar{L}_m} \bar{e}_q - \frac{\bar{L}_m}{\bar{L}_{rr}} \bar{i}_{ds} \\ \bar{i}_{qr} = \left(\frac{\bar{\lambda}_{qr} - \bar{L}_m \times \bar{i}_{qs}}{\bar{L}_{rr}} \right) = -\frac{1}{\bar{L}_m} \bar{e}_d - \frac{\bar{L}_m}{\bar{L}_{rr}} \bar{i}_{qs} \end{cases} \quad [3-11]$$

The electromagnetic torque is calculated using:

$$T_e = \bar{\lambda}_{ds} \times \bar{i}_{qs} - \bar{\lambda}_{qs} \times \bar{i}_{ds} \quad [3-12]$$

Substituting from equation [3-8] to equation [3-12] the following equation can be obtained:

$$\begin{aligned} T_e &= (\bar{X}_1 \times \bar{i}_{ds} + \bar{e}_q) \times \bar{i}_{qs} - (\bar{X}_1 \times \bar{i}_{qs} - \bar{e}_d) \times \bar{i}_{ds} \\ &= \bar{e}_q \times \bar{i}_{qs} + \bar{e}_d \times \bar{i}_{ds} \end{aligned} \quad [3-13]$$

Substituting for \bar{e}_d and \bar{e}_q in terms of $\bar{\lambda}_{dr}$ and $\bar{\lambda}_{qr}$ in equation [3-13]:

$$T_e = \frac{\bar{L}_m}{\bar{L}_{rr}} (\bar{\lambda}_{dr} \times \bar{i}_{qs} - \bar{\lambda}_{qr} \times \bar{i}_{ds}) \quad [3-14]$$

Substituting from equation [3-4] in to equation [3-14]:

$$T_e = \bar{L}_m (\bar{i}_{dr} \times \bar{i}_{qs} - \bar{i}_{qr} \times \bar{i}_{ds}) \quad [3-15]$$

Finally, if T_m is the mechanical torque, dependent upon the local wind speed:

$$\frac{d\omega_r}{dt} = \frac{1}{J} \times (T_m - T_e) \quad [3-16]$$

3.3 Third order model of the DFIG

For power system transient studies inclusion of the network transients and generator stator transients increases the order of the overall system model, thus limiting the size of the system that can be simulated. Further, a small time step is required for numerical integration resulting in an increased computational time. For these reasons, it has become conventional to reduce the order of the generator model and to neglect network transients for the stability analysis of large power systems. A standard method of reducing the order of the induction generator model has been adopted, that is to neglect the rate of change of stator flux linkage. The reduced order model was derived by ignoring the differential term in equation [3-1], which is equivalent to neglecting the stator electric transients [11].

This approach is consisted with the dynamic analysis within IPSA, which, in common with the majority of dynamic/transient analysis programs, ignores network transients since these are relatively high frequency effects.

The reduced order voltage equations for the DFIG are, in pu:

$$\begin{cases} \bar{v}_{ds} = \bar{R}_s \times \bar{i}_{ds} - \bar{\lambda}_{qs} \\ \bar{v}_{qs} = \bar{R}_s \times \bar{i}_{qs} + \bar{\lambda}_{ds} \end{cases} \quad [3-17]$$

$$\begin{cases} \bar{v}_{dr} = \bar{R}_r \times \bar{i}_{dr} - s \times \bar{\lambda}_{qr} + \frac{1}{\omega_s} \frac{d}{dt} \bar{\lambda}_{dr} \\ \bar{v}_{qr} = \bar{R}_r \times \bar{i}_{qr} + s \times \bar{\lambda}_{dr} + \frac{1}{\omega_s} \frac{d}{dt} \bar{\lambda}_{qr} \end{cases} \quad [3-18]$$

When the stator transient is neglected, the machine equations given by [3-9] and [3-10] can be simplified to:

$$\begin{cases} \bar{v}_{ds} = \bar{R}_s \times \bar{i}_{ds} - \bar{X}_l \times \bar{i}_{qs} + \bar{e}_d \\ \bar{v}_{qs} = \bar{R}_s \times \bar{i}_{qs} + \bar{X}_l \times \bar{i}_{ds} + \bar{e}_q \end{cases} \quad [3-19]$$

$$\begin{cases} \frac{d\bar{e}_d}{dt} = -\frac{1}{\bar{T}_o} \left[\bar{e}_d + \frac{\bar{L}_m^2}{\bar{L}_{rr}} \times \bar{i}_{qs} \right] + s \times \omega_s \times \bar{e}_q - \omega_s \times \frac{\bar{L}_m}{\bar{L}_{rr}} \times \bar{v}_{qr} \\ \frac{d\bar{e}_q}{dt} = -\frac{1}{\bar{T}_o} \left[\bar{e}_q - \frac{\bar{L}_m^2}{\bar{L}_{rr}} \times \bar{i}_{ds} \right] - s \times \omega_s \times \bar{e}_d + \omega_s \times \frac{\bar{L}_m}{\bar{L}_{rr}} \times \bar{v}_{dr} \end{cases} \quad [3-20]$$

Where $\bar{T}_o = \frac{\bar{L}_{rr}}{\omega_s \bar{R}_r}$

The electromagnetic torque given in equation [3-15] can be simplified using the following steps:

- Using equations [3-17] and [3-3] and neglecting the resistance term

$$\begin{cases} \bar{i}_{ds} = \frac{1}{\bar{L}_{ss}} \bar{v}_{qs} - \frac{\bar{L}_m}{\bar{L}_{ss}} \bar{i}_{dr} \\ \bar{i}_{qs} = -\frac{1}{\bar{L}_{ss}} \bar{v}_{ds} - \frac{\bar{L}_m}{\bar{L}_{ss}} \bar{i}_{qr} \end{cases} \quad [3-21]$$

- Substituting in equation [3-15]:

$$T_e = -\frac{\bar{L}_m}{\bar{L}_{ss}} (\bar{i}_{dr} \times \bar{v}_{ds} + \bar{i}_{qr} \times \bar{v}_{qs}) \quad [3-22]$$

4 System and Connection Description:

The likely connection scenarios, for three types of wind generation technology; namely (1) variable speed induction or synchronous generators connected via back-to-back static converters; (2) fixed speed induction generators; or (3) doubly fed induction generators are studied in this section. The analyses were conducted by simulating a real-life situation, using the 132kV and 33kV distribution system between Pentir and Connahs Quay within the SP Manweb network. Two offshore wind farms have already been granted planning permission within this network. The first is 'Offshore Farm 1' 6 km offshore from Prestatyn in North Wales, approved in July 2002 with a planned capacity of 60MW from 30 turbines. The second is 'Offshore Farm 2' 8 km offshore from Abergele in North Wales, approved in December 2002 with a planned capacity of 100MW from 30 turbines.

Please note that the details of these arrangements are based on typical published information. However, none of it represents the actual set up being built by the developers. The intention of these configurations is to be generally representative of a 'real world' condition.

4.1 System Description:

This section represents a brief description of the Pentir – Connah 132kV network used for the studies and the current operation practices.

A generic Winter Peak network was supplied to IPSA from SP Power Systems Ltd for this project. Summer Minimum load is typically 34% of the Winter Peak load for this network.

The network used has more than 480 busbars representing the 400kV, 132kV and 33kV voltage levels. It is operating as an interconnected system with more than 700 lines including 110 transformers varying from super grid transformers typically rated 120MVA or higher to 132/33kV transformers with typical ratings of 45-60MVA, and some generator transformers with lower voltage levels. Figure 4.1 presents a single line diagram of the 132kV (in blue) and 33kV (in black) voltage levels.

Pentir is normally operated with one of the two Super Grid Transformers (SGTs) on open standby but may also operate with both SGTs in service and the bus section open to reduce fault levels. Connahs Quay has 4 SGTs, two SGTs feeding the 132kV to Pentir. Two more SGTs are connected to other parts of the network. The remainder of the 132kV network is run solid.

There are number of generators close and/or connected to the system. The major generation from the Seven Year Statement of the National Grid Plc, is at Fiddler's Ferry, Dee Side, Dinorwig and Wyfla. Fiddler's Ferry has registered capacity of 1950MW, Deeside 500MW while Wyfla and Dinorwig have declared generation capacities of 1082MVA and 1728MVA, respectively.

Within the SP Manweb network there is approximately 550MW of independent embedded generation operating, over 50% of which is from renewable sources.



Figure 4-1: The Representative system.

4.2 System Equipment Ratings:

The Pentir and Connahs Quay SGTs are rated at 240MVA each. The 132/33kV transformer ratings are detailed in the network, they are typically 45MVA or 60MVA. Switchgear fault rating for Peak Make duties vary from 22863MVA at Colwyn Bay 132kV substation to 6230MVA at the Holywell 132kV substation. The typical Summer rating for the 132kV lines used in this area is 89 MVA while the Winter rating is typically 111MVA

4.3 Offshore Connection:

A typical large offshore farm has 30 turbines. A common arrangement of a farm is 3 rows with 10 turbines in each row. Two offshore wind farms are presented in 'offshorewindfarms.co.uk' will be connected to the SP Manweb network.

The published information in 'offshorewindfarms.co.uk' indicates that the distance to the nearest turbine is 6km and 8km for the two sites. The turbines are spaced over 4-5km horizon. This provides an average length for under-sea cable of 8km for 'Offshore Farm 1' offshore farm and 10.5km for 'Offshore Farm 2' site.

Presently, typical offshore generation will be connected at 0.69kV to 1kV with a step up generator transformer (for induction generators and doubly-fed induction generators) to 33kV. For synchronous turbine generators back-to-back converters are used for connection to the distribution network with step up transformers. Figure 4.2 shows the typical connection configuration for synchronous generator connections and Figure 4.3 presents a typical connection route for both types of induction generator connections.

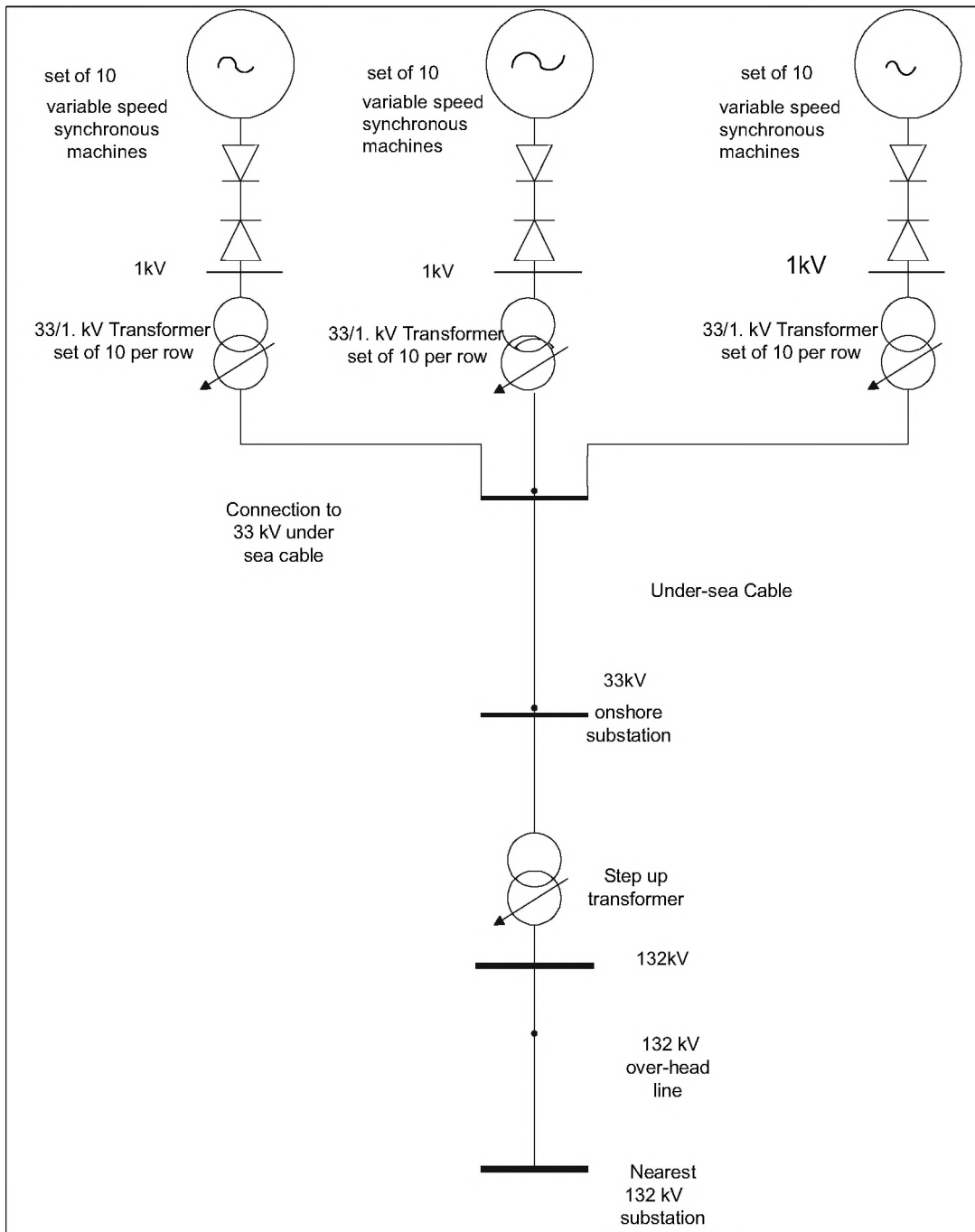


Figure 4.2 Configuration for a 30 turbine variable speed turbine offshore wind farm connection (use of synchronous generators)

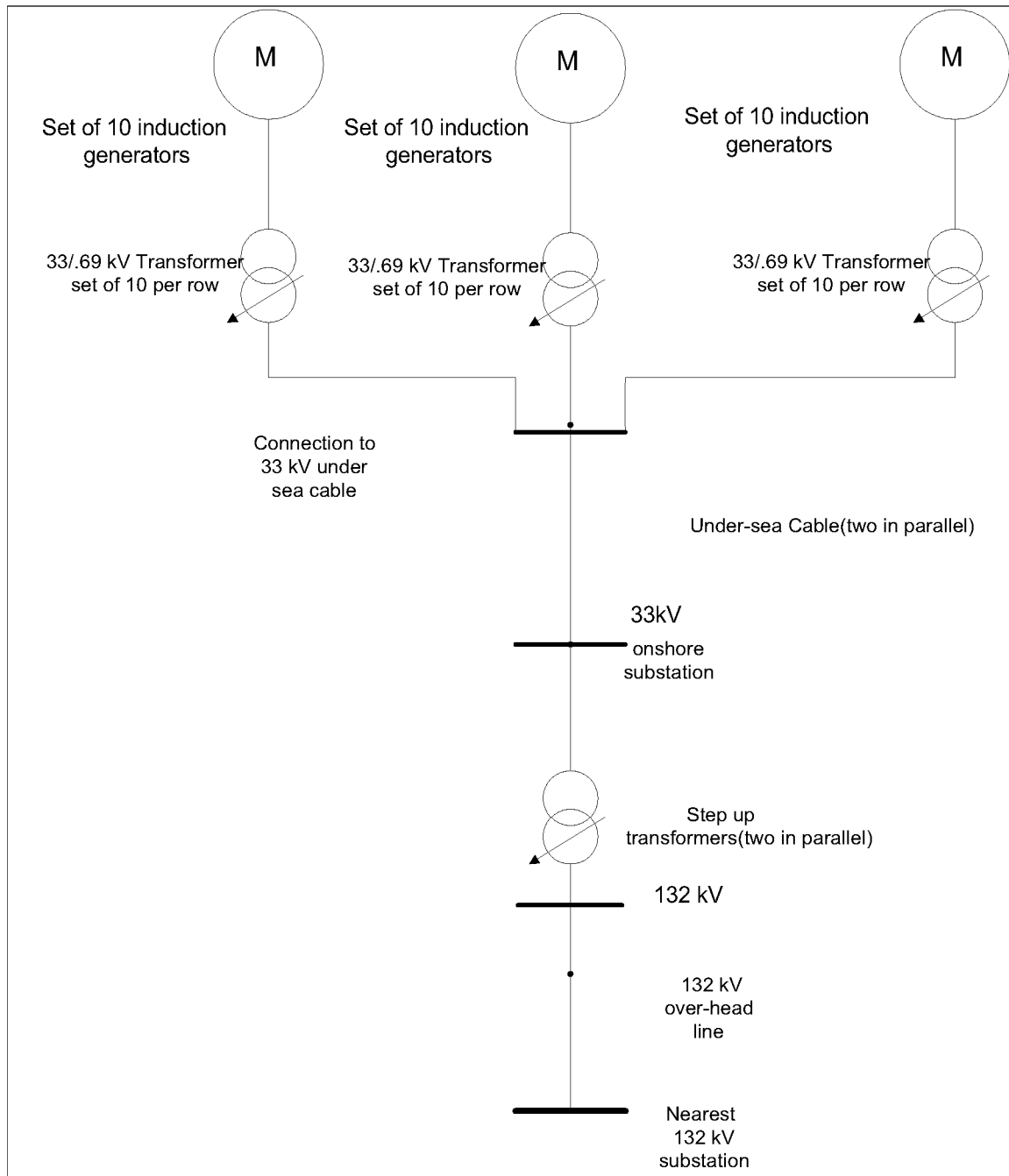


Figure 4.3 Configuration for a 30 turbine variable speed turbine offshore wind farm connection (use of induction generators).

For the level of power transferred and the length of the connection to the network, 33kV undersea cables are used.

An onshore step-up substation is needed for each windfarm connection with 132/33kV transformers. Transformer ratings for 'Offshore Farm 2' are two 132/33kV transformers rated at 60MVA each and for 'Offshore Farm 1', 45MVA each. For the purpose of this study two undersea 33kV cables are used for each farm. The first farm has cables of 57.5MVA rating the second has two cables rated at 68MVA each.

5 Connection Policies, Technical Problems and Merits:

5.1 Connection Policies:

Presently, all of the UK Distribution Network Operators (DNOs) follow the various national technical standards that cover the different aspects of embedded generation (i.e. G59, G75, P2/5, P28, P29, ETR113). These impose some technical constraints. The constraints may require some reinforcements or modifications to the network.

5.2 Technical Problems:

Various technical problems may need to be investigated. The list includes:

- High fault levels: Some networks are designed to operate close to equipment ratings; offshore generation connection will increase the local system connectivity and the fault level currents for local substations.
- Circuit loading: different ratings apply for continuous loadings; summer ratings are lower, but loadings are likely to be higher.
- Voltage regulation and voltage control: existing networks are not well designed for voltage rise; voltage reduction schemes and network voltage control schemes are adversely affected by embedded generation – especially if operating under voltage control, or if the generator output changes rapidly.
- Security Analysis: Circuit loading and voltage regulation may not be a problem with normal network configuration, however the connection of embedded generation may cause overloads or unacceptable voltages in some local lines or substations during an outage scenario.
- Some transformer on-load tap changers are not designed for reverse power flow (this more likely in lower voltage distribution transformers rather than at the 132kV voltage level).
- Operational problems: a high penetration of (variable) wind generation replacing thermal plant; encountering unknown embedded generation when undertaking a ‘black start’.
- Protection: distribution systems are not generally designed for ‘reverse’ power flow; the presence of generation can upset protection schemes, e.g. distance protection.
- Nuisance tripping.
- Impact on power quality: some types of wind generators need to be connected through back-to-back converter devices. These devices introduce some harmonics. While the level of harmonics generated is usually within the specified regulations, studies are needed to ensure that there is no resonance.
- The power output from wind farms may vary continuously, not only during power-up and power-down but also during normal running. This variation leads to a continuously changing network voltage at the point of connection with the DNO. The customers connected at lower voltages rely on the automatic on-load tap changers employed on 132/33kV and 33/11kV transformers to maintain their voltage within acceptable limits. In order to reduce the number of tap changer operations, the automatic voltage control schemes have a built in time delay (1 or 2 minutes). The wind farm may therefore have to limit the rate of change of voltage at the point of connection to avoid exposing large numbers of customers to unacceptable voltage fluctuations.

- The DNOs have a continuing obligation to comply with P2/5. This may need some security and contingency studies with the new system loading conditions.
- The fault ride-through capability is a problem for the network transmission operator. If the wind farm disconnects itself when a fault occurs on the transmission system then the integrity of the transmission system can be undermined as the lost generation may exceed the amount of spinning reserve. Closely related here is the frequency responsiveness of the machines capability to enable windfarm power output to be increased if the system frequency falls.

5.3 Offshore Windfarm Connection Merits:

For distribution networks the offshore wind generation connection may present some merits to the DNOs as follows:

- May possibly lower network losses and reduced costs of network investments.
- May reduce reinforcement required by load growth in some conditions.
- May increase the generation availability in the area.

6 Connection Studies:

6.1 Synchronous Machine based offshore wind farm:

Although the synchronous machines used for offshore wind farms have many special design features, the conventional decoupled loadflow with PV and PQ models cover all the needs. Load flow solutions can be tweaked to represent the output of these generator sets. Whether the cost to get converters actually deliver the specified operating condition for the whole bulk of active and reactive power from the farm is another question.

A full simulation of the behaviour under fault conditions to consider contribution from converters as well as generators and must involve modelling of the converter current control and protection systems used. These are not factors can be considered accurately within the AC system fault level calculation algorithms. A full short circuit fault simulation can, therefore, only be carried out as a dynamic simulation exercise. However, for fault level analyses of the AC areas of the network, it is reasonable to assume that the converters will have current control facilities limiting the converter fault contributions to something of the order of 120% rated current, which is mostly included in the solution as load currents and are taken into the account.

Typical data for synchronous machines are used for ‘Offshore Farm 1’ and are presented in Table 6.1.1. The farm will have 3 rows of 10 turbine-generator sets. Each set will have its own back-to-back converter set and a step up transformer (33/0.69kV, 2.2MVA and impedance of 7%). The network model configuration is shown in Figure 4.2

Parameter	Value	Units
kVA (rated kVA)	2000	kVA
V (rated voltage)	.69	kV
R_a (armature resistance)	.018	pu
X_d (direct axis reactance)	2.65	pu
R_o (zero-sequence resistance)	.018	pu
X_o (zero-sequence reactance)	.054	pu
X_d' (direct axis transient reactance)	.22	pu
T_d' (direct axis transient open-circuit time constant)	3.5	secs
X_d'' (direct axis sub-transient reactance)	.15	pu
T_d'' (direct axis sub-transient open-circuit time constant)	.03	secs
X_q (q-axis reactance)	2.16	pu
X_q'' (q-axis sub-transient reactance)	.25	pu

Table 6.1.1: Typical Synchronous Machine data for Offshore Farm 1.

Similarly, typical data for synchronous machines are used for ‘Offshore Farm 2’ and are presented in Table 6.1.2. The farm has 3 rows of 10 turbine-generator sets. Each set has its own back-to-back converter set and a step up transformer (33/1.0kV, 3.4MVA and impedance of 8.3%) with the same basic network configuration. Figure 4.1 presents the single line diagram illustrating the connection of the two farms into the 132kV network.

Parameter	Value	Units
kVA (rated kVA)	3400	kVA
Rated voltage	1.0	kV
R_a (armature resistance)	.01	pu
X_d (direct axis reactance)	2.65	pu
R_o (zero-sequence resistance)	.01	pu
X_o (zero-sequence reactance)	.03	pu
X_d' (direct axis transient reactance)	.22	pu
T_d' (direct axis transient open-circuit time constant)	3.5	secs
X_d'' (direct axis sub-transient reactance)	.15	pu
T_d'' (direct axis sub-transient open-circuit time constant)	.03	secs
X_q (q-axis reactance)	2.16	pu
X_q'' (q-axis sub-transient reactance)	.25	pu

Table 6.1.2: Typical Synchronous Machine data for Offshore Farm 2.

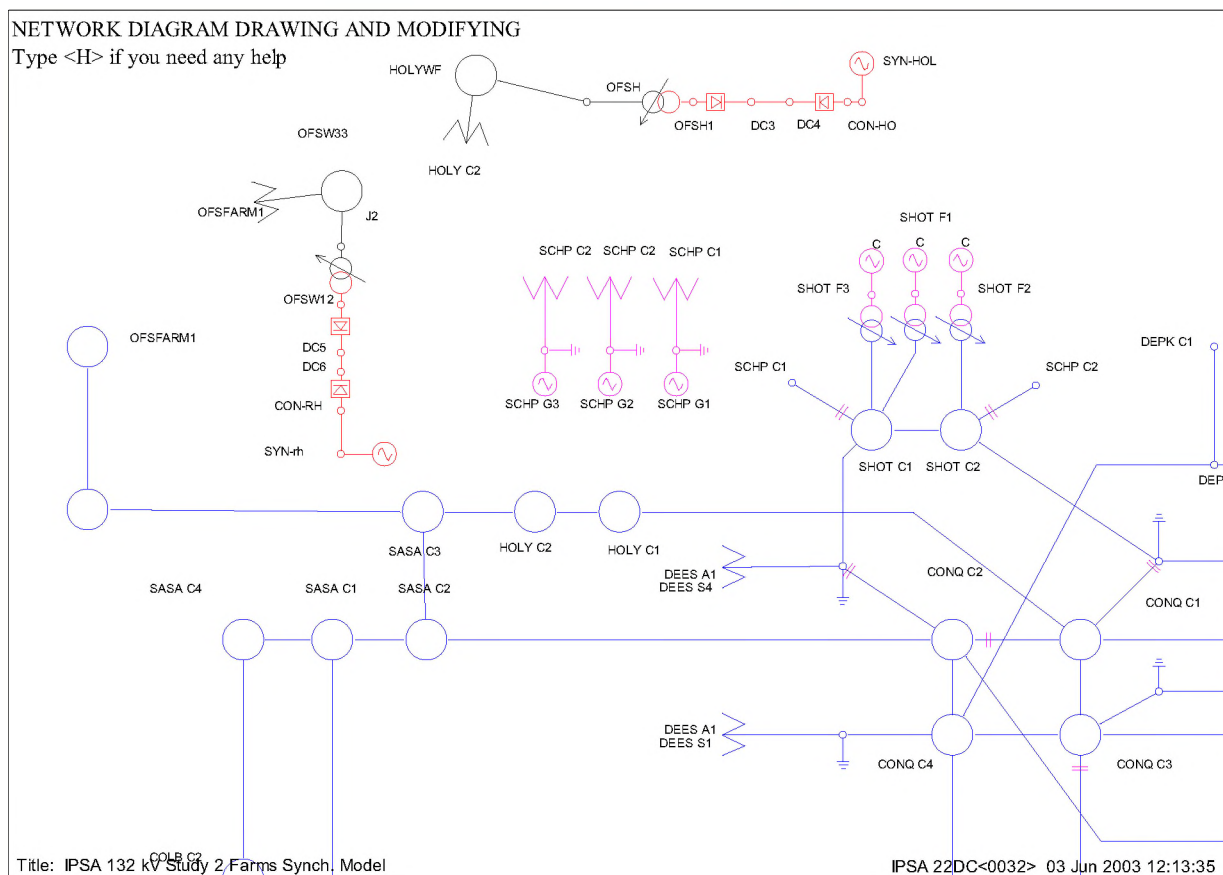


Figure 6.1: Connection of Synchronous generator type offshore farm via back-to-back converter-inverter set.

6.1.1 Load flow studies:

The following load flow studies were carried out for this generation type:

- Peak winter load without the offshore farms.
- Peak winter load with both farms at full generation.
- Minimum summer loading without the farms.

- Minimum summer loading with both farms at full generation.

The same network configuration is used to focus on the effect of the generation of the offshore farm. Table 6.1.3 presents a summary of the results for the studies conducted for the minimum summer load. The main voltage increase noticed on the 132kV section of the network with maximum increase at 'RHYL C1'. The other noticeable effect is the increase in the transmission losses. This is due to the shift of the generation pool as a result of the connection of the farms.

The analysis based on unity power factor supply to the back-to-back converter/inverter sets.

Voltage Level	400 kV	132 kV	33 kV
Maximum voltage increase in % when offshore farms connected.	No voltage increase	1.3 %	1.1%
Location of maximum voltage rise.	-	RHYL C1	RHYL E1, RHYL E2
Number of Nodes with voltage increase of 0.5 % or more.	-	14	20
Number of nodes higher than 1.1 PU	5	1	-
Number of Overloaded Circuits	-	-	-
Total Real Power Loss (MW) – no offshore farms	194.5 MW 137 MVAR 201.83 MW 183.3 MVAR $P_{NET\ LOAD} = 561 - 99* = 462$ $Q_{NET\ LOAD} = 147.1 + 53* = 200.1\text{MVAR}$ $P_{NET\ LOAD} = 561 - 262.5* = 298.5\text{MW}$ $Q_{NET\ LOAD} = 147.1 + 52.2* = 199.3\text{MVAR}$		
Total Reactive Power Loss (MVAR)– no offshore			
Total Real Power Loss (MW)– offshore farms connected			
Total Reactive Power Loss (MVAR) – offshore farms connected.			
Total network real load in MW – no offshore farms. (The '*' value represents distributed generation)			
Total network reactive load in MVAR– no offshore farms. (The '*' value represents distributed generation)			
Total network real load in MW – offshore farms connected. (The '*' value represents distributed generation)			
Total network reactive load in MVAR– offshore farms connected. (The '*' value represents distributed generation)			

Table 6.1.3: Summary of the load flow studies for minimum summer load condition (Use of synchronous generators -no reinforcements)

Voltage Level	400 kV	132 kV	33 kV
Maximum voltage increase in % when offshore farms connected.	0.4 %	1.5 %	1.0%
Location of maximum voltage rise.	-	RHYL C1	RHEIWF
Number of Nodes with voltage increase of 0.5 % or more	-	17	11
Number of nodes higher than 1.1 PU	-	-	-
Number of additional overloaded circuits	-	1	-
Total Real Power Loss (MW) – no offshore farms	206 MW 365 MVAR 208.456 MW 355.63 MVAR $P_{\text{NET LOAD}} = 1650 - 98.9^* = 1551.1\text{MW}$ $Q_{\text{NET LOAD}} = 436 + 50.2^* = 486.2\text{MVAR}$ $P_{\text{NET LOAD}} = 1652 - 259.8^* = 1392.2\text{MW}$ $Q_{\text{NET LOAD}} = 436 + 50.9^* = 486.9\text{MVAR}$		
Total Reactive Power Loss (MVAR)– no offshore			
Total Real Power Loss (MW)– offshore farms connected			
Total Reactive Power Loss (MVAR) – offshore farms connected.			
Total network real load in MW – no offshore farms. (The ‘*’ value represents distributed generation)			
Total network reactive load in MVAR– no offshore farms. (The ‘*’ value represents distributed generation)			
Total network real load in MW – offshore farms connected. (The ‘*’ value represents distributed generation)			
Total network reactive load in MVAR– offshore farms connected. (The ‘*’ value represents distributed generation)			

Table 6.1.4: Summary of the load flow studies for peak winter load condition
(Use of synchronous generators - no reinforcements)

6.1.2 Fault Level studies:

The following fault level studies were carried out for both minimum summer loading and peak winter loading for this generation type as follows:

- Minimum summer loading: Three phase asymmetrical peak fault level calculation at each busbar at 10ms (switchgear make duties) and asymmetrical RMS at 100ms (break duties).
- Minimum summer loading: Single line to ground asymmetrical peak fault level calculation at each busbar at 10ms (switchgear make duties) and asymmetrical RMS at 100ms (break duties).
- Peak winter loading: Three phase asymmetrical peak fault level calculation at each busbar at 10ms (switchgear make duties) and asymmetrical RMS at 100ms (break duties)
- Peak winter loading: Single line to ground asymmetrical peak fault level calculation at each busbar at 10ms (switchgear make duties) and asymmetrical RMS at 100ms (break duties).

The network fault level results of the minimum summer loading condition for both fault types have higher values than the winter peak condition. This is specially the case for the 132kV network, due to the generally higher pre-fault voltage level for the minimum summer loading condition. Therefore, the minimum summer loading condition results are compared before and after the

connection of the farms. It must be noticed that the fault level calculations assume that the generator converters protection will operate and hence the contribution is limited to the full load currents. Table 4.1.5 represents the maximum fault level increase as a result of the connection of the offshore farms for the three-phase fault and line-to-ground fault at each busbar.

Voltage Level	400 kV	132 kV	33 kV
Maximum three phase fault level increase in % at 10ms, as a result of offshore farms connected. (PEAK VALUES)	0.21 %	1.66 %	.81%
Maximum single-line-to-ground fault level increase in % at 10ms, as a result of offshore farms connected. (PEAK VALUES)	0.22 %	1.83 %	.85%
Maximum three phase fault level increase in % at 100ms, as a result of offshore farms connected. (ASYMMETRICAL RMS VALUES)	0.18%	1.77 %	.8%
Maximum single-line-to-ground fault level increase in % at 100ms as a result of offshore farms connected. (ASYMMETRICAL RMS VALUES)	0.18 %	1.78 %	.81%

Table 6.1.5: Summary of the fault level studies for minimum summer load condition (Use of synchronous generators - no reinforcements)

Although, these values are within the switchgear limits, it must be pointed out that accurate contributions to the faults of the converter/inverter sets can only be calculated using transient stability routines to consider the effect of the converter controllers and the operating time of converter over-current protect.

6.2 Induction generator connection (IG)

The steady-state analysis of the connection for an offshore windfarm using a traditional induction generator designed to be driven at fixed speed from a wind turbine and supplying the 132kV network is presented.

Typical data for the ‘Offshore windfarm 1’ induction generators are presented in Table 6.2.1. The windfarm has 3 rows of 10 turbine-generator sets. Each set has its own step up transformer to 33kV (33/0.69kV, 2.2MVA and impedance of 7%). The network model configuration is as seen in Figure 4.3

Parameter	Value	Units
kVA (rated kVA)	2000	kVA
Rated voltage	0.690	kV
R_1 (stator resistance)	.0061	pu
X_1 (stator reactance)	.0821	pu
R_2 (rotor resistance referred to stator side – run parameters)	.0169	pu
X_2 (rotor reactance referred to stator side – run parameters)	.1072	pu
R_3 (rotor resistance referred to stator side – standstill parameters)	.021	pu
X_3 (rotor reactance referred to stator side – standstill parameters)	.0329	pu
X_m (magnetizing reactance)	2.556	pu
Frequency	50	Hz

Table 6.2.1: Typical Induction Generator data for ‘Offshore Windfarm 1’.

Similarly, typical data for induction generators are used for ‘Offshore Farm 2’ are presented in Table 6.2.2. The farm has 3 rows of 10 turbine-generator sets. Each generator has its step up

transformer (33/1.0kV, 3.4MVA and impedance of 8.3%) with the same basic network configuration. Figure 6.2 presents the single line diagram illustrating the connection of the two farms into the 132kV network.

Parameter	Value	Units
KVA (rated kVA)	3400	KVA
Rated voltage	0.690	kV
R_1 (stator resistance)	.0061	pu
X_1 (stator reactance)	.0821	pu
R_2 (rotor resistance referred to stator side – run parameters)	.0169	pu
X_2 (rotor reactance referred to stator side – run parameters)	.1072	pu
R_3 (rotor resistance referred to stator side – standstill parameters)	.021	pu
X_3 (rotor reactance referred to stator side – standstill parameters)	.0329	pu
X_m (magnetizing reactance)	2.556	pu
Frequency	50	Hz

Table 6.2.2: Typical Induction Generator data for ‘Offshore Windfarm 2’.

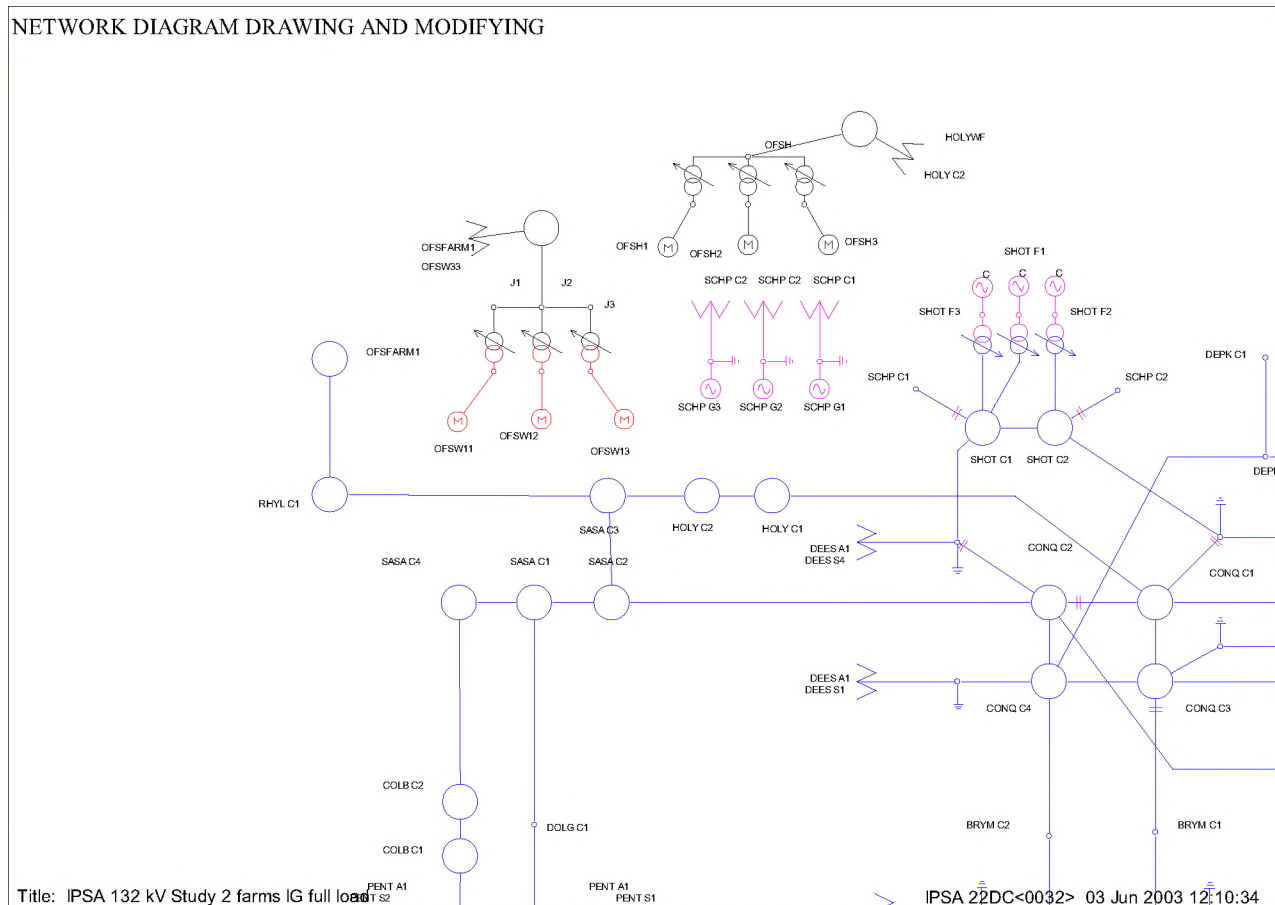


Figure 6.2: Connection of Offshore induction generator type wind farm.

6.2.1 Load flow studies:

The following loadflow studies were carried out for this generation type:

- Peak winter load without the offshore farms.
- Peak winter load with both farms at full generation.

- Minimum summer loading without the farms.
- Minimum summer loading with both farms at full generation.

The same network configuration is used to focus on the effect of the generation of the offshore farm. Table 6.2.3 presents a summary of the results for the studies conducted for the minimum summer load. The main voltage increase noticed on the 132 kV section of the network with maximum increase at 'RHYL C1'.

Voltage Level	400 kV	132 kV	33 kV
Maximum voltage increase in % when offshore farms connected.	No voltage increase	0.6 %	1.0%
Location of maximum voltage rise.	-	RHEI C1	RHYL E1 RHYL E2
Number of Nodes with voltage increase of 0.5 % or more.	-	2	32
Number of nodes higher than 1.1 PU.	3	1	-
Number of Overloaded Circuits.	-	1	-
Total Real Power Loss (MW) – no offshore farms.	194.5 MW 137 MVAR 204.83 MW 214.853 MVAR $P_{NET\ LOAD} = 561 - 99* = 462$ $Q_{NET\ LOAD} = 147.1 + 53* = 200.1\ MVAR$ $P_{NET\ LOAD} = 561 - 250.5* = 310.5\ MW$ $Q_{NET\ LOAD} = 147.1 + 140.5* = 287.6\ MVAR$		
Total Reactive Power Loss (MVAR)– no offshore.			
Total Real Power Loss (MW)– offshore farms connected.			
Total Reactive Power Loss (MVAR) – offshore farms connected.			
Total network real load in MW – no offshore farms (The '*' value represents distributed generation)			
Total network reactive load in MVAR– no offshore farms (The '*' value represents distributed generation)			
Total network real load in MW – offshore farms connected. (The '*' value represents distributed generation)			
Total network reactive load in MVAR– offshore farms connected. (The '*' value represents distributed generation)			

Table 6.2.3: Summary of the loadflow studies for minimum summer load condition (Use of induction generators - no reinforcements)

Voltage Level	400 kV	132 kV	33 kV
Maximum voltage increase in % when offshore farms connected.	No Voltage increase	No Voltage Increase	0.3%
Location of maximum voltage rise.	-		CGEI E1
Number of Nodes with voltage increase of 0.5 % or more.	-	-	
Number of nodes higher than 1.1 PU.	-	-	-
Number of additional overloaded circuits.	-	5	-
Total Real Power Loss (MW) – no offshore farms.	206 MW 365 MVAR 212.285 MW 402.9 MVAR $P_{\text{NET LOAD}} = 1650 - 98.9* = 1551.1 \text{ MW}$ $Q_{\text{NET LOAD}} = 436 + 50.2* = 486.2 \text{ MVAR}$ $P_{\text{NET LOAD}} = 1652 - 253.54* = 1398.5 \text{ MW}$ $Q_{\text{NET LOAD}} = 436 + 137.45* = 573.45 \text{ MVAR}$		
Total Reactive Power Loss (MVAR)– no offshore			
Total Real Power Loss (MW)– offshore farms connected.			
Total Reactive Power Loss (MVAR) – offshore farms connected.			
Total network real load in MW – no offshore farms (The ‘*’ value represents distributed generation)			
Total network reactive load in MVAR– no offshore farms. (The ‘*’ value represents distributed generation)			
Total network real load in MW – offshore farms connected. (The ‘*’ value represents distributed generation)			
Total network reactive load in MVAR– offshore farms connected. (The ‘*’ value represents distributed generation)			

Table 6.2.4: Summary of the loadflow studies for peak winter load condition
(Use of induction generators - no reinforcements)

6.2.2 Fault Level studies:

The following fault level studies were carried out for both minimum summer loading and peak winter loading for this generation type as follows:

- Minimum summer loading: Three-phase asymmetrical peak fault level calculation at each busbar at 10ms (switchgear make duties) and asymmetrical RMS at 100ms (break duties).
- Minimum summer loading: Single-line-to-ground asymmetrical peak fault level calculation at each busbar at 10ms (switchgear make duties) and asymmetrical RMS at 100ms (break duties).
- Peak winter loading: Three phase asymmetrical peak fault level calculation at each busbar at 10ms (switchgear make duties) and asymmetrical RMS at 100ms (break duties).
- Peak winter loading: Single line to ground asymmetrical peak fault level calculation at each busbar at 10ms (switchgear make duties) and asymmetrical RMS at 100ms (break duties).

The network fault level results of the minimum summer loading condition for both fault types have higher values than the winter peak condition. This is specially the case for the 132kV network, due to the generally higher pre-faults voltage level for the minimum summer loading condition.

Therefore, the minimum summer loading condition results are compared before and after the connection of the farms.

Voltage Level	400 kV	132 kV	33 kV
Maximum three phase fault level increase in % at 10ms, as a result of offshore farms connected. (PEAK VALUES)	2 %	22 %	5.7%
Maximum single-line-to-ground fault level increase in % at 10ms, as a result of offshore farms connected. (PEAK VALUES)	1.1 %	11 %	3.6%
Maximum three phase fault level increase in % at 100ms, as a result of offshore farms connected. (ASYMMETRICAL RMS VALUES)	.4%	6.6 %	4 %
Maximum single-line-to-ground fault level increase in % at 100ms as a result of offshore farms connected. (ASYMMETRICAL RMS VALUES)	2.2 %	4.1 %	2.4%

Table 4.2.5: Summary of the fault level studies for minimum summer load condition
(Use of induction generators - no reinforcements)

These values will put limitation on the operation of the network with regard to the connection of both Pentir Super grid transformers (SGTs). Whilst local 132kV substations can handle the fault level increase when a single SGT is connected at Pentir, ‘St Asaph’ switchgears, which are rated 2492RMS MVA, 6230 Peak MVA and 137MVA continuous will need to be upgraded if the connectivity of the network is to be maintained with the present option of having both Pentir SGTs connected to remain available. The protection time and current settings also need to be reviewed to insure the correct sequence of operation for both symmetrical and asymmetrical faults.

6.3 Doubly-fed induction generator connection (DFIG)

The steady-state analysis of the connection for offshore windfarms using DFIGs designed to be driven at variable speed from wind turbines and supplying the 132 kV network is presented. Two back-to-back PWM voltage-fed inverters connected between the stator and rotor allow for each generator for sub- and super-synchronous operation with low distortion currents.

Typical data for the DFIGs used for ‘Offshore Windfarm 1’ are presented in Table 6.3.1. The windfarm has 3 rows of 10 turbine-generator sets. Each set has its own step up transformer to 33kV (33/0.69kV, 2.2MVA and impedance of 7%). The network model configuration is as seen in Figure 4.3

Parameter	Value	Units
kVA (rated kVA)	2000	kVA
Rated voltage	0.690	kV
R_1 (stator resistance)	.0043	pu
X_1 (stator reactance)	.0809	pu
R_2 (rotor resistance referred to stator side)	.0048	pu
X_2 (rotor reactance referred to stator side)	.0871	pu
X_m (magnetizing reactance)	3.459	pu
Frequency	50	Hz

Table 6.3.1: Typical DFIG data for ‘Offshore Windfarm 1’.

Similarly, data for induction generators used for ‘Offshore Windfarm 1’ are presented in Table 6.3.2. The windfarm has 3 rows of 10 turbine-generator sets. Each set has its own step up transformer (33/0.69kV, 3.4MVA and impedance of 8.3%) with the same basic network configuration.

Parameter	Value	Units
kVA (rated kVA)	3400	kVA
Rated voltage	0.690	kV
R_1 (stator resistance)	.0043	pu
X_1 (stator reactance)	.0809	pu
R_2 (rotor resistance referred to stator side)	.0048	pu
X_2 (rotor reactance referred to stator side)	.0871	pu
X_m (magnetizing reactance)	3.459	pu
Frequency	50	Hz

Table 6.3.2: Typical DFIG data for ‘Offshore Windfarm 2’.

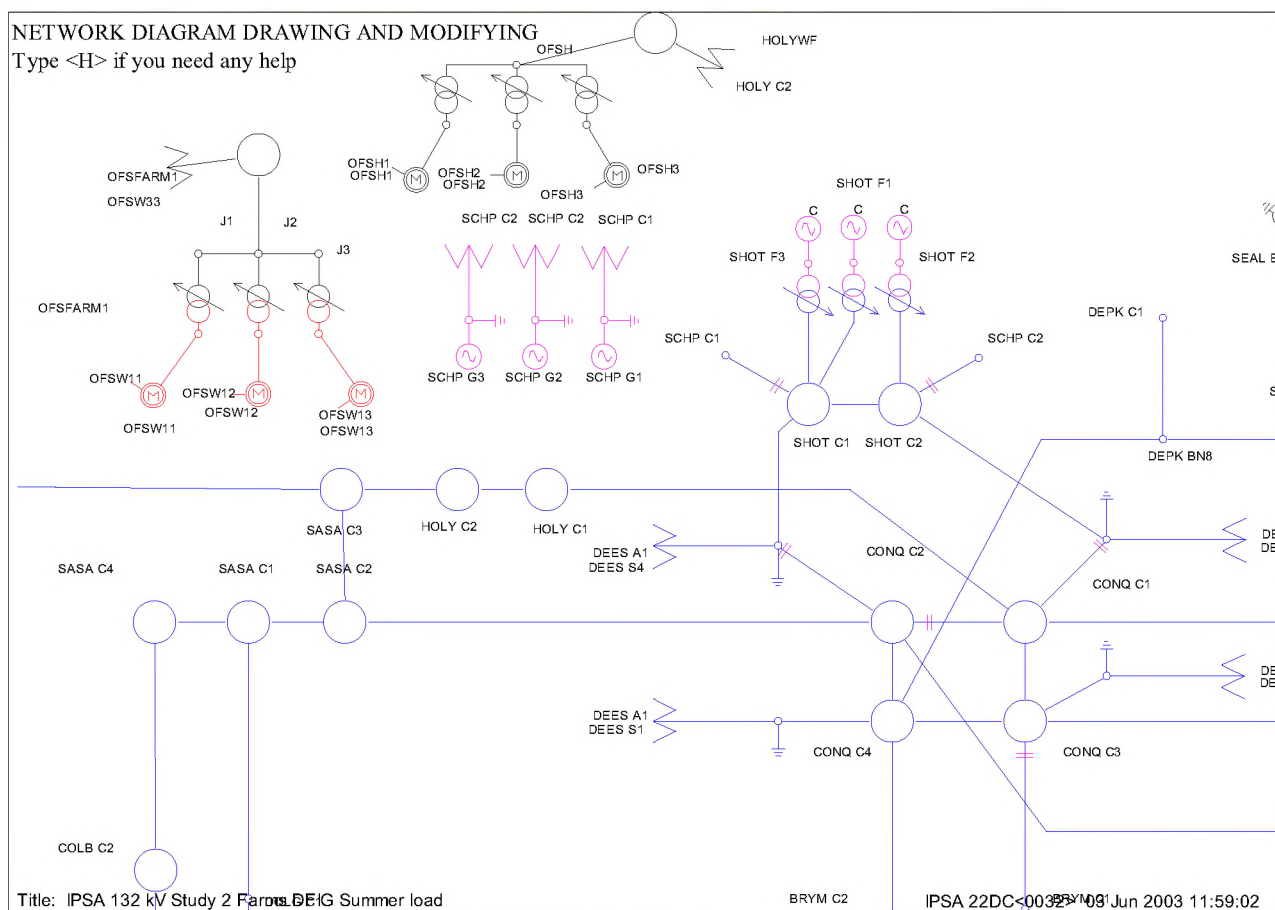


Figure 6.3: DFIG connection for 2 offshore windfarms.

6.3.1 Loadflow studies:

The following loadflow studies were carried out for this generation type:

- Peak winter load without the offshore farms.
- Peak winter load with both farms at full generation.
- Minimum summer loading without the farms.
- Minimum summer loading with both farms at full generation.

The same network configuration is used to focus on the effect of the generation of the offshore farm. Table 6.3.3 presents a summary of the results for the studies conducted for the minimum summer load. The main voltage increase noticed on the 132kV section of the network with maximum increase at 'RHYL C1'.

Voltage Level	400 kV	132 kV	33 kV
Maximum voltage increase in % when offshore farms connected.	No voltage increase	1.13 %	1.1%
Location of maximum voltage rise.	-	RHYL C1	RHYL E1 RHYL E2
Number of Nodes with voltage increase of 0.5 % or more	-	12	32
Number of nodes higher than 1.1 PU	5	1	-
Number of Overloaded Circuits	-	1	-
Total Real Power Loss (MW) – no offshore farms	194.5 MW 135 MVAR 201.936MW 182.966 MVAR $P_{\text{NET LOAD}} = 561 - 99* = 462 \text{ MW}$ $Q_{\text{NET LOAD}} = 147.1 + 53* = 200.1\text{MVAR}$ $P_{\text{NET LOAD}} = 561 - 257.55* = 303.45\text{MW}$ $Q_{\text{NET LOAD}} = 147.8 + 53* = 200.8\text{MVAR}$		
Total Reactive Power Loss (MVAR)– no offshore			
Total Real Power Loss (MW)– offshore farms connected			
Total Reactive Power Loss (MVAR) – offshore farms connected.			
Total network real load in MW – no offshore farms. (The '*' value represents distributed generation)			
Total network reactive load in MVAR– no offshore farms. (The '*' value represents distributed generation)			
Total network real load in MW – offshore farms connected. (The '*' value represents distributed generation)			
Total network reactive load in MVAR– offshore farms connected. (The '*' value represents distributed generation)			

Table 6.3.3: Summary of the loadflow studies for minimum summer load condition (Use of doubly-fed induction generators - no reinforcements)

Voltage Level	400 kV	132 kV	33 kV
Maximum voltage increase in % when offshore farms connected.	No Voltage increase	1.3 %	1.0%
Location of maximum voltage rise.	-	RHYL C1	RHYL E1 RHYL E2
Number of Nodes with voltage increase of 0.5 % or more	-	12	22
Number of nodes higher than 1.1 PU	-	-	-
Number of additional overloaded circuits	-	4	-
Total Real Power Loss (MW) – no offshore farms	206 MW 365 MVAR 208.756 MW 356.63 MVAR $P_{\text{NET LOAD}} = 1650 - 98.9* = 1551.59 \text{ MW}$ $Q_{\text{NET LOAD}} = 436 + 50.2* = 486.2 \text{ MVAR}$ $P_{\text{NET LOAD}} = 1652 - 260.54* = 1391.5 \text{ MW}$ $Q_{\text{NET LOAD}} = 436 + 50.86* = 486.86 \text{ MVAR}$		
Total Reactive Power Loss (MVAR)– no offshore			
Total Real Power Loss (MW)– offshore farms connected			
Total Reactive Power Loss (MVAR) – offshore farms connected.			
Total network real load in MW – no offshore farms. (The ‘*’ value represents distributed generation)			
Total network reactive load in MVAR– no offshore farms. (The ‘*’ value represents distributed generation)			
Total network real load in MW – offshore farms connected. (The ‘*’ value represents distributed generation)			
Total network reactive load in MVAR– offshore farms connected. (The ‘*’ value represents distributed generation)			

Table 6.3.4: Summary of the loadflow studies for peak winter load condition
(Use of doubly-fed induction generators - no reinforcements)

6.3.2 Fault Level studies:

The following fault level studies were carried out for both minimum summer loading and peak winter loading for this generation type as follows:

- Minimum summer loading: Three-phase asymmetrical peak fault level calculation at each busbar at 10ms (switchgear make duties) and asymmetrical RMS at 100ms (break duties).
- Minimum summer loading: Single line to ground asymmetrical peak fault level calculation at each busbar at 10ms (switchgear make duties) and asymmetrical RMS at 100ms (break duties).
- Peak winter loading: Three-phase asymmetrical peak fault level calculation at each busbar at 10ms (switchgear make duties) and asymmetrical RMS at 100ms (break duties)
- Peak winter loading: Single line to ground asymmetrical peak fault level calculation at each busbar at 10ms (switchgear make duties) and asymmetrical RMS at 100ms (break duties).

The network fault level results of the minimum summer loading condition for both fault types have higher values than the winter peak condition. This is specially the case for the 132kV network, due to the generally higher pre-fault voltage level for the minimum summer loading condition.

Therefore, the minimum summer loading condition results are compared before and after the connection of the farms.

Voltage Level	400 kV	132 kV	33 kV
Maximum three phase fault level increase in % at 10ms, as a result of offshore farms connected. (PEAK VALUES)	1.2 %	16 %	6.04%
Maximum single-line-to-ground fault level increase in % at 10ms, as a result of offshore farms connected. (PEAK VALUES)	1.1 %	10.1 %	2.45%
Maximum three phase fault level increase in % at 100ms, as a result of offshore farms connected. (ASYMMETRICAL RMS VALUES)	0.4%	11.9 %	4 %
Maximum single-line-to-ground fault level increase in % at 100ms as a result of offshore farms connected. (ASYMMETRICAL RMS VALUES)	1.1 %	8.78 %	2.11%

Table 6.3.5: Summary of the fault level studies for minimum summer load condition
(Use of doubly-fed induction generators - no reinforcements)

As seen from Table 6.3.5 the main affected voltage level is the 132kV with a sizable fault level currents increase in a number of the local substations in this voltage level for the initial fault currents. Local 132kV substations can handle the fault level increase when a single SGT is connected at Pentir. However the fault level increase will put limitation on the operation of the network with regard to the connection of both Pentir Super grid transformers (SGTs) as the three-phase fault level peak values for minimum summer loading at 10 ms at 'St Asaph' is critically close to switchgear make rating, which are rated 2492RMS MVA, 6230 Peak MVA and 137MVA continuous. The protection time and current grading and/or settings also need review to insure the correct sequence of operation for both symmetrical and asymmetrical faults for the new configuration.

7 Comments on the Steady State Results

Three types of offshore wind farm turbine generator farm connections were analysed for load flow and fault level. Summary of the load flow and fault level results for each type is presented in section 6.

The variable speed synchronous generator connected via back-to-back static converters impact on the local 132kV system may not create a major problem as far as thermal overloads or increase in fault level as simplified analysis suggests the converters overload protection will switch the converters off. Transient analysis calculations are needed to simulate the behaviour of the converter controllers and its effects on the converter contribution before arriving to a final conclusion.

It must be mentioned that the connection caused an increase in the real power loss of 2.45MW at peak winter load and 7.3MW at minimum summer load. The effect on the reactive power loss was mixed, for minimum summer load there was an increase in the network losses of 47MVAR while there was a reduction in the reactive power losses of 9.5MVAR for the peak winter load condition. The variation of losses is due the shift of the pole of generation due to the offshore generation connection.

The fixed speed induction generator type without reinforcements presents a number of technical problems. The main one the high reactive power consumption with the associated increase in the flows and its problems such as increase in active loss between 10MW at minimum summer loading and 6MW for peak winter loading condition. The reactive power loss jumped by 77MVAR for minimum summer loads and 35MVAR for peak winter loads. The high increase in reactive power demand causes some drop in the voltage of 1.1% at the local 'RHYL C1' 132kV substation. This is of course will improve if capacitive compensators are used.

The fault level analysis presented an increase in the initial half-cycle peak values for symmetrical faults (make duties) of 22% at the local 132kV substation. The maximum increase for the initial peak asymmetrical line-to-ground faults is 11% for the same substation. While the switchgears can handle this increase if one of the two super grid transformers at Pentir is open, the peak value exceeds at substation 'St Asaph' the make duties when both transformers are connected. As the contribution from the induction generators is decaying to zero at steady state the increase in the break values is not critical.

The doubly fed induction generator off-share wind farm alternative presents fewer technical problems. The losses in the network increased by 7.4MW for minimum summer loading and 2.7MW for peak winter loading. The effect on the reactive power loss was mixed, for minimum summer load there was an increase in the network losses of 45.9MVAR while there was a reduction in the reactive power losses 9.37MVAR for the peak winter load condition.

The fault level analysis presented an increase in the initial half-cycle peak values for symmetrical faults (make duties) of 16% at the local 132kV substation. The maximum increase for the initial peak asymmetrical line-to-ground faults is 10.1% for the same substation. The increase in local 132kV substations is critically close to the make duties rating for 'St Asaph' substation. The maximum increase for the asymmetrical RMS values for three-phase faults at 100ms is 11%.

8 Stability Connection Studies for Wind farms with Synchronous Generators:

From Figure 4.2 it is clear that the synchronous generator configuration has three main elements with significant influence in the dynamic analysis, namely: the synchronous machine, the machine and turbine governor and automatic voltage regulators, and thirdly the converters with their controllers. The first three sections discuss briefly the dynamic modelling each of these elements. This is followed by the transient stability studies for the system using the synchronous generator option.

8.1 Synchronous Machine:

Although the synchronous machines used for offshore wind farms have many special design features, the conventional direct and quadratic axis synchronous machine models can be used to represent the output of these generator sets. In modelling terms, the following must be considered:

- Machine rotational speeds are normally expected to change by no more than 1% for grid connection increasing to perhaps 10% for islanded systems. Therefore, machine saturation and variations in parameters must be considered.
- Whereas normally the dynamic behaviour of synchronous machines are based on known output power and prime mover torque/speed characteristics, for wind energy systems the torque and speed are functions of wind velocity. Therefore, it may be necessary to consider special turbine/governor models for simulation of dynamic performance of wind energy systems.

Direct and quadrature axis synchronous machine models based on the above assumptions yield accurate modelling for transients arising from faulted or operational switching conditions. Under these conditions, wind turbine-generator sets, can be modelled by an equivalent conventional synchronous machine model.

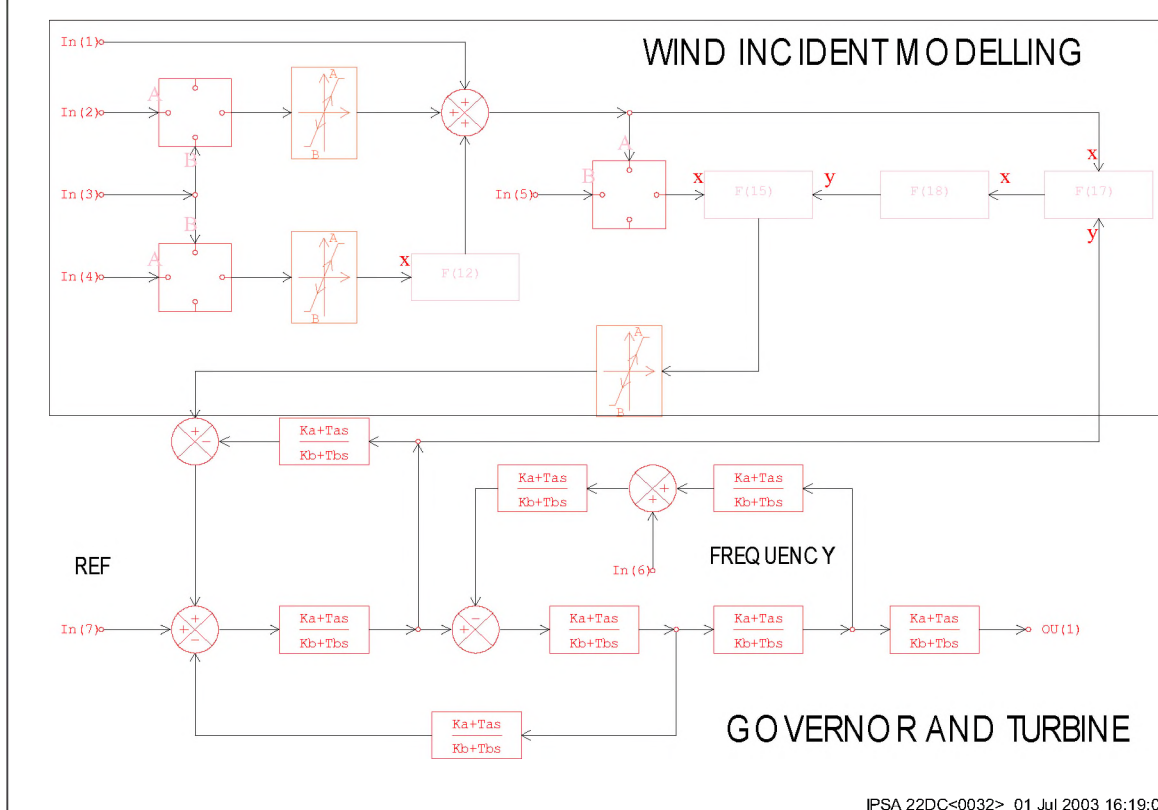
Typical data for synchronous machines are used for Offshore Farm 1 and are presented in Table 6.1.1. The farm will have 3 rows of 10 turbine-generator sets. Each set will have its own back-to-back converter set and a step up transformer (33/0.69kV, 2.2MVA and impedance of 7%). The network model configuration is shown in Figure 4.2

Similarly, typical data for synchronous machines are used for 'Offshore Farm 2' and are presented in Table 6.1.2. The farm has 3 rows of 10 turbine-generator sets. Each set has its own back-to-back converter set and a step up transformer (33/1.0kV, 3.4MVA and impedance of 8.3%) with the same basic network configuration. Figure 6.1 presents the single line diagram illustrating the connection of the two farms into the 132kV network.

8.2 Wind Turbine and Governor:

The turbine/governor is modelled using the IPSA 'User Defined Models' program to represent the special wind requirements. The turbine and governor section accommodates a frequency input, simulation of damping and the gear train etc. The reference signal is set automatically to balance the initial wind and frequency input against the set power output.

An example of a typical user defined controller for a combined wind turbine and governor model with simulation of the wind incident is shown in Figure 8.1. This controller can also be used with Induction Generators models.



IPSA 22DC<0032> 01 Jul 2003 16:19:07

Figure 8.1 Example of the combined wind turbine, governor and wind incident model.

This model is split into two parts. The upper part of the block diagram represents the wind incident part of the model. The limiter at the top allows a linear change in the wind velocity with time, up to a set limit, to be simulated. The lower branch can model wind gusting to any user-selected pattern.

The lower part represents the turbine and governor section, which includes a frequency input, simulation of damping and the gear train etc.

As the wind incident varies with location and time, the effect on the turbine depends upon a number of mechanical design factors beyond the scope of this work. Therefore, simplified governor turbine models have been used for the analysis in this report.

8.3 Converters:

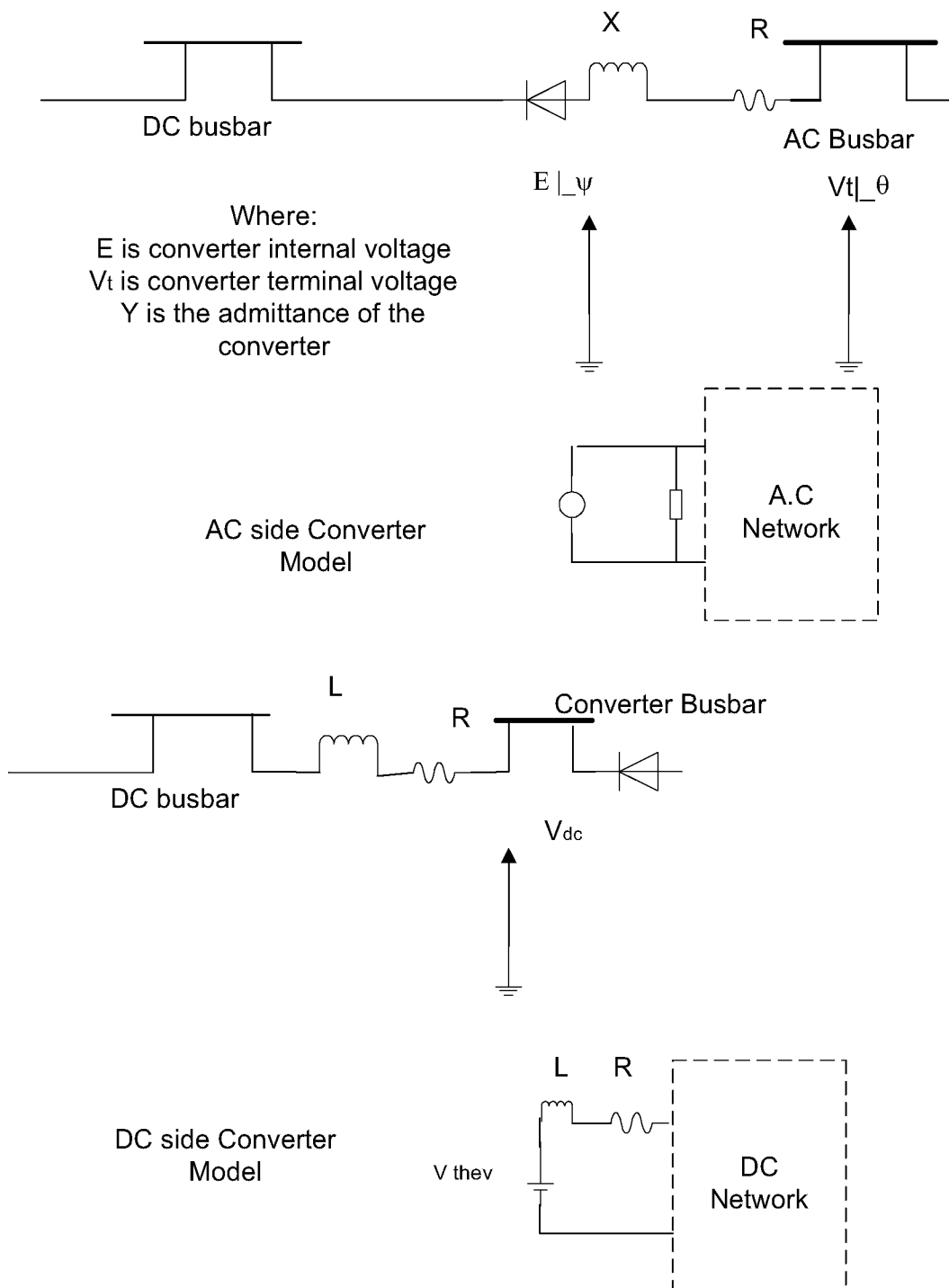


Figure 8.2 Single line diagram of back-to-back converter model.

8.4 Transient Analysis of Fault at The Local Network:

In this section transient stability analysis of the offshore farms (shown in Figure 6.1) is presented. The wind farms are modelled in the analysis with synchronous machines with their controllers behind back-to-back converters. Each wind farm is presented with an equivalent generator and transformer for a set of 30 synchronous generators. Each is connected in series with its own step up transformer and a converter equivalence set for each wind farm is also presented.

a) Transient analysis for a fault at the local 33kV node (busbar 'OFSW33'):

In this analysis the effect of a fault applied at the converter busbar 'OFSW33' at $t = .05\text{secs}$ and cleared at $.15\text{secs}$ is presented. Figure 8.3 shows the transient stability graphs over time for AC voltages, active and reactive power of the converters and frequency deviation.

The analysis shows that for faults at 'OFSW33' the over-current converter protection for the 100MW wind farm operated at 80ms. Disconnection of the farm caused the frequency to decrease for a short time.

The fault flow at the converters of 'Offshore farm 2' initially was 125% of the farm rated current with an increased reactive power flow and reduced active power flow. The flow reactive power flow is reduced after approximately 10ms but the windfarm remained connected to the system (see Figure 8.3).

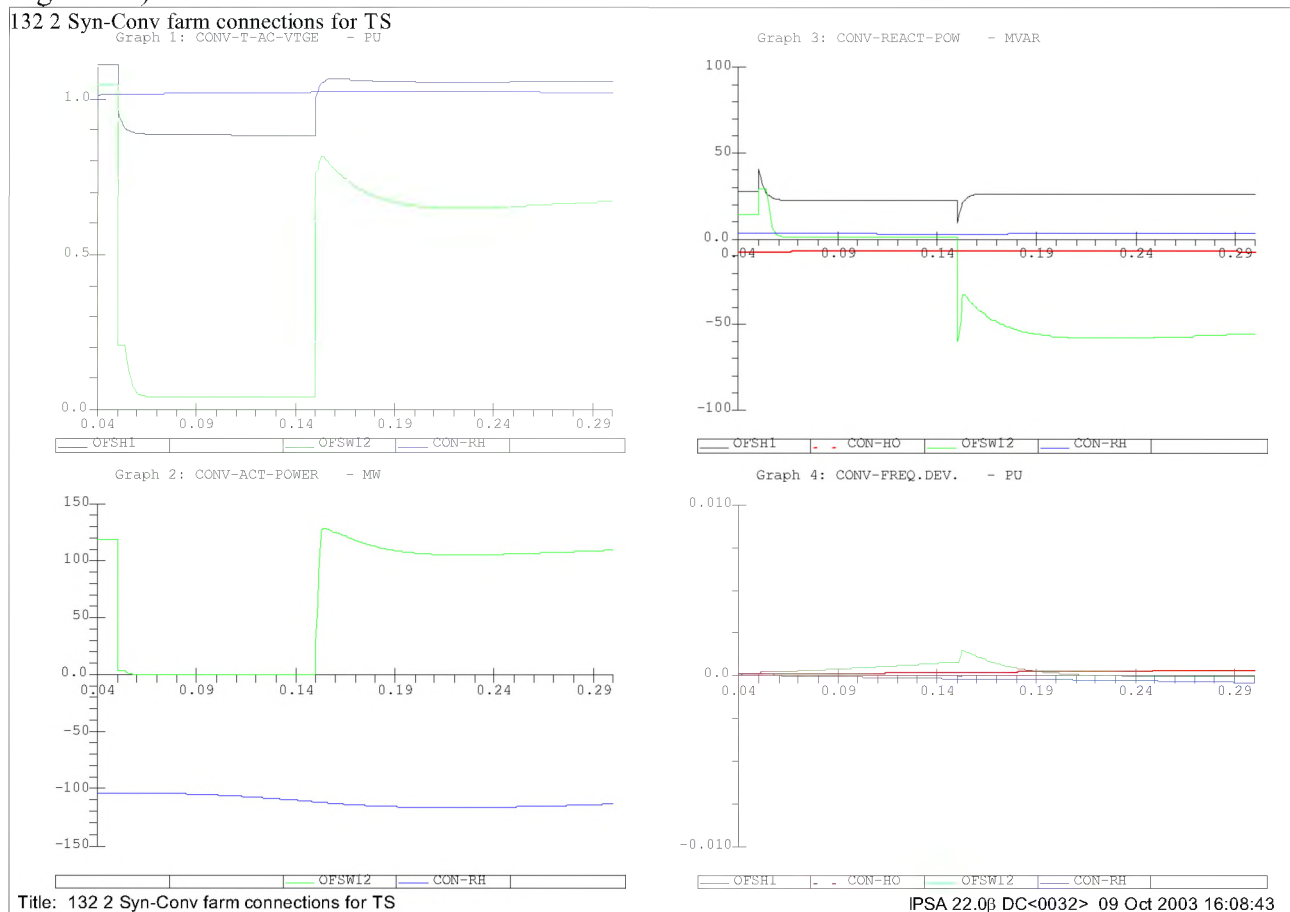


Figure 8.3 Transient results for a fault at 33kV busbar of the converter transformer at 'Offshore windfarm 1' (busbar 'OFSW33')

b) Transient analysis for a fault at the local 132kV network (busbar 'HOLY C2'):

In this analysis the effect of a fault applied at the converter busbar 'HOLY C2' .05secs and cleared at 0.15secs is presented. Figure 8.4 shows the transient stability graphs over time for AC voltages, active and reactive power of the converters and frequency deviation.

The analysis shows that for faults at 'HOLY C2' converter protection for the 60MW farm operated at 100ms. Disconnection of the farm caused the frequency to decrease for a short time.

The fault flow at the converters of 'Offshore farm 2' initially was 120% of the farm rated current with an increased reactive power flow and reduced active power flow. The flow of reactive power flow is reduced after less than 10ms. The windfarm remained connected to the system (see Figure 8.4).

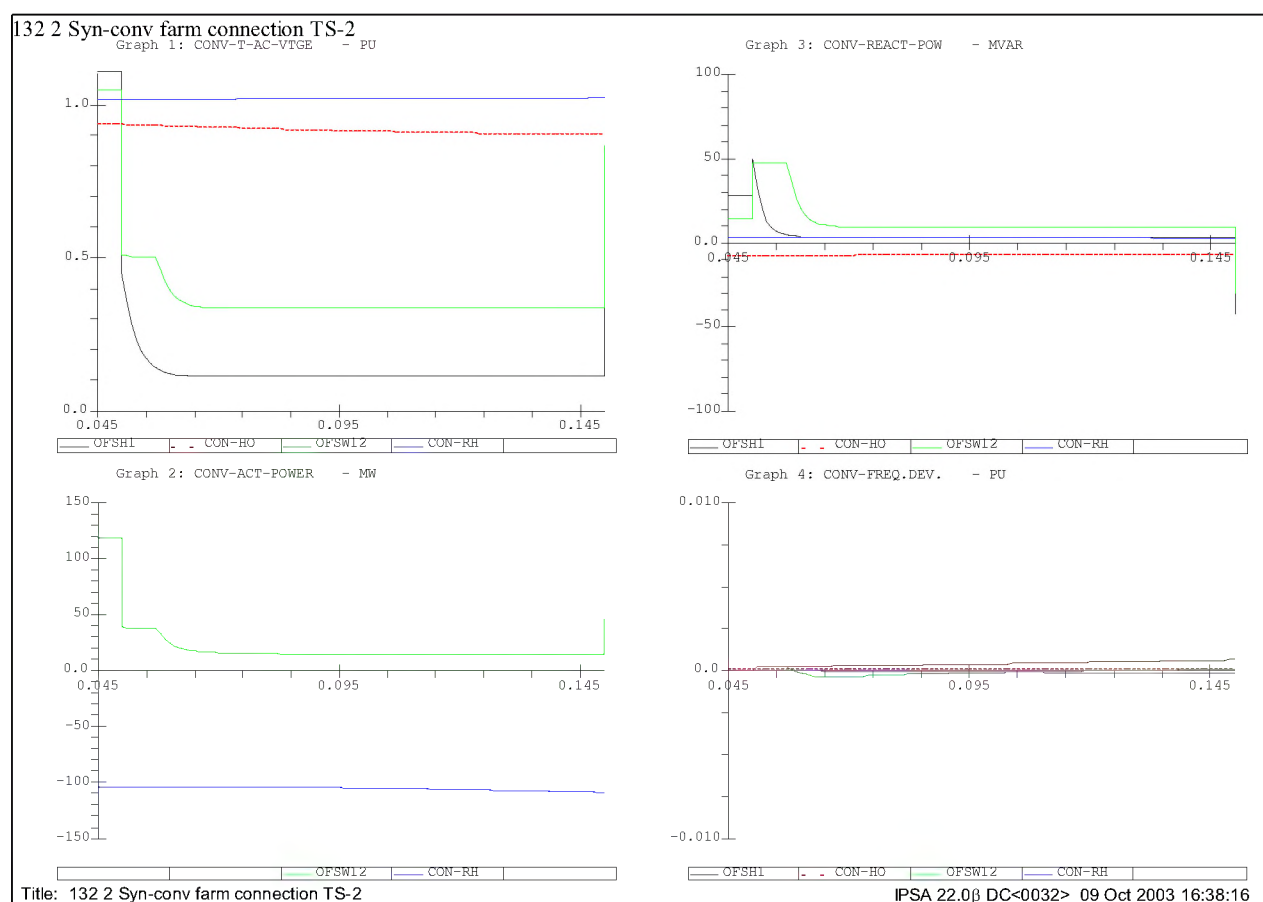


Figure 8.4 Transient results for a 132kV busbar fault at busbar 'HOLY C2'.

8.5 Comments on the Variable Speed Generator dynamic Results:

Section 8.4 presents the transient stability analysis for the variable speed synchronous generator connected via back-to-back static converters to the network. Two faults are investigated in details using transient, one at the local 33kV busbar (OFSW33) and the other is in the local 132kV network (busbar 'HOLY C2').

Transient analysis calculations showed that for a fault in the local 33kV to 'Offshore windfarm 1' the fault caused the converter protection to isolate the whole farm while 'Offshore windfarm 2' continues to operate. A fault at local 132kV network caused the converter overload protection at 'Offshore windfarm 2' wind farm to be switched off the network as flow exceeds overloading setting of the protection. The impact on the local 132kV network may not create a major problem as far as thermal overloads or increase in fault level.

The fault ride through capability is a problem for the network transmission operator. This action protects the windfarm and limits any overloads for the switchgears.

Section 7 of the G75/1 (Engineering recommendations for the connection of embedded generation plant to the public distribution systems above 20kV or with outputs over 5MW) recommends that any 'Offshore Wind Farm' connection should allow the full MVA capacity to be exported to the Distribution System at all times of the year and after one outage. If a firm connection is required, it shall be achieved by installing at least two connections between the 'Offshore Wind Farm' and the Major Busbar. It is in the interest of Generators, DNOs, and the TSO, to maintain system stability of generation within limits of Generating Plant capability during network disturbances and disconnect reliably for true "loss of mains" situations. As some forms of loss of mains protection may not achieve the required level of discrimination. However, if the wind farm disconnects itself when a fault occurs on the transmission system then the integrity of the transmission system can be undermined as the lost generation can exceed the amount of spinning reserve.

9 Transient Stability Connection Studies for Wind farms with Fixed Speed Induction Generators:

From Figure 4.3 fixed speed induction generator configuration has two main elements with influence in the dynamic analysis, namely the machine and the machine controllers (governor and turbine and automatic voltage regulators). In this section, details of the Induction generator parameters are given followed by transient stability studies for the system using the fixed speed induction generator.

Presently, the induction generator controllers are not fully represented in the IPSA software. For this reason the turbine input power assumed to remain constant during any network transient.

9.1 Fixed Speed Induction Generators:

Typical data for the ‘Offshore windfarm 1’ induction generators are presented in Table 6.2.1. The windfarm has 3 rows of 10 turbine-generator sets. Each set has its own step up transformer to 33kV (33/0.69kV, 2.2MVA and impedance of 7%). The network model configuration is as seen in Figure 4.3

Similarly, typical data for induction generators are used for ‘Offshore Farm 2’ are presented in Table 6.2.2. The farm has 3 rows of 10 turbine-generator sets. Each generator has its step up transformer (33/1.0kV, 3.4MVA and impedance of 8.3%) with the same basic network configuration. Figure 6.2 presents the single line diagram illustrating the connection of the two farms into the 132kV network.

Although the induction generators used for offshore wind farms have many special design features, the conventional direct and quadratic axis induction machine models can be used to represent the output of these generator sets. In modelling terms, the following must be considered:

- Machine rotational speeds are normally expected to change by no more than 1% for grid connection, increasing to perhaps 10% for islanded systems. Therefore, machine saturation and variations in parameters must be considered.
- Whereas normally the dynamic behaviour of induction generators is based on known output power and prime mover torque/speed characteristics, for wind energy systems the torque and speed are functions of wind velocity. Therefore, it may be necessary to consider special turbine/governor models for simulation of dynamic performance of wind energy systems. Presently, the induction generator controllers are not fully represented in the IPSA software. For this reason the turbine input power assumed to remain constant during any network transient.

9.2 Transient Analysis of Faults at The Local Network:

In this section transient stability analysis of the offshore wind farms (shown in Figure 6.2) is presented. The wind farms are modelled in the analysis by induction generators with their governors. Each windfarm is modelled with three equivalent generators and their transformers. Each represents 10 induction generators and each is connected in series with its own step up transformer.

a) Transient analysis for a fault at the local 33kV node to ‘Offshore windfarm 1’:

In this analysis the effect of a fault applied the local 33kV busbar ‘OFSW33’ at $t = .05\text{secs}$ and cleared at $.4\text{secs}$ is presented. The results are presented in Figures 9.1 and 9.2.

The results show that for a fault at ‘OFSW33’ the initial contribution to the fault from the each set of induction generators is 1.16 per-unit, which is 310% of the full load current at a power factor of 0.1. As induction generators are not self-excited, the currents and voltages on the generator terminals decay to zero in less than 200ms. The generators accelerate from -2% slip to around -8% slip as the output active power decreases to zero with the voltage collapse.

For fault clearance at 400ms, on recovery of the generators terminal voltage, the inertia and slip will give a transient increase in real power to 58MW for each set of generators. This represents 175% of the full load power. This output reduces to the original full load output after 5 seconds.

The second windfarm (Offshore windfarm 2) output current and power actually decreases during the fault (see Figures 9.1 and 9.2).

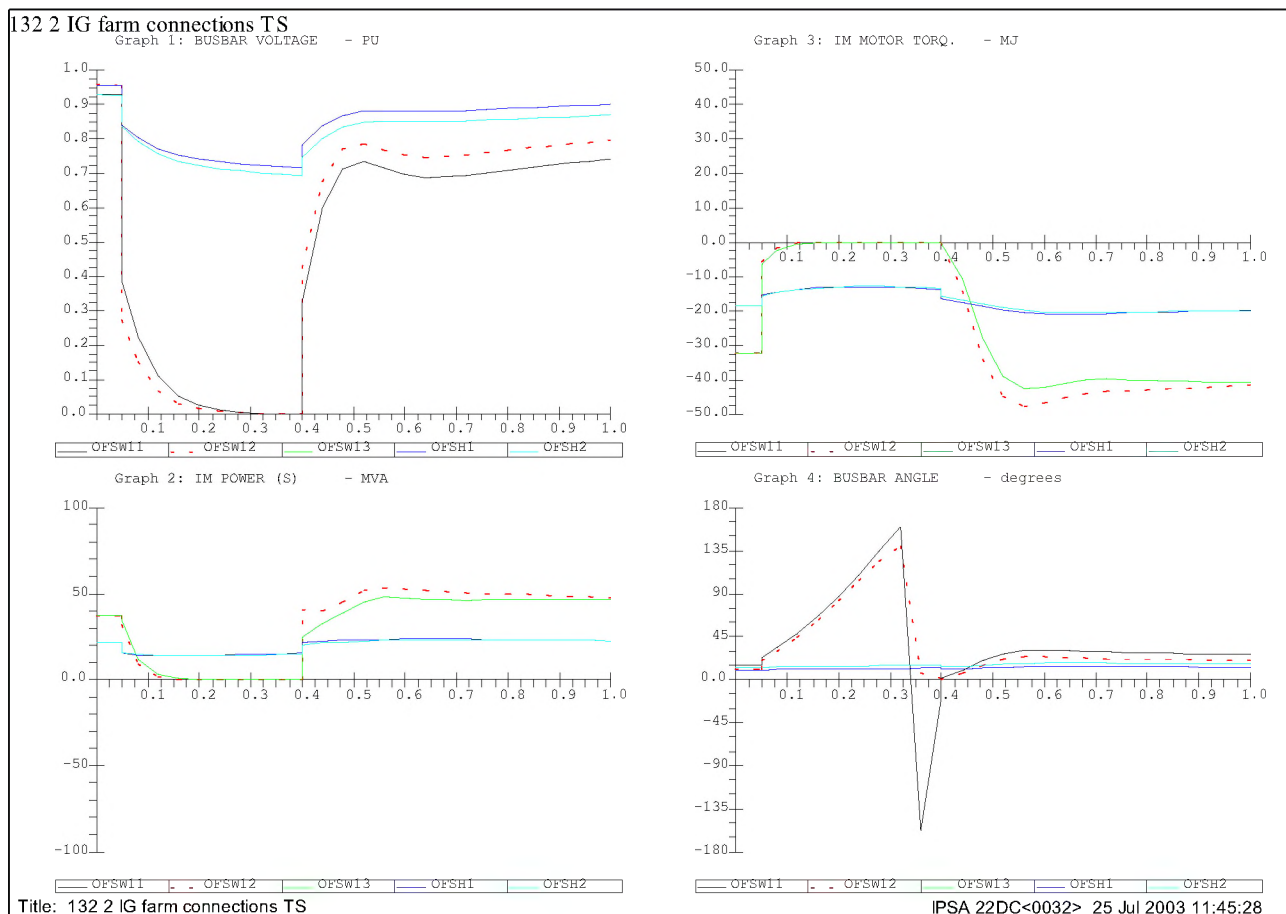


Figure 9.1: Transient stability study for a fault simulation and clearance at the local 33kV busbar (busbar ‘OFSW33’) connecting ‘Offshore windfarm 1’ for fixed speed IG - Busbar voltage in pu, generators MVA, torque in MJ and busbar angles in degrees.

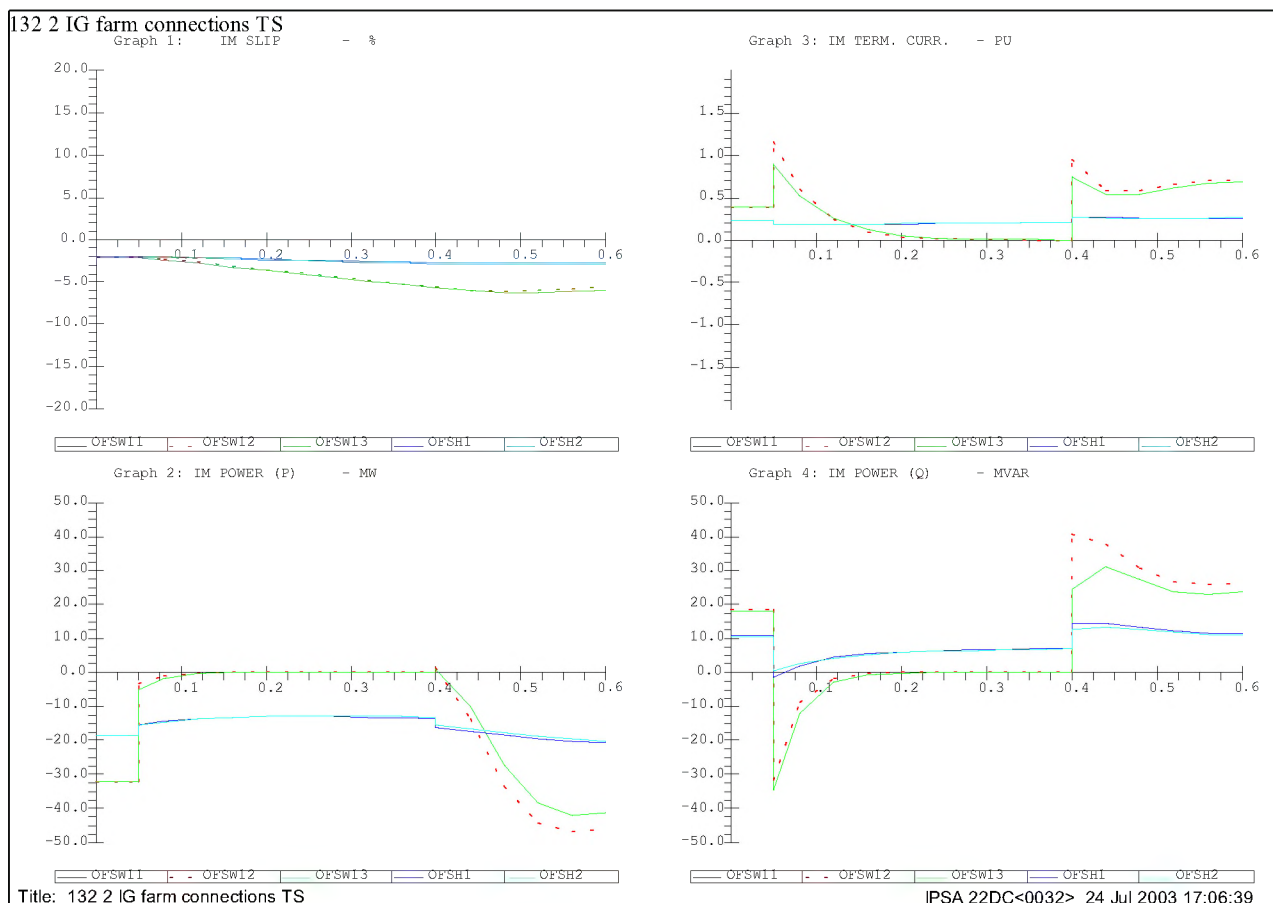


Figure 9.2: Transient stability study for a fault simulation and clearance at the local 33kV busbar (busbar 'OFSW33') connecting 'Offshore windfarm 1' for fixed speed IG- generator slips in %, real power in MW, terminal currents in pu and reactive power in MVAR.

b) Transient analysis for a fault at the local 132kV node (busbar 'HOLY C2'):

In this analysis the effect of a fault applied at the 132kV busbar 'HOLY C2' at .05secs from the start of the study and cleared at .4secs is presented. Figures 5.4 and 5.5 show the transient stability graphs over time for AC voltage, generators torque in MJ, power MVA, busbar angle in degrees, generators slip in %, real power MW, terminal currents in pu, and reactive power in MVAR.

The results show that for a fault at the local 132kV network (busbar 'HOLY C2') the initial contribution to the fault from the each set of induction generators is .58 per-unit, which is 290% of the full load current at a power factor of 0.1. As induction generators are not self-excited, the currents and voltages at the generator terminals decay to zero in less than 200ms. The generators accelerate from approximately -2% slip to -5% as the output active power decreases to zero with the voltage collapse. Obviously, this increase in the speed will be affected (reduced) if the generator turbine controller were to act to reduce the turbine input power within this period.

For fault clearance at 400ms, on recovery of the generators terminal voltage, the inertia and slip will give transient increase in real power to 48MW for each set of generators represents 145.5% of the full load power. The output reduces to the original full load output after 5 seconds.

The other windfarm (Offshore windfarm 1) output current and power actually decreases during the fault (see Figures 9.3 and 9.4).

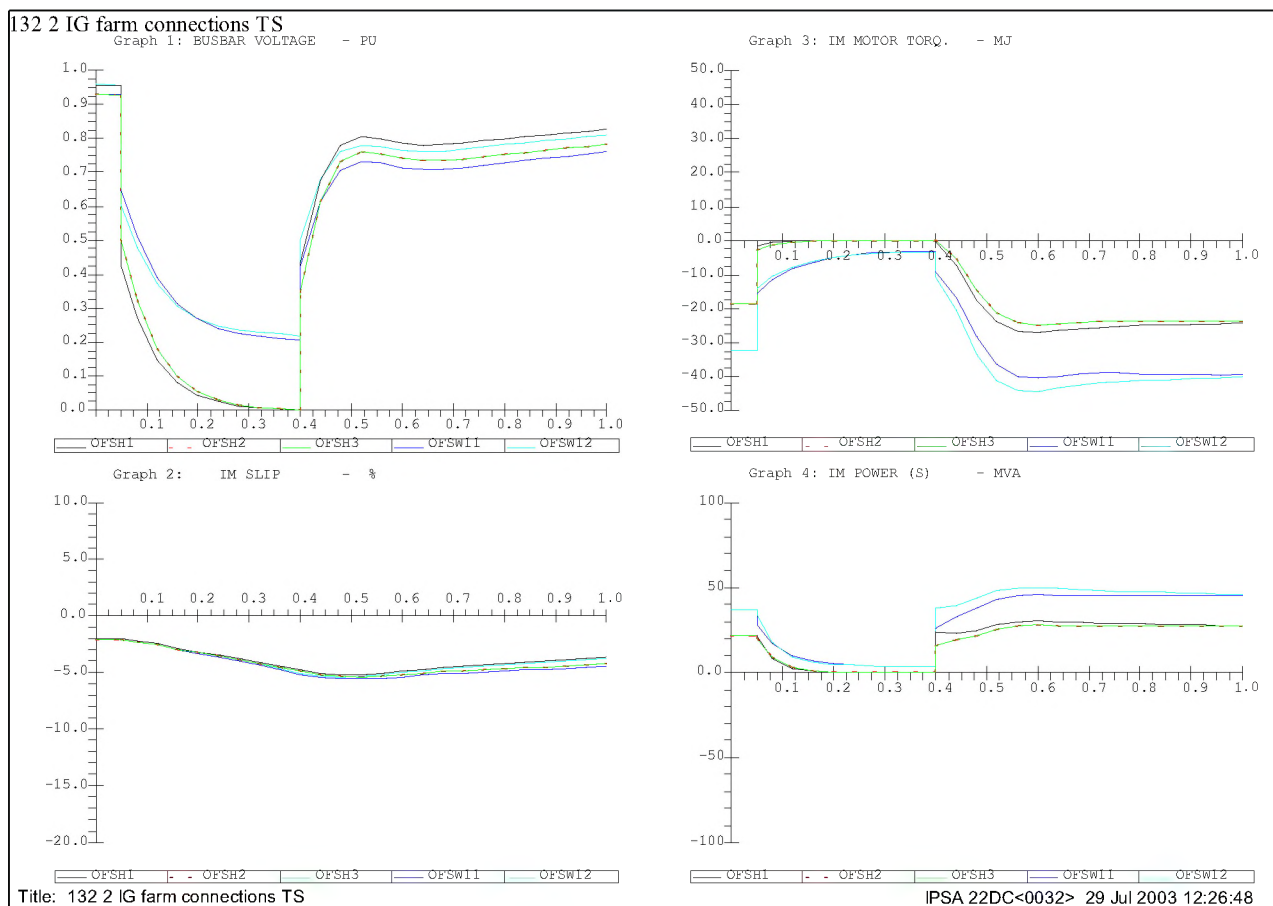


Figure 9.3: Transient stability study for a fault simulation and clearance at the local 132kV busbar (busbar 'HOLY C2') 'Offshore windfarm 2' for fixed speed IG - busbar voltage in pu, generators slip, torque and MVA.

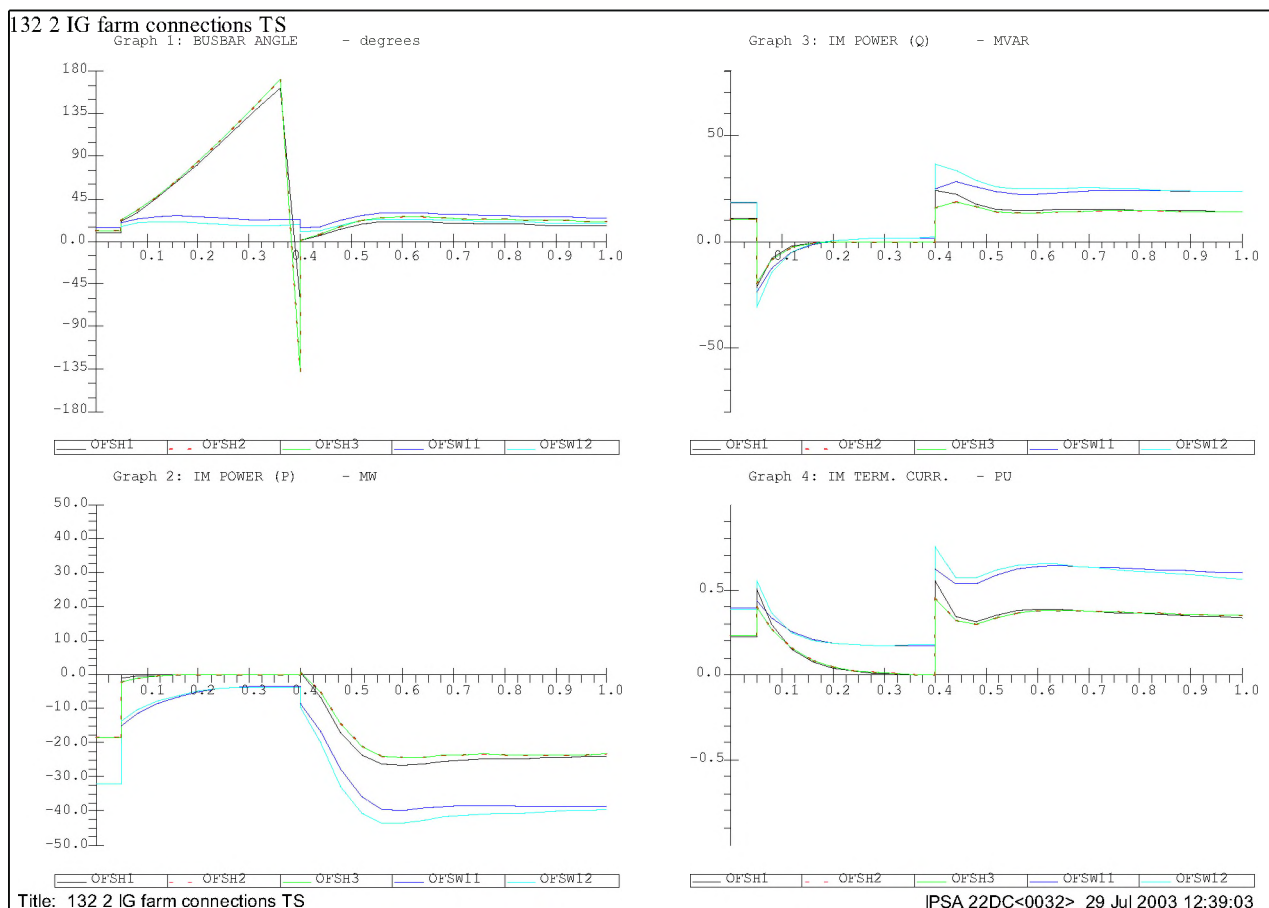


Figure 9.4: Transient stability study for a fault simulation and clearance at the local 132kV Busbar (busbar 'HOLY C2') 'Offshore windfarm 2' for fixed speed IG - Busbar angle in degrees, generators MW, generators MVAR and terminal currents in pu.

9.3 Comments on the Induction Generator Dynamic Results:

Section 9.2 presents the transient simulation of the behaviour of the fixed speed induction generator type under fault conditions. Two faults are investigated in details; one at the local 33kV busbar (busbar 'OFSW33') and the other is in the local 132kV (busbar 'HOLY C2') network.

For a fault in the local 33kV network of 'Offshore windfarm 1', since the induction generators are not self excited the voltage at the machine terminals drops to zero after 200 ms. The initial contribution of a set of 10 induction generators to the fault is 1.38pu this value decreases to zero as the voltage collapses. The 'Offshore windfarm 1' machines accelerate to a slip -8% for a fault duration of 350ms while the turbine controllers try to adjust the input power. The second windfarm 'Offshore windfarm 2' terminal voltage and power output decrease as a result of this fault.

For a fault at the local 132kV network the initial contribution to the fault from each windfarm is approximately 290% of its full load current and as the voltage drops the real power decreases causes an increase in the machines speed to an approximate slip of -5%.

When the fault is cleared, the initial generator terminal currents for both farms are 180% of the full load current, but decreases to 130% of the full load current in less than 300ms.

10 Transient Stability Connection Studies for Wind farms with Doubly-Fed Induction Generators (DFIGs):

From Figure 4.3, the Doubly Fed Induction Generator (DFIG) configuration has two main elements with significant influence in the dynamic analysis, namely: the machine and the machine governor and turbine and automatic voltage regulators.

While the effect of the injected currents from the back-to-back converters to the machines rotor windings in these studies are taken into consideration, the dynamic modelling details of the back-to-back converters and their controller connected to the rotor windings at reduced frequency are approximated.

Presently, the DFIGs controllers are not fully represented in the IPSA software. For this reason the turbine input power assumed to remain constant during any network transient.

10.1 DFIG Connection:

The dynamic analysis of the connection for offshore wind farms using DFIGs designed to be driven at variable speed from wind turbines and supplying the 132kV network is presented. Two back-to-back PWM voltage-fed converters connected between the stator and rotor allow for sub- and/or super-synchronous operation of each machine.

Figure 6.3 presents the single line diagram of the 132kV network section with the connection of the two DFIG offshore wind farms.

Typical data for the DFIGs used for ‘Offshore Windfarm 1’ are presented in Table 6.3.1. The windfarm has 3 rows of 10 turbine-generator sets. Each set has its own step up transformer to 33kV (33/0.69kV, 2.2MVA and impedance of 7%). The network model configuration is as seen in Figure 4.3

Similarly, data for induction generators used for ‘Offshore Windfarm 1’ are presented in Table 6.3.2. The windfarm has 3 rows of 10 turbine-generator sets. Each set has its own step up transformer (33/0.69kV, 3.4MVA and impedance of 8.3%) with the same basic network configuration.

10.2 Transient Analysis of Faults at the Local Network:

In this section transient stability analysis of the offshore wind farms (shown in Figure 6.3) is presented. The wind farms are modelled in the analysis with DFIGs. Each windfarm is modelled with three equivalent generators and their transformers. Each represents 10 DFIGs and each is connected in series with its own step up transformer.

For a DFIG, the optimal speed of the wind turbine at full load varies from synchronous speed to super synchronous speed of -12% slip. In order model the effect of the slip, three fault conditions are modelled. The first is for a fault in the local 33kV connecting busbar (busbar ‘OFSW33’) with DFIGs running at rated output power and speed. The second and the third are for a fault at the 132kV network (busbar ‘HOLY C2’) with DFIGs running at steady state rated power output at synchronous speed, and -12% slip respectively.

a) Transient analysis for a fault at the local 33kV node to ‘Offshore windfarm 1’ (busbar ‘OFSW33’):

In this analysis the effect of a fault applied at the local 33kV busbar ‘OFSW33’ at $t = 0.2$ secs from the start of the transient stability study and cleared at 0.4secs is presented. The results are presented in Figures 10.1 and 10.2.

The results show that for a fault on ‘OFSW33’ the initial contribution to the fault from each set of DFIGs is 1.46 per-unit. This represents 424% of the full load current at a power factor of 0.1. These currents decay to the full load current after 200ms of applying the fault. The generators accelerate from the synchronous speed to -2.2% slip as the output active power decreases as a result of the voltage collapse.

For fault clearance at 400ms(200ms after applying the fault), on recovery of the generators terminal voltage, the inertia and slip will give transient increase in real power to 40MW for each set of generators. This represents 121% of the full load power. The power output reduces to the original full load output after 5 seconds.

The change in output of the second windfarm (Offshore windfarm 2) over the fault duration is very limited. This is shown in a small decrease in the output of real power to 82% of full load, resulting in a transient increase in speed and a decrease of the generator power factor. The increase in the terminal current of this windfarm was limited to 7% (see Figures 10.1 and 10.2).

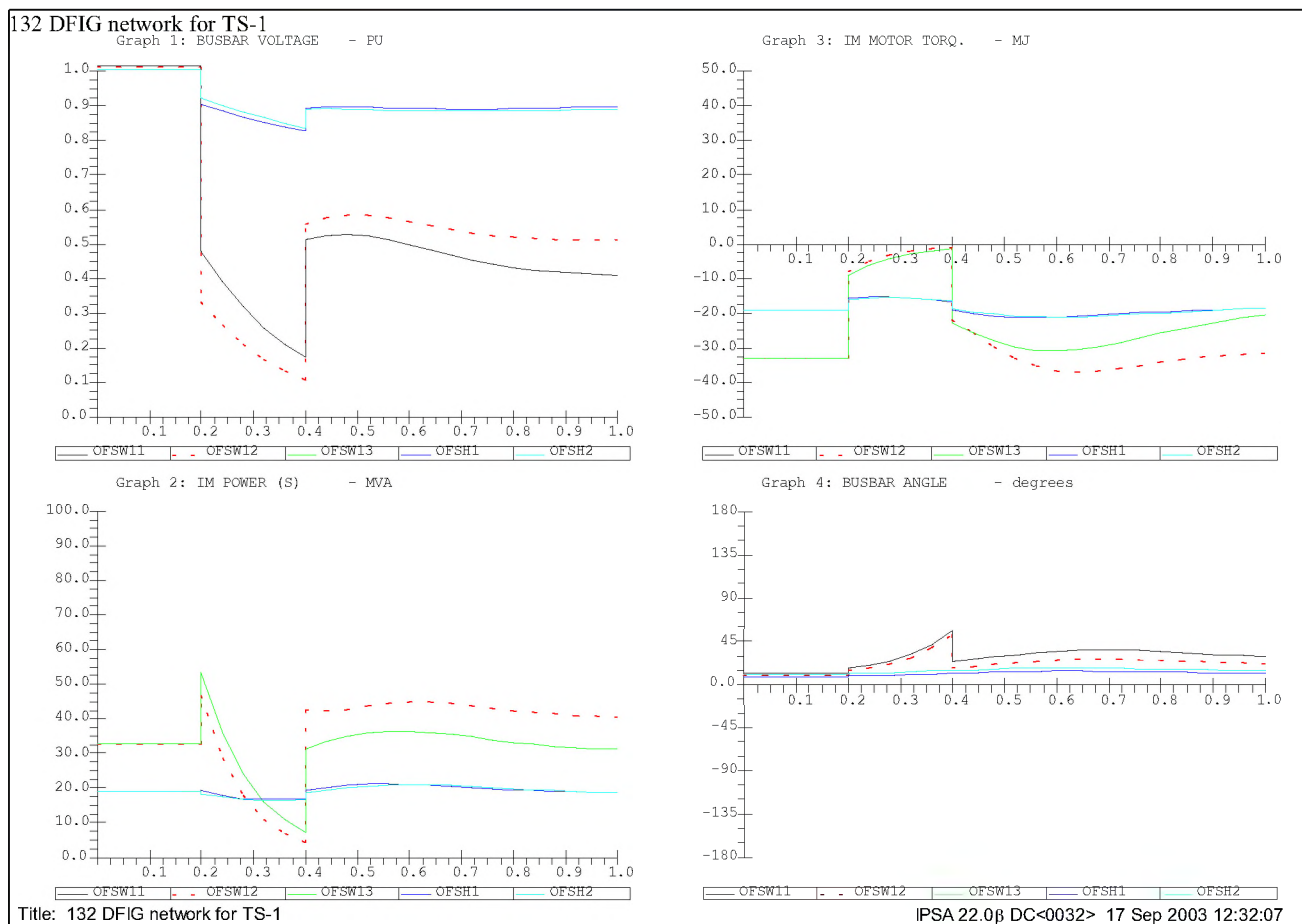


Figure 10.1: Transient stability study for fault simulation and clearance at the local 33kV busbar for ‘Offshore windfarm 1’ for DFIGs - busbar voltage in pu, Generators MVA, Torque and busbar angle.

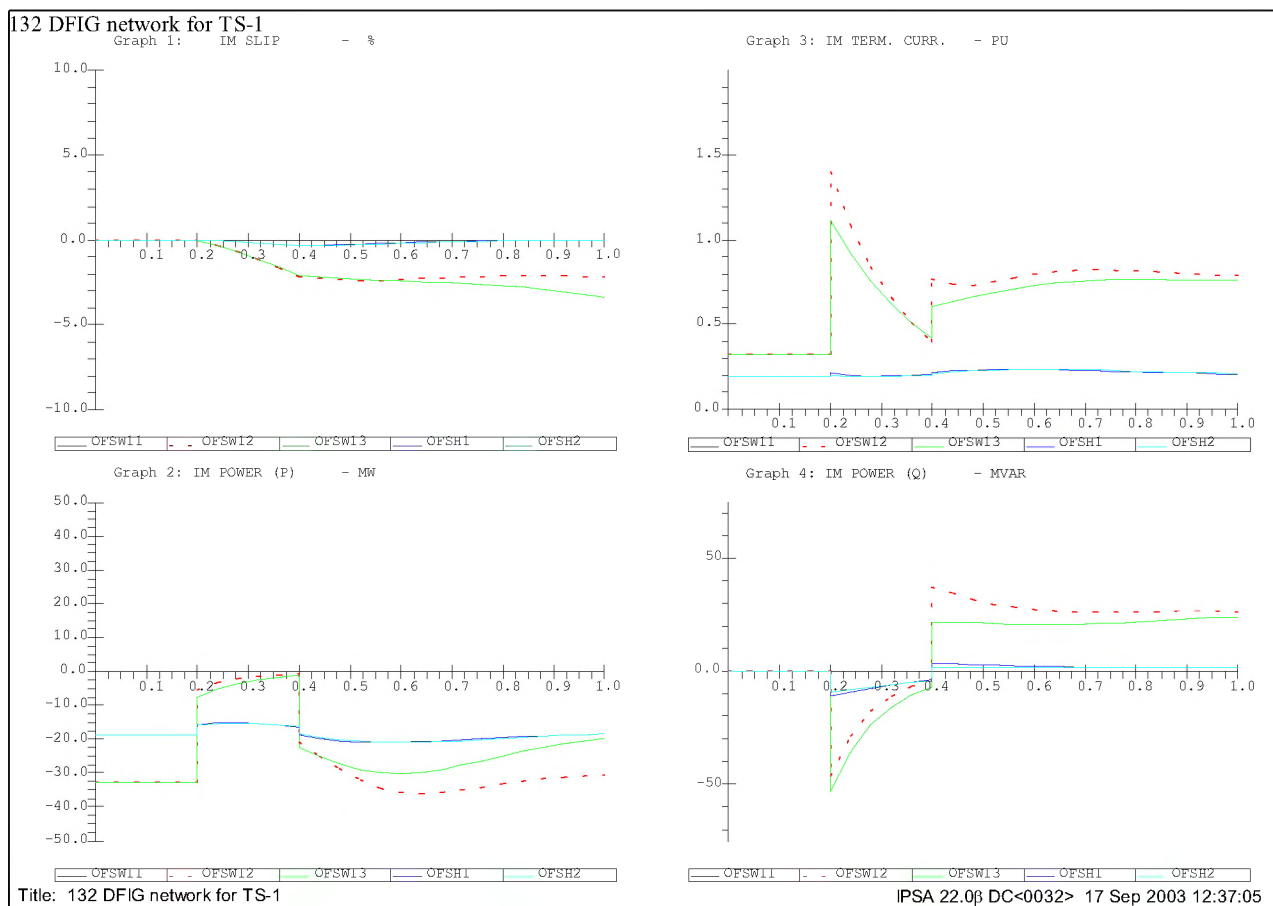


Figure 10.2: Transient stability study for fault simulation and clearance at the local 33kV busbar for 'Offshore windfarm 1' for DFIGs – generator slip, MW, terminal currents in pu and MVAR.

b) Transient analysis for a fault at the local 132kV node (busbar 'HOLY C2') (DFIGs steady state full load slip =0):

In this analysis the effect of a fault applied at the 132kV busbar 'HOLY C2' at .2secs from the start of the study and cleared at .4secs is presented. Figures 10.3 and 10.4 show the transient stability graphs over time for AC voltage, generators torque in MJ, power MVA, busbar angle in degrees, generators slip in %, real power MW, terminal currents in pu, and reactive power in MVAR.

The results show that for a fault in the local 132kV busbar for the 'Offshore windfarm 2' the initial contribution to the fault from the each set of the DFIGs is 0.46 and 0.75 per-unit respectively for sets in 'Offshore windfarm 2' and 'Offshore windfarm 1'. These represent 230% of the full load current at a power factor of 0.3. The currents at the DFIGs terminals decay to close to full load current after 200ms from applying the fault. The generators at 'Offshore windfarm 2' accelerate from the synchronous speed to -1% as the output active power decreases with the voltage collapse. Obviously, this increase in speed will be affected (reduced) if the generator turbine controller acted to reduce the turbine input power within this period.

For fault clearance after 200ms from applying the fault, the recovery of the generators terminal voltage, the inertia and slip will give transient increase in real power to 48MW for each set of generators represents 141% of the full load power. The power output reduces to the original full load output after 5 seconds.

The effect of the fault in the other windfarm (Offshore windfarm 1) is less. The increase in the terminal current of the wind farm is 170% of the full load. The results graphs are shown in Figures 10.3 and 10.4.

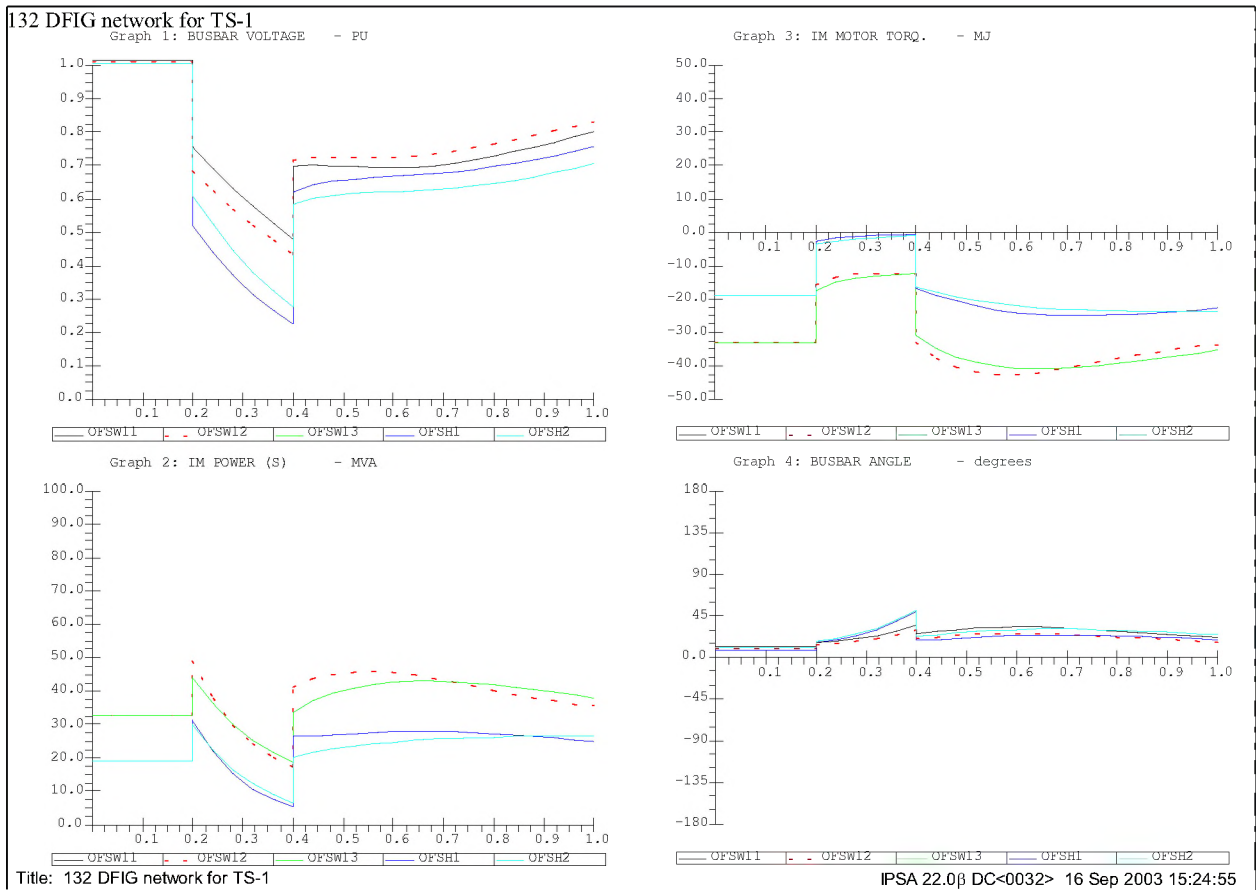


Figure 10.3: Transient stability study for fault simulation and clearance at the local 132kV busbar (HOLY C2) at 'Offshore windfarm 2' for DFIGs - busbar voltage in pu, Generators MVA, Torque and busbar angle (DFIGs steady state full load slip =0).

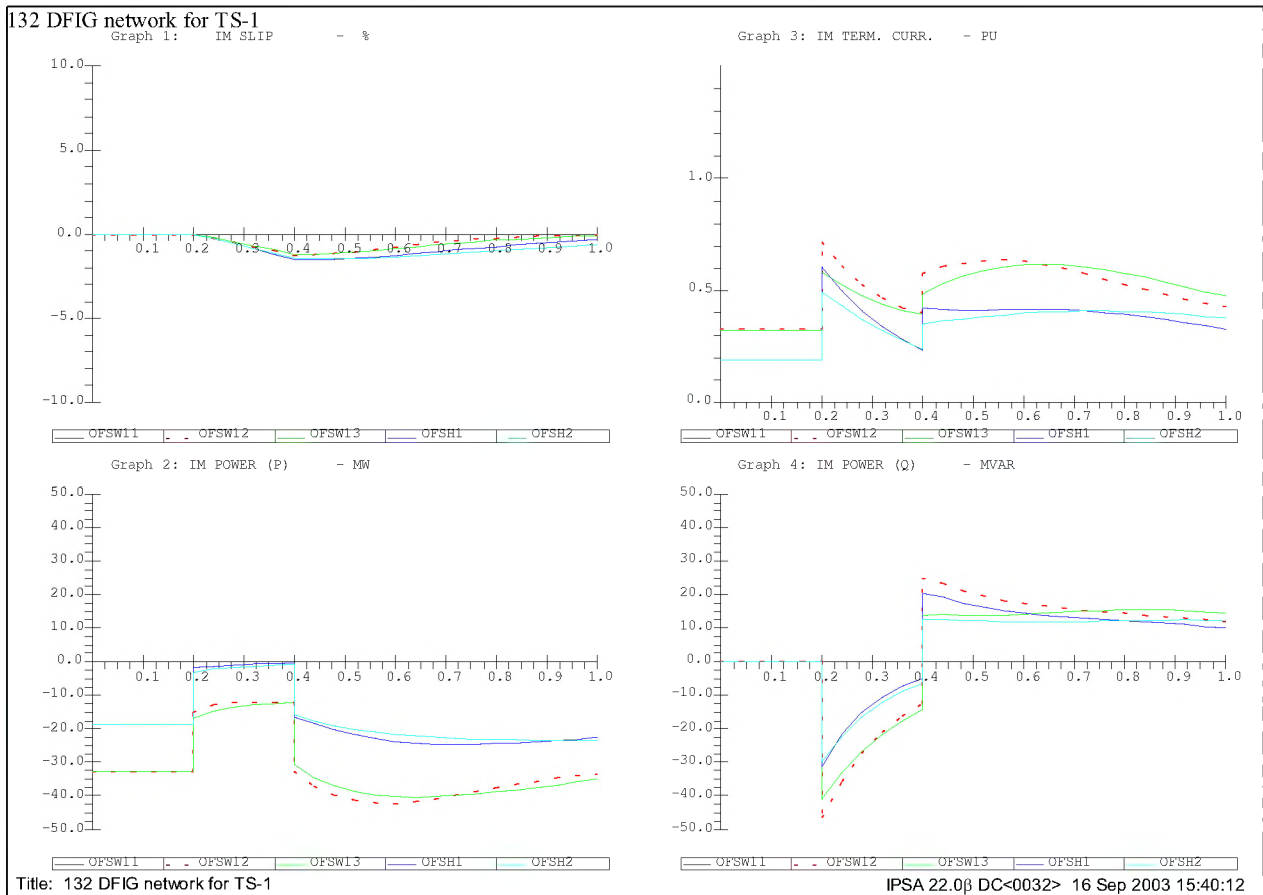


Figure 10.4: Transient stability study for fault simulation and clearance at the local 132kV busbar (HOLY C2) at 'Offshore windfarm 2' for DFIGs – generator slip, MW, terminal currents in pu and MVAR (DFIGs steady state full load slip =0).

c) Transient analysis for a fault at the local 132kV node (busbar 'HOLY C2') (steady state DFIGs full load slip =-12%):

In this analysis the effect of a fault applied at the 132kV busbar 'HOLY C2' at .22secs from the start of the study and cleared at 0.3secs is presented. Figures 6.6 and 6.7 show the transient stability graphs over time for AC voltage, generators torque in MJ, power MVA, busbar angle in degrees, generators slip in %, real power MW, terminal currents in pu, and reactive power in MVAR. The DFIGs running at steady state with full load slip is -12%.

The results show that for a fault in the local 132kV busbar for the 'Offshore windfarm 2' the initial contribution to the fault from the each set of the DFIGs is .56 and .73 per-unit respectively for sets in 'Offshore windfarm 2' and 'Offshore windfarm 1' represent 230% of the full load current at a power factor of 0.3. The generators at 'Offshore windfarm 2' accelerate from the synchronous speed to -1% as the output active power decreases with the voltage collapse. Obviously, this increase in speed will be affected (reduced) if the generator turbine controller acted to reduce the turbine input power within this period.

If the fault is cleared at 80ms, on recovery of the terminal voltage the generators inertia and slip will give transient maximum power of 75MW for each set of 10 generators at 'Offshore windfarm 2' represents 272% of the full load power. The output power decreases to the original full load output power after 5 seconds.

It must be mentioned here that if the fault duration under these condition is longer, and there is no AVR representation for the DFIGs. Then the voltage and power fluctuation may be higher and the results may not represent the actual response with DFIG controlled by AVR and governors.

The effect of the fault in the other windfarm (Offshore windfarm 1) is lesser with an increase in the current to 170% of the full load current. The graphs of other components are shown in Figures 10.5 and 10.6.

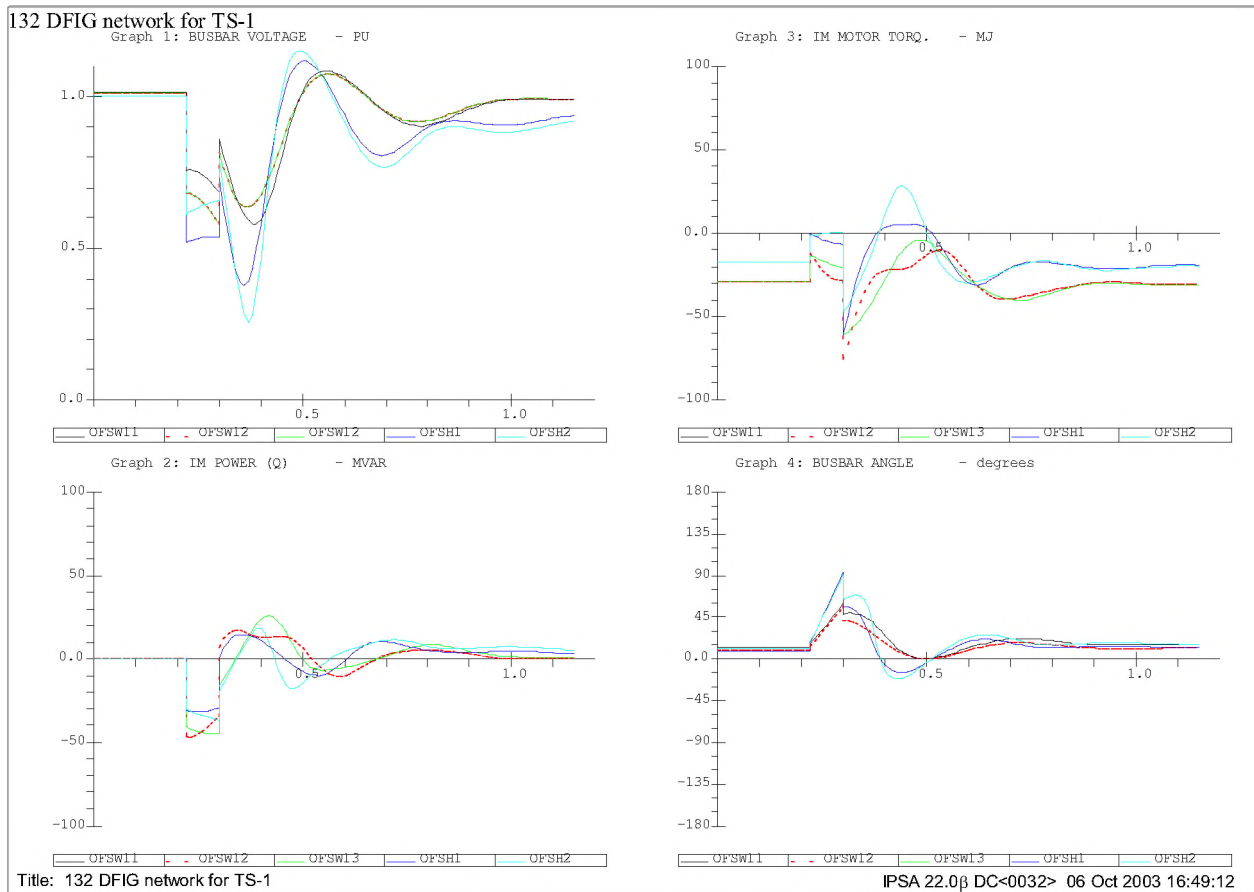


Figure 10.5: Transient stability study for fault simulation and clearance at the local 132kV busbar (HOLY C2) at 'Offshore windfarm 2' for DFIGs - busbar voltage in pu, Generators MVA, Torque and busbar angle. (DFIG full load slip= -12%)

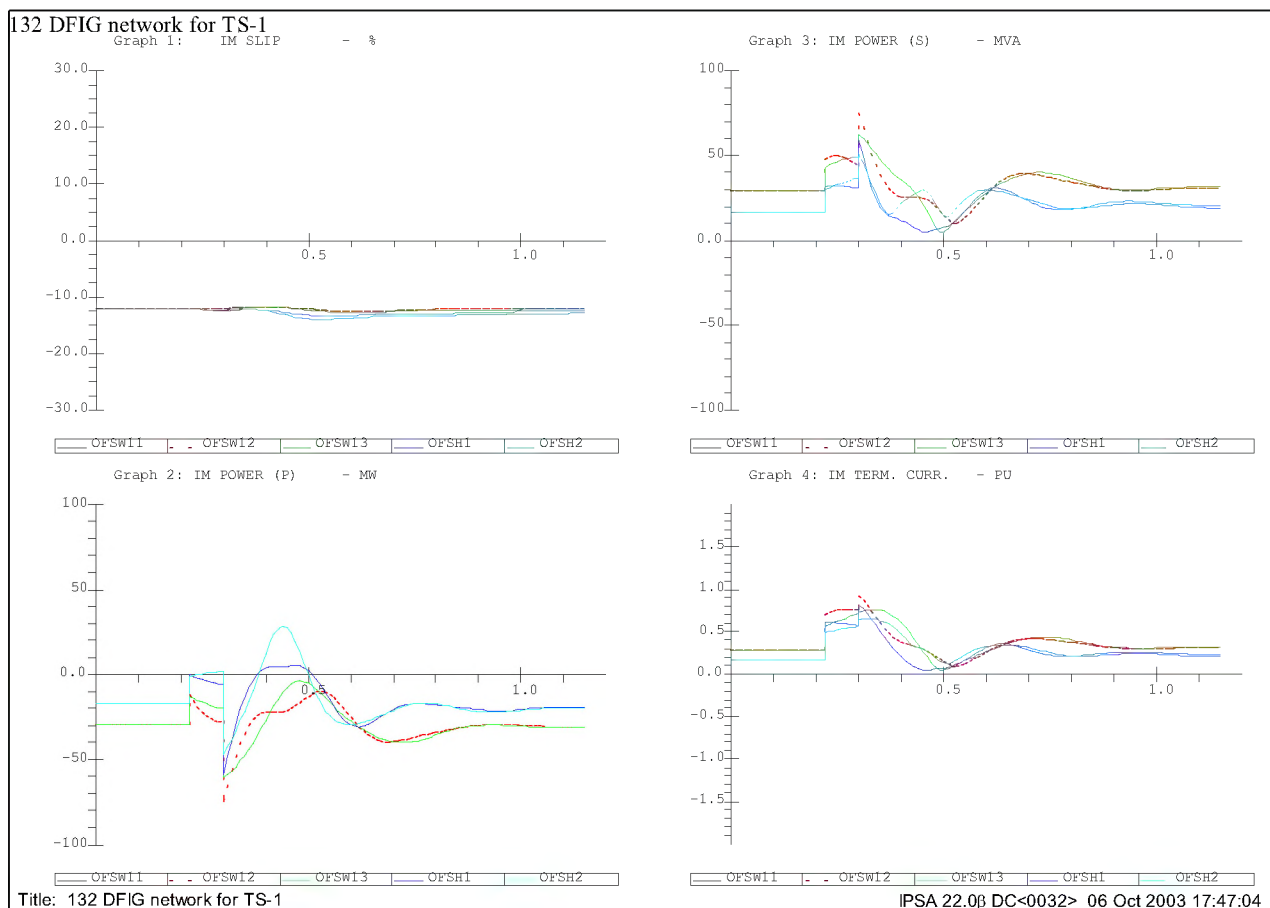


Figure 10.6: Transient stability study for fault simulation and clearance at the local 132kV busbar (HOLY C2) at 'Offshore windfarm 2' for DFIGs – generator slip, MW, terminal currents in pu and MVAR. (DFIG full load slip = -12%)

10.3 Comments on the DFIGs Results:

Section 10.2 presents the transient simulation of the behaviour of the DFIG type under fault conditions. The same two faults are investigated in detail; one at the local 33kV busbar (busbar 'OFSW33') and the other is in the local 132kV network (busbar 'HOLY C2').

For a fault in the local 33kV network of 'Offshore windfarm 1', the voltage at the machine terminals drops to .2pu after 200ms. The initial contribution of a set of 10 DFIGs to the fault is 1.46 per-unit. This represents 424% of the full load current (mainly reactive power) feeding the fault, and this value decreases as the voltage collapses. The 'Offshore windfarm 1' accelerates to a slip of -2.2% for a fault duration of 200ms. The changes in the second windfarm (Offshore windfarm 2) terminal voltage and power output are limited as a result of this fault. However on fault clearance 'Offshore windfarm 1' draws an initially high reactive power of 110% of rating. This depresses the terminal voltage to .9pu until the controllers react to adjust the power factor.

For a fault at the local 132kV network (full wind farm generation at synchronous speed), the initial contribution to the fault from each windfarm is approximately 230% of its full load current. The voltage drops causes the real power decreases and this causes an increase in the machines speed to an approximate slip of -1%. When the fault is cleared, the initial generator terminal currents for the

farms are 170% and 150% of full load current. This decreases to 110% of the full load in less than 300ms.

For a fault at the local 132kV network (full generation at -12% slip), the initial contribution to the fault from each windfarm is approximately 227% of its full load current and the real power decrease causes an increase in the machines speed to an approximate slip of -1% .

It is noted that the active and reactive power fluctuate more in this case. Therefore, with fault durations longer than 80ms, the modelling of DFIGs controllers (the AVR and governor) is important.

11 Comments on the Dynamic Results

Three types of offshore wind farm turbine generator connections have been analysed for transient stability. The results for each type are presented in sections 8 to 10.

It must be mentioned that in all cases, the generators are modelled with a set of three equivalent machines. Although, these generators are of a similar type and characteristics, it is inevitable that, with 30 turbines, they all will be at different power outputs and slips. The studies assumed that an approximate representation of the worst case condition is to consider that all the generators are at full load at the fault instant. This will maximize their initial fault contribution.

Section 8.4 presents transient stability analyses for the variable speed synchronous generator connected via back-to-back static converters to the network. Two faults are investigated in detail using transient simulation, one at the local 33kV busbar and the other in the local 132kV network.

Transient analysis calculations showed that for a fault in the local 33kV to 'Offshore windfarm 1' the fault caused the converter protection to isolate the whole farm while 'Offshore windfarm 2' continued to operate. A fault at local 132kV network caused the converter overload protection at 'Offshore windfarm 2' wind farm to operate as current flow exceeded the overloading setting of the protection. The impact on the local 132kV network may not create a major problem as far as thermal overloads or increase in fault level. However, the fault ride-through capability is a problem for the network transmission operator. This action protects the windfarm and limits any overload on the switchgear. However, if the wind farm disconnects itself when a fault occurs on the transmission system then the integrity of the transmission system can be undermined as the lost generation can exceed the amount of spinning reserve.

Section 9.2 presents the transient simulation of the behaviour of the fixed speed induction generator type under fault conditions. Two faults are investigated in detail; one at the local 33kV busbar and the other in the local 132kV network.

For a fault in the local 33kV network of 'Offshore windfarm 1' since the induction generators are not self excited the voltage at the machines terminals drops to zero after 200 ms. The initial contribution of a set of 10 induction generators to the fault is 1.38pu, and this value decreases to zero as the voltage collapses. The 'Offshore windfarm 1' accelerates to a slip of -8% for a fault duration of 350ms while the turbine controllers try to adjust the input power. The second windfarm 'Offshore windfarm 2' terminal voltage and power output decrease as a result of this fault.

For a fault at the local 132kV network the initial contribution to the fault from each windfarm is approximately 290% of its full load current. The voltages drop causes the real power to decrease; and this causes an increase in the machines speed to an approximate slip of -5%.

When the fault is cleared, the initial terminal currents for both farms are 180% of the full load current.

Section 10.2 presents the transient simulation of the behaviour of the doubly fed induction generator type under fault conditions. The same two faults are investigated in detail; one at the local 33kV busbar and the other in the local 132kV network.

For a fault in the local 33kV network of 'Offshore windfarm 1', the voltage at the machine terminals drops to .2pu after 200ms. The initial contribution of a set of 10 DFIGs to the fault is 424% of the full load current. This value decreases as the voltage collapses. The 'Offshore windfarm 1' accelerates to a slip of -2.2% for a fault duration of 200ms. The changes in the second windfarm (Offshore windfarm 2) terminal voltage and power output are limited in this case. However on fault clearance 'Offshore windfarm 1' draws an initial high reactive power of 110% of rating, and this depresses the terminal voltage to .9pu until the controllers react to adjust the power factor.

For a fault at the local 132kV network the initial contribution to the fault from each windfarm is approximately 230% of its full load current. The voltage drops cause the real power to decrease and this causes an increase in the machines speed to an approximate slip of -1% . When the fault is cleared, the initial terminal currents for the farms are 170% and 150% of full load current. This decreases to 110% of full load in less than 300ms.

The results for DFIGs operating at a slip of -12% for steady state full generation show higher levels of disturbance for a fault clearance of 80ms. Details of the DFIGs controller models are needed for a credible overall analysis for longer duration of faults.

12 Optimal Power Flow Development

In April 2002 IPSA Power Ltd. acquired an Optimal Power Flow package from the EEPs Group at UMIST. Induction generator and Static VAR Compensator (SVC) models have been developed and incorporated into the OPF code.

A Ph.D. thesis has been submitted in June 2003 (see References) that contains information on the development of the Optimal Power Flow package. This includes details on SVCs, but it does not include developments on induction generators. It is expected that a paper will be published in future in regards to how induction generators were modelled in the OPF.

12.1 Capabilities

The Optimal Power Flow attempts to make the best use of system resources subject to a number of constraints and requirements. More specifically it aims to minimise an objective function (usually dealing with costs) by the optimal setting of control parameters, while obeying the various constraints on the system (such as power and voltage limits).

The OPF models busbars, loads (as part of busbars), generation, induction generation, shunts, SVCs, lines and transformers. The following can be optimised in relation to minimising cost:

- shedding load on a bus (only if enabled and only up to specified maximum amount of load shed)
- adding new generation to a bus
- setting existing generation output (with real and reactive power cost functions)
- setting existing induction generation output (with real and reactive power cost functions)
- setting shunt output (with a reactive power cost function)
- setting SVC output
- increasing the rated capacity of a branch (if enabled)
- transformer tap position (according to each transformers working mode)
- shunts (according to each shunts working mode)

In addition, busbar voltages around the network can also be optimised, and optionally voltage controlled busbars can be allowed to become unregulated.

12.2 Further Developments

Work is still ongoing on the OPF software to develop and extend it's features. An increase in functionality usually means an increase in the number of functions and parameters. Conversely, as time progresses some functions may become superseded or even be deleted altogether. These considerations were important when deciding how to integrate the OPF into IPSA.

12.3 Development of an Application Programming Interface (API) to the OPF

The OPF calculation code was originally developed to run as a self-contained application running in simple console mode. This amounts to:

- All user interaction being done at a command line interface.
- All network modelling data being read from files.
- All results and data messages being written both to the console and to files.

While this is fine during the initial development phase, any general use of the OPF software requires it to be ‘Enginised’, i.e. the removal of all user interaction and its replacement with an API. This enables the main application to call the OPF directly, with all user interaction handled by the main application not the OPF.

12.3.1 The structure of the API

The API is composed of a number of layers, of which only the external one is visible to the application programmer. The choice of language for each of these layers is a function of what propose they serve.

12.3.1.1 Language considerations

For a general API, which may be interfaced to most programming languages on most platforms, a basic C style function call is generally considered most effective. This should be the only user-visible layer in the OPF Engine, and should be fully documented for the Application programmer.

The OPF software is written in Fortran 90 (F90) and makes extensive use of the *Module* construct which enables data and procedure hiding in a similar way to the class concept in C++. While this is perfectly acceptable when calling from other Fortran 90 code, the routine name decorations used to incorporate the module name can cause problems when calling from C. There are no such problems when the routines are not defined in a *Module*, so the outer layer of the core F90 code is not inside any *Modules*.

12.3.2 API Layers

The Engine consists of the following layered structure:

- User visible API – written in C, language bindings in C and C++
- Internal private layer written in C that calls the F90 API layer, the F90 routine definitions expressed in C format
- Engine interface layer - Fortran 90 API layer – calls the main OPF routines in their respective modules
- Core Engine written in F90 using Modules.

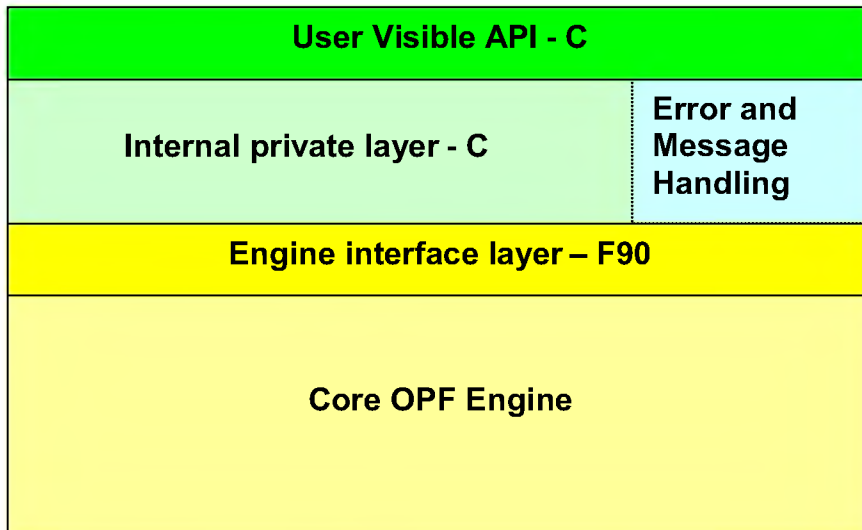


Figure 12.1: Engine architecture

The Engine Interface layer could also be thought of as the basic Fortran API, for instances where the OPF module is called directly from Fortran.

12.3.3 Message and Error handling

The internal private API layer provides a message and error reporting function, allowing the OPF Engine to report and store messages and errors. These can then be queried through the main user visible API.

12.3.4 Types of API routines

The User Visible API function calls may be broadly split into the following groups:

- Initialisation routines – sets up the Engine ready for use
- Data set routines – set up the network model to be analysed
- Data get routines – get the values of the network model parameters
- Control and run time routines – setting the analysis parameters used during the study
- Run routines – runs the actual calculation
- Results get routines – get the results of the calculation
- Reporting routines – get the messages, warnings and error messages encountered during a study
- Reset routines – reset the Engine to be re-used.

12.3.5 Packaging of the OPF

The OPF routines with the API layer (the OPF Engine) are packaged together as an object library. This has been developed on both Windows and Unix platforms, and is how the Engine is linked in to the IPSA software. The language bindings for both C and C++ are defined in the Engine API definition header file. This enables the main IPSA program to compile in the calls to the OPF Engine.

12.4 Addition of OPF Data to IPSA

While some of the data required for OPF calculations was already in IPSA, most of the OPF data would be new information. There were cases where the same piece of information in IPSA was handled differently in the OPF module (e.g. induction generator power), cases where a network item in IPSA was handled differently by the OPF (e.g. shunts), and cases where a network item did not exist at all in one program but did in the other (e.g. DC equipment, static VAR compensators, and many others).

12.5 Separation and Conversion of Data

Clearly each relevant network item in IPSA had to be extended to store OPF data. Due to the many differences in representing the network between IPSA and the OPF, the decision was made not to share data between the normal IPSA representation and the OPF data. This means for example that the specified output power of a generator in IPSA can be different to that specified in the OPF.

To avoid unnecessary overheads in memory allocation, OPF data is not created by default for network items in IPSA until the user specifically requests to convert the network to OPF form. After the program receives this instruction, each item in IPSA that has a representation in the OPF module has its data extended to include the relevant pieces of OPF data.

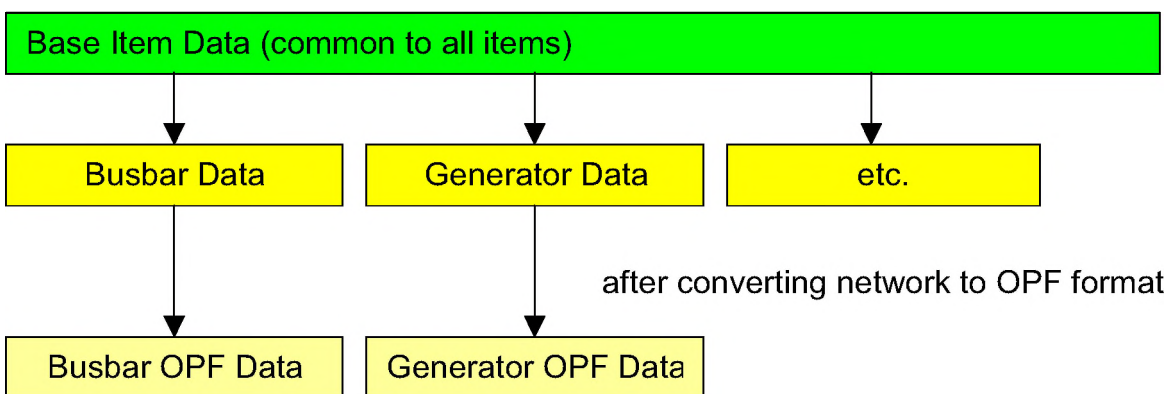


Figure 12-2: Extending IPSA data to include OPF information via inheritance

As the OPF data is separate from the existing IPSA data information already entered for these items is not altered in any way by the conversion process. This means that other parts of the IPSA program do not have to be altered because of the addition of the OPF module. Note that the existing data is used as a starting point for the OPF data when it is sensible to do so, e.g. the existing in or out of service status for an item is copied to the OPF status, applying conversions where necessary.

The latest version of IPSA is largely written in C++. The OPF data for each item is generally a derived class from the base IPSA data for the item in question.

12.5.1 Busbars

Busbars are represented in the OPF with the following information:

- Type (e.g. unregulated, swing, etc.)
- Base voltage
- Minimum and maximum intact voltages
- Minimum and maximum fault voltages
- Voltage limit type
- Target voltage
- Real and reactive power demand
- Maximum load shedding
- Cost of load shedding
- Cost of new real and reactive power generation at bus

Busbars in IPSA other than swing buses do not have a type, but the OPF type can be inferred from the settings of the equipment connected to the busbar.

12.5.2 Loads

Loads are represented in the OPF on their connected busbar as real and reactive power demand.

12.5.3 Generators

Generators are represented in the OPF with the following information:

- Status
- Optimise real and reactive power flags
- Real power minimum and maximum output
- Reactive power minimum and maximum output
- Actual real and reactive power output
- Quadratic, linear and constant coefficients of the real power cost function
- Quadratic, linear and constant coefficients of the reactive power cost function

12.5.4 Induction machines

Induction motors are represented in the OPF on their connected busbar as real and reactive power demand.

Fixed speed induction generators are represented in the OPF with the following information:

- Status
- Stator resistance and reactance
- Rotor resistance and reactance
- Magnetising reactance
- Mechanical power
- Linear coefficients of real and reactive power cost functions

Note that this is a single cage representation. IPSA allows for double cage induction machines. If a double cage entry has been made for an induction generator in IPSA then one set of rotor values is discarded.

DFIGs are represented in the OPF as generators.

12.5.5 Branches

Branches are modelled in the OPF as follows:

- Status
- Type (e.g. line, fixed tap transformer, etc.)
- Resistance, reactance and susceptance
- Rating
- Capacity cost

Note that in IPSA there are several branch status values dealing with which end(s) of the branch are in or out of service and available to be switched. In the OPF the branch is simply either in or out of service.

12.5.6 Shunts

In IPSA shunts are treated as a special case of a branch (one whose “from” and “to” busbars are the same). In the OPF module they are separate items and have the following data:

- Status
- Shunt mode (preventative or corrective)
- Minimum and maximum B
- Actual G and B
- Quadratic, linear and constant coefficients of the reactive power cost function

12.5.7 Transformers

Tap changing transformers are modelled in the OPF as follows:

- Status
- Mode (e.g. fixed tap)
- Present tap position
- Minimum and maximum tap positions

Quadrature boosters are modelled in the OPF as follows:

- Status
- Mode
- Angle
- Minimum and maximum angles

12.5.8 Static VAr Compensators (SVCs)

SVCs have no representation in IPSA but they are present in the OPF and use the following information:

- Status
- Mode
- Present value of reactive power
- Maximum and minimum limits of reactive power
- Present voltage reference
- Maximum and minimum limits of the voltage reference
- Present droop
- Maximum and minimum values of droop
- Cost of reactive generation

12.5.9 OPF Control

As well as the OPF information for each item of equipment, IPSA also had to be extended to include the necessary control information for running the OPF, such as the number of iterations and which parameters to optimise.

12.6 Further Developments

Until recently it was not possible to add elements to an IPSA network without drawing them on the single line diagram. As SVCs are not modelled in the present version of IPSA there was hence no way to include their OPF data into IPSA either. However, the latest beta version of IPSA now does allow items to be added to a network without being drawn. It will therefore now be possible to add SVCs to a network that has already been converted to OPF form without having to add them to the single line diagram as well.

At present all induction generators are modelled as OPF induction generators. This will be changed so that DFIGs are modelled as OPF generators, while fixed speed induction generators remain modelled as OPF induction generators.

13 Addition of OPF Results to IPSA

Each of the network items added to the OPF network has results that are returned by the OPF program. Additionally the network itself has results, these being a summary of the performance of the OPF and various totals for specific types of equipment.

13.1 Stored Results

IPSA stores results for all of its calculations and allows them to be viewed on the diagram, in tables, or as part of an HTML report (like an off-line web page). The result types hence had to be extended to include OPF results.

The latest version of IPSA is largely written in C++. The OPF results for each item is generally a derived class from the base IPSA results for the item in question.

13.1.1 Busbars

The following results are returned for each busbar from the OPF:

- Voltage magnitude and angle
- Minimal and maximal voltages
- Target voltage
- Island number
- Voltage status (i.e. was the busbar voltage optimised?)
- PV / PQ status (i.e. was switching from PV to PQ enabled?)
- Slack status (i.e. is this busbar slack?)
- Local marginal costs of supplying additional real and reactive powers to this bus. The value of the Lagrange multipliers for real and reactive power balance.
- Real and reactive power mismatch
- Real and reactive power demand
- Real and reactive load shedding
- Cost of load shedding
- Real and reactive new generation
- Cost of new generation

13.1.2 Generators

Note that new generation is a busbar result. The following results are returned for each existing generator from the OPF:

- Real and reactive power generation

13.1.3 Induction generators

The following results are returned for each induction generator from the OPF:

- Real and reactive power generation
- Slip

13.1.4 Branches

The following results are returned for each branch from the OPF:

- Sending end real, reactive and total power
- Receiving end real, reactive and total power
- Real and reactive losses
- Required extra capacity
- Penalty (Lagrange multiplier)

13.1.5 Shunts

The following results are returned for each shunt from the OPF:

- Values of G and B

13.1.6 Transformers

The following results are returned for each transformer from the OPF:

- Tap position (for tap changers)
- Angle (for quadrature boosters)

13.1.7 Static VAr compensators

The following results are returned for each SVC from the OPF:

- Reactive power
- Voltage reference
- Droop

13.1.8 Network results

The following results are returned from the OPF for the network as a whole

- Item numbers and status (e.g. number of disconnected generators, number of fixed tap transformers, etc.)
- Total real and reactive load
- Total real and reactive load shed
- Total real and reactive load shedding costs
- Total real and reactive new generation
- Total real and reactive new generation costs
- Total real and reactive existing generation
- Total real and reactive existing generation costs
- Total real and reactive induction generation
- Total real and reactive induction generation costs
- Total real and reactive shunt powers
- Total real and reactive branch losses
- Total new branch capacity and costs
- High and low voltages
- Overall real and reactive losses
- Overall cost

14 Integrating the OPF into IPSA

After an API had been created for the OPF module and classes created to store the required OPF data and results, work then began on integrating the OPF module into the IPSA program.

14.1 OPF Façade

A façade class was created to handle interaction between IPSA and the OPF. Façade classes minimise the communication and dependencies between subsystems in a program in two ways:

- All calls to the subsystem must go through the façade. In this case, all calls to the Optimal Power Flow API pass through the façade.
- The façade provides a simplified interface to the subsystem. In IPSA the façade only offers general functions to the rest of the program, such as “initialise the OPF” and “fetch OPF results”.

These are both useful features when the subsystem in question (the OPF) is still subject to change, as it limits the impact such changes have on the rest of the program.

14.2 Interface Changes

The IPSA interface was extended to allow OPF data entry, display OPF results, and perform OPF operations, namely converting the network to OPF format and running the OPF calculation.

Operations in IPSA can be performed in one or more ways:

- by selecting the operation from a menu entry
- by selecting the operation from an icon on a toolbar
- by selecting the operation from an icon on the stack bar

From the user's (and interface's) point of view there are only two basic OPF operations, namely converting the network to OPF form, and running the OPF. Both of these operations were made available by menu selection and icons on the stack bar. The option to run the OPF is disabled until the network has been converted to OPF format.

Once a network has been converted to Optimal Power Flow format, OPF data can be entered using IPSA's normal data table entry mechanism. The tables are available from menu selection and from icons on the stack bar. IPSA's tables adapt to display as much information as is present, so before the network is converted no OPF data is displayed, and after the network is converted all the OPF data is displayed.

The single exception to data entry via table is the OPF control parameters. As there is only one set of parameters per network there was no point creating a table with a single row of data. For the control parameters, therefore, the IPSA Analysis Settings property page was extended to provide OPF support, once the network has been converted.

Analysis Properties

General and Load Flow Fault Level and Waveforms Protection Transient Stability Breakers **OPF**

Base MVA: 100

Maximum Iterations: 150

Active Power Tolerance (MW): 0.1 Reactive Power Tolerance (MVar): 0.2

Load Shedding Tolerance (MW, MVar): 0.01

Optimise Active Power Generation: -1 Optimise Taps: 0

Optimise Voltages: 0 Optimise Shunts: 0

Optimise Quad Boosters: 0

☒ Enable PV to PQ Busbars Centering Parameter: 0.1

☒ Enable Load Shedding

☒ Enable Flow Constraint Gap Tolerance: 0.0001

☒ Enable New Branch Capacity Maximum Gap Divergence: 1e+010

☐ Maximum Load Capability

OK Cancel Help

Figure 14.1: IPSA Analysis Properties dialog showing OPF Parameters

While an OPF calculation is being performed the OPF module generates information, warning and error messages. These messages are colour-coded and displayed in the progress window of IPSA.

After an OPF calculation has been performed, the results can be seen in tabular form. The results tables are available by menu selection and icons on the stack bar. The menu entries and icons for OPF results will be disabled until a successful OPF calculation has been performed.

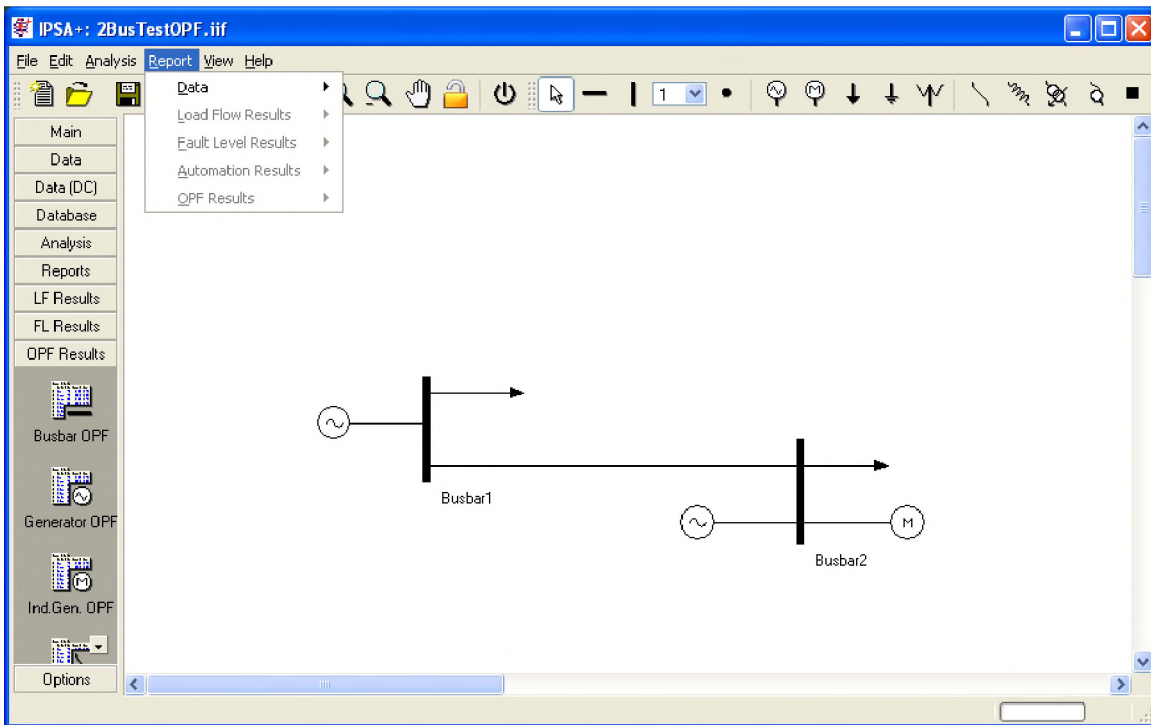


Figure 14.2: OPF Results disabled until available

Note that the precision to which the results are displayed can be changed in IPSA from 0 to 6 decimal places using the Results Settings dialog.

14.3 File Format Changes

IPSA uses a file format that is both forward and backward compatible; that is each version can read files written by both previous versions and by future versions too (the program ignores data added in future that does not exist in the present version). The file format was extended to include OPF data if the network had been converted to OPF form.

The Optimal Power Flow package is an optional part of the IPSA program. Users without the OPF module will still be able to view OPF data, but they cannot create it nor convert a network to OPF form.

14.4 Further Developments

IPSA can display property pages for each individual item of equipment. The property pages allow a more user-friendly approach to data entry than the tables; the range of acceptable values can be indicated by pull-down lists or a series of buttons, true or false values can be shown by check boxes, and so on. In future the OPF values will be added to the property pages.

For most calculations IPSA displays results on the single line diagram. No results are displayed on the diagram at the moment after an OPF calculation, but this may change in future.

IPSA can produce HTML reports for calculations. These can be viewed using an Internet browser, or imported into a modern word processor document. In future an HTML report will be created for the results of OPF calculations.

At present IPSA displays OPF results to the same precision as it displays Load Flow results. In future OPF results will have their own precision settings separate from Load Flow.

15 Validating the OPF in IPSA

Once all the changes had been made to IPSA to incorporate the OPF module a small test network was used to demonstrate that the same results were obtained running the OPF from within IPSA and from running the OPF in stand-alone console mode.

15.1 The Test Network

The test network consisted of a two bus network with one line, one swing generator and one induction generator.

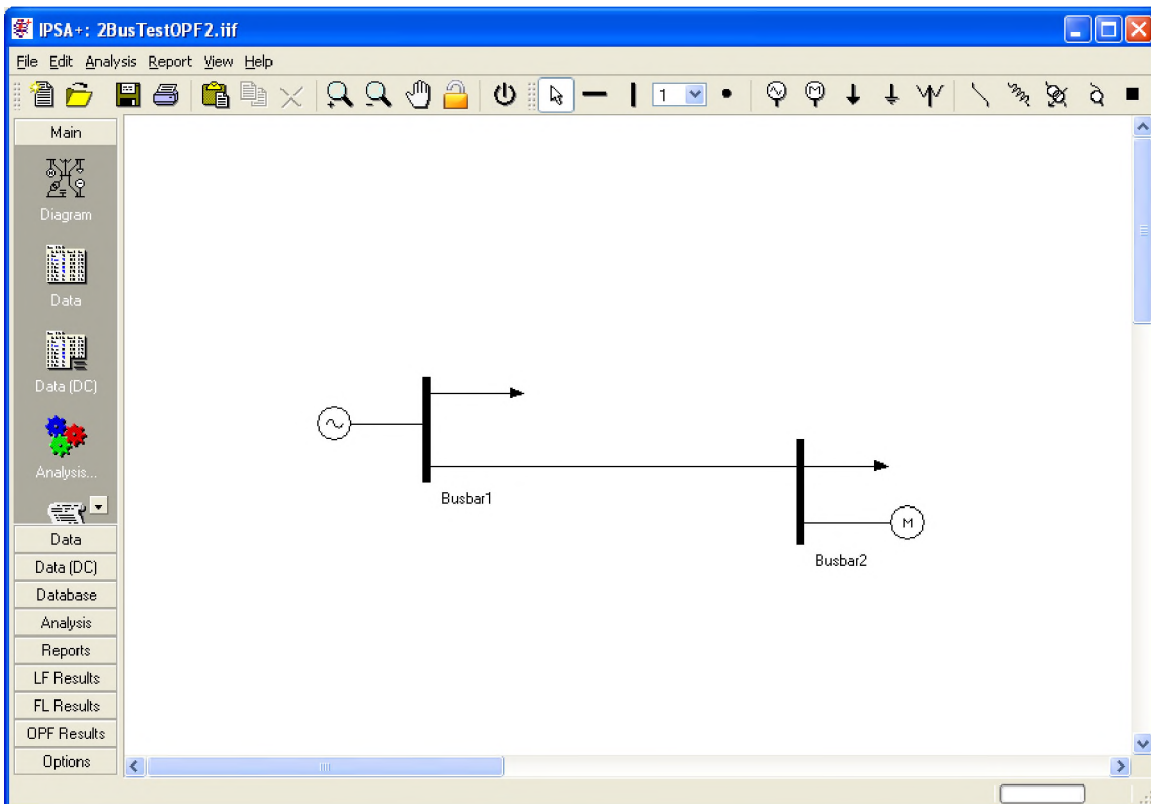


Figure 15.1: The test network in IPSA

Note that the loads displayed on the busbars are both zero in this case.

15.1.1 Test Network Data

The OPF data for the test network is shown in the following tables. For IPSA this data can be entered directly. For the OPF operating in console mode the data is entered into several plain text files.

15.1.1.1 Busbars

Name	Type	Base Voltage (kV)	Minimum Intact V. (pu)	Maximum Intact V. (pu)	Minimum Fault V. (pu)	Maximum Fault V. (pu)	Voltage Limit Type	Target Voltage (pu)
Busbar1	3	0.69	0.97	1.01	0.90	1.10	1	1.0
Busbar2		0.69	0.90	1.10	0.85	1.15	1	1.0

Name	Active Power Demand (MW)	Reactive Power Demand (MVar)	Maximum Load Shedding (%)	Cost Load Shedding	Cost New Generation P	Cost New Generation Q
Busbar1			100.0	2000.0	50000.0	10000.0
Busbar2			100.0	2000.0	50000.0	10000.0

15.1.1.2 Generators

Busbar	Optimise P	Optimise Q	P Minimum (MW)	P Max. (MW)	Q Minimum (MVar)	Q Max. (MVar)	P (MW)	Q (MVar)
Busbar1	1	1	-9999.0		-9999.0	9999.0		

Busbar	Quadratic Coeff. P	Linear Coeff. P	Constant Coeff. P	Quadratic Coeff. Q	Linear Coeff. Q	Constant Coeff. Q
Busbar1						

15.1.1.3 Induction Generators

Busbar	Stator R (pu)	Stator X (pu)	Rotor R (pu)	Rotor X (pu)	Magnet. X (pu)	Mech. P (MW)	Lin. Coeff. P	Lin. Coeff. Q
Busbar2	0.001164	0.022000	0.001309	0.023700	0.940964	2.000	10.000	

15.1.1.4 Lines

From Busbar	To Busbar	Type	Resistance (pu)	Reactance (pu)	Susceptance (pu)	Rating 1 (MVA)	Capacity Cost
Busbar1	Busbar2		0.050	0.500		3.0	4000.0

15.1.1.5 Control Parameters

As well as the data for each network item, the control parameters for the OPF analysis have to be entered.

```
Base MVA:          100
Max. Iterations:   150
Active Power Tol:   0.1           Reactive Power Tol: 0.2
Load Shedding Tol: 0.01

Optimise Active Power: -1         Optimise Taps:      0
Optimise Voltages:    0           Optimise Shunts:    0
Optimise Quad Boosters: 0

Enable PV to PQ Bus:      True
Enable Load Shedding:     True
Enable Flow Constraint:    True
Enable New Branch Capacity: True
Enable Maximum Load Capability: False

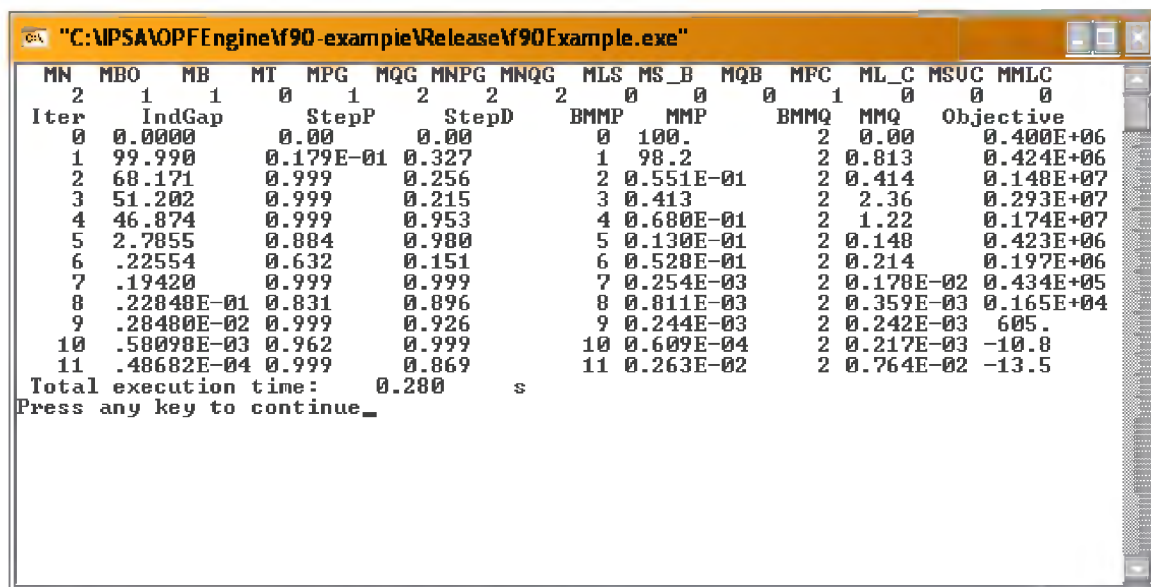
Centering Parameter:    0.1
Gap Tolerance:          0.0001
Maximum Gap Divergence: 1e10
```

Figure 15.2: Test network OPF control parameters

For IPSA the control parameters are entered on the Analysis Properties dialog (see Figure 15.2). For the OPF operating in console mode the parameters are entered into a plain text file.

15.2 Results from OPF Console

In console mode the OPF reached an answer in 11 iterations.



The screenshot shows a console window titled "C:\IPSA\OPFEngine\90-example\Release\90Example.exe". It displays a table of iteration results for 11 iterations. The table has columns for iteration number (Iter), and various parameters: MN, MBO, MB, MT, MPG, MQG, MNPG, MNQG, MLS, MS_B, MQB, MFC, ML_C, MSUC, MMLC. The 'Objective' column shows the value of the objective function at each iteration. The results show a steady decrease in the objective function value from approximately 0.400E+06 in iteration 0 to -13.5 in iteration 11. The console also displays the total execution time as 0.280 seconds and prompts the user to press any key to continue.

Iter	MN	MBO	MB	MT	MPG	MQG	MNPG	MNQG	MLS	MS_B	MQB	MFC	ML_C	MSUC	MMLC	Objective
0	0.0000	0.00	0.00	0.00	0.00	0.00	0.00	0.00	100.	0.00	0.00	0.00	0.00	0.00	0.00	0.400E+06
1	99.990	0.179E-01	0.327	0.256	0.215	0.215	0.215	0.215	98.2	0.813	0.424E+06	0.414	0.148E+07	0.148E+07	0.148E+07	0.424E+06
2	68.171	0.999	0.256	0.215	0.215	0.215	0.215	0.215	0.551E-01	0.413	0.148E+07	2.36	0.293E+07	0.293E+07	0.293E+07	0.148E+07
3	51.202	0.999	0.215	0.215	0.215	0.215	0.215	0.215	0.413	0.680E-01	0.174E+07	1.22	0.174E+07	0.174E+07	0.174E+07	0.174E+07
4	46.874	0.999	0.953	0.953	0.953	0.953	0.953	0.953	0.680E-01	0.148	0.423E+06	0.148	0.197E+06	0.197E+06	0.197E+06	0.423E+06
5	2.7855	0.804	0.980	0.980	0.980	0.980	0.980	0.980	0.130E-01	0.214	0.197E+06	0.214	0.434E+05	0.434E+05	0.434E+05	0.197E+06
6	.22554	0.632	0.151	0.151	0.151	0.151	0.151	0.151	0.528E-01	0.178E-02	0.434E+05	0.178E-02	0.165E+04	0.165E+04	0.165E+04	0.434E+05
7	.19420	0.999	0.999	0.999	0.999	0.999	0.999	0.999	0.254E-03	0.359E-03	0.165E+04	0.359E-03	605.	605.	605.	0.359E-03
8	.22848E-01	0.831	0.896	0.896	0.896	0.896	0.896	0.896	0.811E-03	0.244E-03	605.	0.244E-03	-10.8	-10.8	-10.8	0.811E-03
9	.28480E-02	0.999	0.926	0.926	0.926	0.926	0.926	0.926	0.244E-03	0.609E-04	-10.8	0.609E-04	0.217E-03	0.217E-03	0.217E-03	0.244E-03
10	.58098E-03	0.962	0.999	0.999	0.999	0.999	0.999	0.999	0.609E-04	0.263E-02	0.217E-03	0.263E-02	-13.5	-13.5	-13.5	0.609E-04
11	.48682E-04	0.999	0.869	0.869	0.869	0.869	0.869	0.869	0.263E-02	0.764E-02	-13.5	0.764E-02				0.263E-02

Total execution time: 0.280 s
Press any key to continue_

Figure 15.3: The OPF in console mode

The results are saved to a text file when the OPF is operated in console mode (Figure 15.4).

SYSTEM SUMMARY

[AREAS : 1] [ZONES: 1] [ISLANDs: 1] VRANGE: 0.9973 <= V <= 1.0000

Buses	PV	PQ	Load	Gen	Shunt	LS	SVC
2	1	1	0	1	0	0	0

	[TOTAL]	[OFF]	[FIX]	[PREV]	[CORR]	[GENTAP]
Branches:	1	0				
Generators:	1	0				
Wind Gens:	1	0				
Taps:	0	0	0	0	0	0
QBs:	0	0	0	0	0	
Shunts:	0	0	0	0	0	
SVCs:	0	0	0	0	0	

Energy:	[P]	[P+]	[P-]	[Q]	[Q+]	[Q-]
Capacity:		0.0000	-9999.0		9999.0	-9999.0
Used:	1.3496			0.68400		
Generation:	-1.3496	0.0000	1.3496	0.68400	0.68400	0.0000
Wind Gen.:	1.3481			-0.68038		
Shunts:	0.0000			0.0000		
Loads:	0.0000			0.0000		
Load Shed.:	0.0000			0.0000		
Losses:	-0.15299E-02			0.36183E-02		

[OBJECTIVE]	[EXIST PG]	[EXIST QG]	[New PG]	[New QG]
-13.481	0.0000	0.0000	0.0000	0.0000

[ACTIVE LS]	[REACTIV LS]	[LINE CAPAC]	[SVC]
0.0000	0.0000	0.0000	0.0000

BUSES

No	T A	I	Voltage	[PLoad]	[PLS]	[Pgen]	[PShnt]	[LP]	[MismP]
Name	S Z		Angle	[QLoad]	[QLS]	[Qgen]	[QShnt]	[LQ]	[MismQ]
1	3 1	1	1.0000	0.00	0.00	-1.35	0.00	0.20309	-0.43E-04
	0 1		0.00	0.00	0.00	0.684	0.00	0.853E-07	-0.19E-03
2	0 1	1	0.9973	0.00	0.00	1.35	0.00	-1.2211	-0.26E-02
	1 1		0.41	0.00	0.00	-0.680	0.00	0.631	-0.76E-02

BRANCHES

[ID]	[Fr]	C T	[Tap]	[Pij]	[Sij]	[Pji]	[Sji]	[PLoss]	[Max]	[Pot]	[No]
	[To]	O	[Angle]	[Qij]		[Qji]		[QLoss]	[Usage]	[Lambda]	
1	1 1	0	0.00	-1.3	1.5	1.4	1.5	0.11E-02	3.0	0.0	1
	2 1		0.00	0.68		-0.67		0.11E-01	50.437	0.37	

TOTAL PLoss = 0.00 QLoss = 0.01 Additional Capacity = 0.00

EXISTING GENERATORS

[ID]	[Bus]	T P	[PG]	[PMin]	[PMax]	[M.PCost]	[Pcost]		[No]
		O Q	[QG]	[QMin]	[QMax]	[M.QCost]	[QCost]	[QPProp]	[QNProp]
1	1	1 1	-1.35	-9999.00	0.00	0.00	0.00		1
		1 1	0.68	-9999.00	9999.00	0.00	0.00	9999.00	-9999.00
			-1.35			0.00			
			0.68			0.00	9999.00	-9999.00	

INDUCTION GENERATORS

No	Bus	T	Pgen	s	LP	MismP
		S	Qabs		LQ	MismQ
1	2	1	1.348	-0.3966E-02	0.000	0.000
1	0.6804		0.000	0.000		

Figure 15.4: Console mode OPF results

15.3 Results from IPSA OPF

In IPSA the OPF reached an answer in 11 iterations. In Figure 15.5 the OPF iterations are displayed in the progress window at the bottom of the IPSA program.

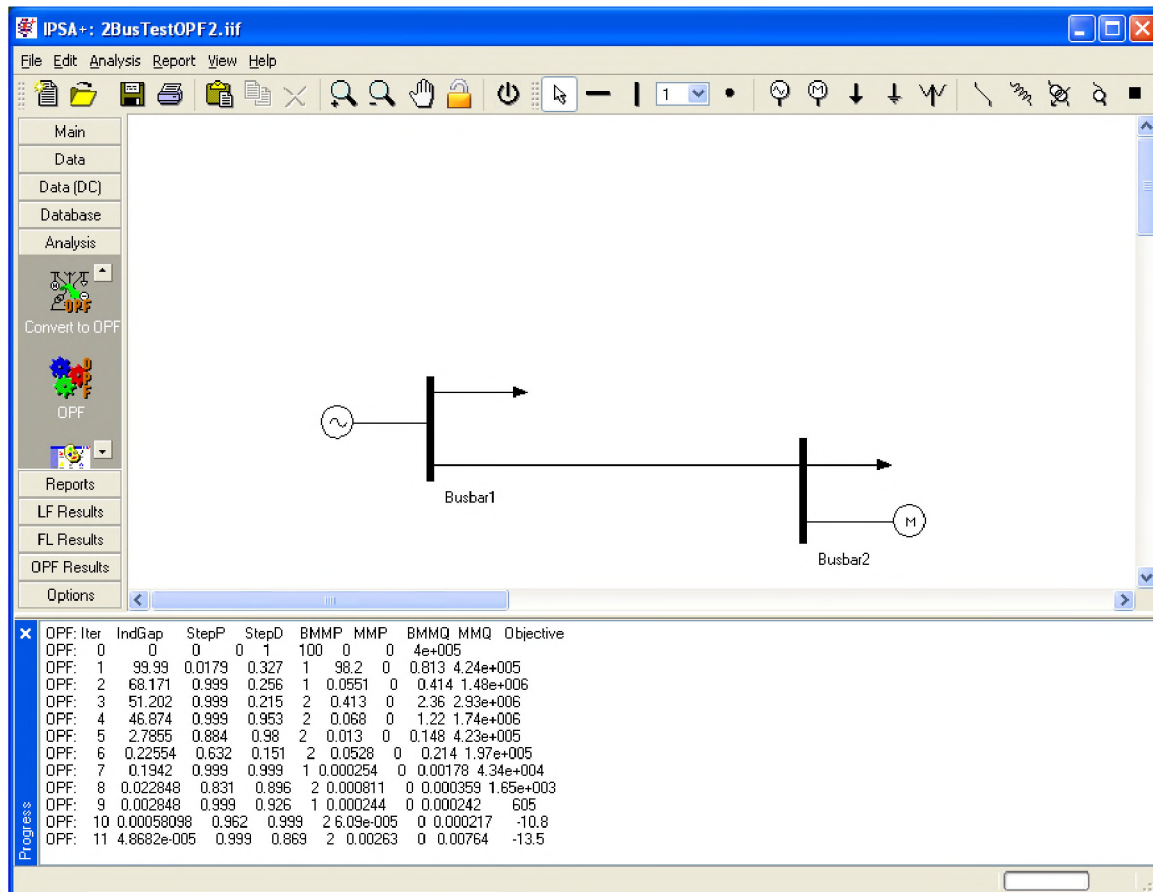


Figure 15.5: The OPF in IPSA

Once the OPF analysis is complete the results tables within IPSA become active.

15.3.1 Busbars

Name	Volt. Mag. (pu)	Volt. Angle (deg)	Minimal Volt. (pu)	Maximal Volt. (pu)	Target Volt. (pu)	Volt. Status	Island No.	PV/PQ Status	Slack Status
Busbar1	1.000		0.970	1.010	1.000				
Busbar2	0.997	0.41	0.900	1.100	1.000				

Name	Lambda P	Lambda Q	Mismatch (MW)	Mismatch (MVar)	P Dem. (MW)	Q Dem. (MVar)	P Shed (MW)	Q Shed (MVar)	Load Shedding Cost
Busbar1	0.203	0.000	-0.000	-0.000					2000.0
Busbar2	-1.221	0.631	-0.003	-0.008					2000.0

Name	New Active Generation (MW)	New Reactive Generation (MVar)	New Active Generation Cost	New Reactive Generation Cost
Busbar1			50000.00	10000.00
Busbar2			50000.00	10000.00

15.3.2 Generators

Busbar	Name	Active Power Generation (MW)	Reactive Power Generation (MVar)
Busbar1		-1.350	0.684

15.3.3 Induction Generators

Busbar	Name	Active Power Output (MW)	Reactive Power Output (MVar)	Slip
Busbar2		1.348	0.680	-0.004

15.3.4 Lines

From Busbar	To Busbar	Send P (MW)	Send Q (MVar)	Send P (MVA)	Receive P (MW)	Receive Q (MVar)	Receive Power (MVA)
Busbar1	Busbar2	-1.350	0.684	1.513	1.351	-0.673	1.509

From Busbar	To Busbar	P Losses (MW)	Q Losses (MVar)	Required Capacity (MVA)	Extra	Penalty
Busbar1	Busbar2	0.001	0.011			0.374

15.4 Further Developments

Further testing using larger networks needs to be carried out to verify that the OPF module in IPSA behaves in the same manner as the OPF in console mode.

16 Voltage Control

This study utilises the Optimal Power Flow program and the DFIG model developed by IPSA Power Ltd, to analyse a range of issues pertaining to the connection of both DFIG and standard IG based wind farms.

After some initial analysis it was decided that the investigation into wind farms using either variable speed induction or synchronous generators connected via back-to-back static convertors lead to similar results to installations containing DFIG machines. For this reason and to avoid the relative duplication of similar results, it was felt that investigating DFIG machines operated in both power factor and voltage control modes would provide a greater degree of insight.

In Section 16.1, the test network utilised in the studies is detailed and assumed data commented on. This network is representative of a small part of a real 132kV network in the UK where a proposed 100MW wind farm is planned to be connected. Section 16.2 briefly discusses the Optimal Power Flow program that is utilised in the study to determine the optimal voltage control strategy.

In Sections 16.3-16.6, the voltage control study analysis is carried out for the following tasks:-

- Contrast the network voltage performance associated with the application of (1) fixed speed (2) doubly fed induction machines under various loading conditions for various levels of penetration of off-shore wind generation (Section 14.3).
- Determine the optimal control strategy of doubly-fed induction generators to maximise penetration of wind generation on the existing 132kV network, considering full spectrum of network loading conditions (Section 16.4).
- Determine the benefits of the application of on-shore reactive compensation in conjunction with (1) fixed speed induction machine and (2) variable speed based off-shore wind generation and contrast it with the results in Section 16.4 (Section 16.5).
- Determine an optimal strategy of coordinated area based voltage control using OLTCs in the local network and controlling active and reactive outputs of doubly-fed induction machines (Section 16.6).

Finally, Section 16.7 presents conclusions of this study and discusses any future work that may be carried out to further the development of wind farm integration into distribution networks.

16.1 System Models

16.1.1 Network Model

The base network model used in the Voltage Control Study is shown below in Figure 16.1.1.

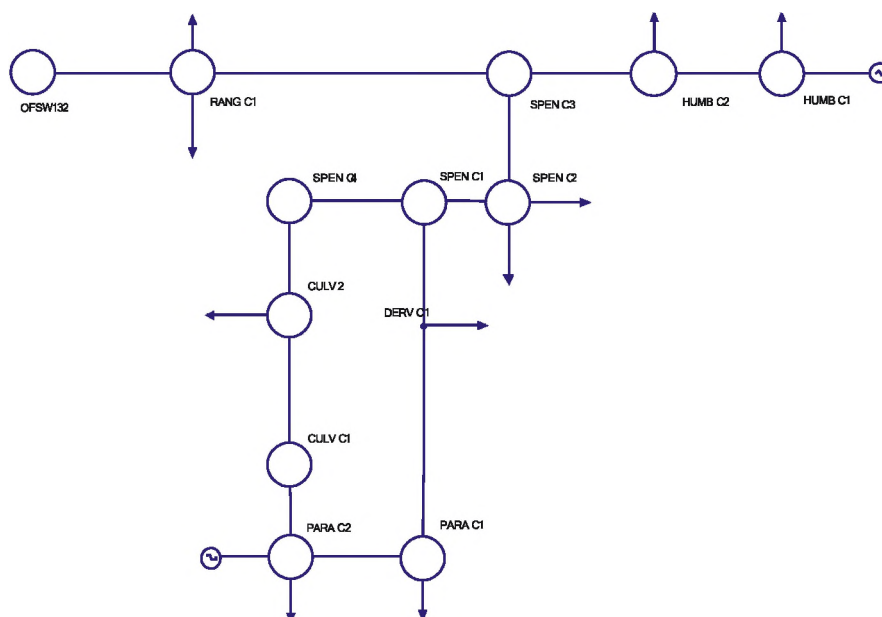


Figure 16.1.1: 132kV network model used for Voltage Control Study

It is a simplified representation of a section of a typical 132kV network with changes to busbar names and in some cases, line impedances and ratings. The network has been constructed for implementation with the OPF to highlight the effect of attaching different types of wind generation and DFIG control implementations.

The network connection of the windfarms will be made at the OFSW132 132kV busbar for the Case 1 studies and at SPEN C3 132kV busbar for the Case 2 studies. The slack busbar is PARA C2 in all studies.

16.1.2 DFIG and IG data

Doubly Fed Induction Generator and Induction Generator machine data for all the wind farms modelled in the studies, are detailed in Tables 16.1.1 and 16.1.2.

IG Parameter	Value	unit
Rating	3.4	MVA
V (rated voltage)	0.69	kV
R1 (stator resistance)	0.0061	pu
X1 (stator reactance)	0.0821	pu
R2 (rotor run resistance referred to stator)	0.0169	pu
X2 (rotor run reactance referred to stator)	0.1072	pu
Xm (magnetising reactance)	2.556	pu

Table 16.1.1: IG machine parameters (to 1.3MW base) used in this analysis.

DFIG Parameter	Value	unit
Rating	3.4	MVA
V (rated voltage)	0.69	kV
R1 (stator resistance)	0.0043	pu
X1 (stator reactance)	0.0809	pu
R2 (rotor resistance referred to stator)	0.0048	pu
X2 (rotor reactance referred to stator)	0.0871	pu
Xm (magnetising reactance)	3.459	pu

Table 16.1.2: DFIG machine parameters used in this analysis.

16.1.3 Load Data

The network used in the study is based on a real part of a typical network, albeit with different line impedances and substation names. This was done to simplify the OPF analysis and to highlight the relevant results in the study. The network reduction and the subsequent equivalent loadings at the 132kV busbars (shown in Table 16.1.3) are based on the load flow of the 100% network load case.

Busbar	100% load Scenario
HUMB C1	5.9 - j25.5 MVA
SPEN C2	41.1 - j17.9 MVA
RANG C1	47 + j33.5 MVA
CULV 2	22.1 + j11.1 MVA
DERV C1	4.7 - j0.7 MVA
PARA C1	27.2 + j15 MVA
PARA C2	27.6 + j19.3 MVA
HUMB C2	33.5 + j15.1 MVA

Table 16.1.3: Network loadings for the equivalenced network

16.2 Using The Optimal Power Flow Program

The Optimal Power Flow or OPF is a relatively new addition to the suite of tools that the power system engineer can use for the design and analysis of electrical networks. There are many different variants on the OPF depending on the solution method and end-user requirements. At its simplest level, the OPF automates the normal iterative process that a normal study would take using a conventional power flow program.

For example, to determine the maximum load a particular node could take, the user would have to gradually increase the load until either a voltage or thermal limit is reached. This may take several iterations of the power flow program and require the user to monitor many different system variables. On a simple system, this approach would usually result in a near optimal solution as there are only a few variables that need to be monitored. The OPF however can do this same study in a single step while monitoring all the system constraints. The advantage is a significant saving in time taken to perform the study.

For more complex systems with a large number of operational variables and system constraints, the OPF can still determine a near optimal solution whereas the corresponding time required for an experienced system analyst using a conventional power flow program would be prohibitive in comparison. For example the use of an OPF in a study to determine the optimal placement of distributed generation and reactive compensation on a meshed network would significantly reduce the amount of time required. By initially identifying the potential nodes where generation could be

added, the OPF would then adjust them all simultaneously to result in a solution that maximises the amount of generation without resulting in any system constraints.

An OPF, like all simulation programs, requires careful use to ensure reasonable results are obtained. More data is generally required such as branch loading limits, over and under voltage limits, additional capacity costings, etc. A significant amount of this data is already available for most studies as it is used for reporting purposes for the analyst. The OPF essentially automates the manual adjustment process thereby freeing up the analyst to consider the overall picture.

There are three key parts to an OPF formulation:

1. Objective Function
This defines the user definition of the optimal solution. It can consist of different system variables such as capacity changes and losses linked together by a common unit such as cost (£).
2. Decision variables
These are the variables by which the solution algorithm tries to maximise or minimise the objective function. They consist of two categories, state variables such as nodal voltages and angles, and control variables such as active and reactive power generation or load shedding.
3. Constraints
These define the satisfactory operating envelope of the network such as maximum and minimum output of a generator, voltage limits at a busbar, maximum power transfer across a transformer, or nodal balance equations.

16.2.1 Variants of the OPF

Not all OPF programs are created equal. The optimal operation of an electrical network is a large, highly complex and non-linear problem. An all encompassing optimisation program would require vast amounts of coherent data and result in a problem that would be questionable if it could be solved.

The OPF started out as an extension to Economic Dispatch programs which determined the optimum loading levels of generators, which had previously been determined from a Unit Commitment program. The Economic Dispatch programs were essentially a single busbar model and so ignored effects and losses of the electrical network.

The early OPF programs incorporated DC loadflows as solution constraints to allow for the effect of losses and capacity constraints. However, the DC loadflow does not account for voltage variation within the network and therefore cannot be used for reactive power dispatch and can only approximate branch thermal constraints.

As electrical networks and many of their associated cost functions are non-linear and often non-convex, a key issue in the construction of an OPF program is the optimisation method. The selection of this method either for speed or robustness has a major influence on the type of OPF that can be formulated. Some of the variants are:

1. DC or AC power flow equations
2. Linear or Non-linear solution engine
3. Linear or Quadratic objective functions
4. Direct or indirect solution of the power flow equations

16.2.2 Formulation of the IPSA-OPF

The OPF used in this project has been implemented in IPSA was originally developed by UMIST as part of a PhD project. The algorithm uses a non-linear optimisation routine with an AC power flow directly implemented. The non-linear optimisation routine is a Primal-Dual Interior Point Method. The OPF has been proven to be robust on a real 1000+ busbar transmission system.

The objective function can consist of any one, or combination, of the following:

1. Cost of existing Active power generation dispatch (quadratic)
2. Cost of existing Reactive power generation dispatch (quadratic)
3. Cost of new Active power generation capacity (linear)
4. Cost of new Reactive power generation capacity (linear)
5. Cost of Load Shedding (linear)
6. Cost of New Branch Capacity (linear)
7. Maximise the network loading

The constraints that are put on the optimal solution are:

1. Nodal active power balance (equality)
2. Nodal reactive power balance (equality)
3. Operational voltage limits (in-equality)
4. Active and Reactive Generation limits (in-equality)
5. Load shedding limits (in-equality)

All of these constraints are normally used however the in-equality constraints can be removed by setting the minimum and maximum operation limits to define a wide envelope, i.e. $0.5 < V < 1.5$.

It is also possible to allow certain system parameters to be modified during the optimisation process. This allows the solution additional scope with which to minimise or maximise the objective function. The controls that can be fixed or variable are:

1. Active power generation
2. Voltage control setpoints
3. Transformer tap changers
4. Quadrature boost transformer phase angles
5. Shunt reactance/capacitances

The specific OPF formulation used requires all variables to be continuous and so tap changers are not modelled as discrete taps. If tap changers have been used, it may be necessary to fix the tap positions and re-run the OPF to ensure that the near optimum solution has been obtained.

16.2.3 Summary

The Optimal Power Flow (OPF) program is another tool in for the power system engineer to use in order to determine the best system design and operation in terms of technical feasibility and least cost. Like all simulation tools, the OPF is not intelligent in its own right and so care must be taken in constructing the network model and interpreting the results. However, a properly configured OPF will significantly reduce the study work-load of the engineer by removing the trial and error approach to determining the optimal network loading and capacity. The OPF can also highlight

new operational network conditions that previously have not been considered due to the limitations of the iterative approach using conventional power flow programs.

16.3 Voltage Control Study – Case 1

In this section the Voltage Control Study results are detailed for the following tasks:-

- Contrast the network voltage performance associated with the application of (1) fixed speed and (2) doubly fed induction machines under various loading conditions for various levels of penetration of off-shore wind generation (Section 16.3.1).
- Determine the optimal control strategy of doubly-fed induction generators to maximise penetration of wind generation on the existing 132kV network, considering full spectrum of network loading conditions (Section 16.4).
- Determine the benefits of the application of on-shore reactive compensation in conjunction with (1) fixed speed induction machine and (2) variable speed based off-shore wind generation and contrast it with the results in Section 16.4 (Section 16.5).
- Determine an optimal strategy of coordinated area based voltage control using OLTCs in the local network and controlling active and reactive outputs of doubly-fed induction machines (Section 16.6).

It was decided that the investigation into connection of variable speed generators would serve no additional purpose (for the voltage control studies). This is primarily due to the fact that these types of generators are able to be operated in both voltage and power factor control modes and would therefore yield similar results to DFIG units.

16.3.1 Network Performance Comparison of IG and DFIG machines

In this study, the performance of two types of wind farms are compared. In the first case a wind farm with approximately 100MW capacity, connected at the OFSW132 busbar using standard IG machines, is compared with a similar capacity wind farm using DFIG machines. In this case, the effect of two DFIG control strategies are investigated, namely voltage and power factor control.

Additionally, the study looks at varying levels of wind farm output (100MW, 66MW and 33MW) and network loading (120%, 100% and 80%).

16.3.2 Study results

Table 16.3.1 illustrates the significant difference in network voltage performance for the connection of both types and wind generators, and also DFIG control strategies. For the 120% network loading and IG connection, some bus voltages are seen to drop below 0.9pu, specifically at RANG C1 and OFSW132. This would necessitate some measure of reactive compensation within the 132kV network. It must be noted that the capacitor compensation placed at the IG installation has been calculated to improve the power factor there to 0.95 lagging when the wind farm is at 50% output capacity. This is to ensure that if the wind farm capacity rapidly reduces due to a fault, the fixed capacitance doesn't lead to excessive voltages within the network. Due to this design constraint, a

large capacity IG based wind farm will draw a significant reactive component, and this may adversely impact on the 132kV network voltages.

132kV Busbars	120% network load		
	IG voltage (pu)	DFIG pf control voltage (pu)	DFIG voltage control voltage (pu)
HUMB C1	0.916	0.973	1.001
SPEN C2	0.912	0.967	0.994
RANG C1	0.887	0.957	0.991
SPEN C1	0.914	0.967	0.993
CULV 2	0.941	0.972	0.988
CULV C1	0.942	0.973	0.987
DERV C1	0.958	0.984	0.996
PARA C2	1.000	1.000	1.000
PARA C1	0.998	0.999	1.000
HUMB C2	0.915	0.971	0.999
SPEN C4	0.915	0.967	0.992
SPEN C3	0.909	0.966	0.994
OFSW132	0.884	0.956	0.991

Table 16.3.1: Comparison of 132kV busbar voltages for IG and DFIG based wind farm installations

When the two DFIG control modes are compared, it seems clear in this case that the best network voltage performance occurs when in the DFIG Voltage Control mode. In this mode the DFIG units are configured to control the OFSW132 busbar voltage to 1.0pu. Practically this would additionally require some form of line drop compensation within the DFIG controller. In the power factor control mode, which anecdotally seems to be the preferred mode of operation for the presently installed DFIG based wind farm installations, the units are set to operate at unity power factor.

The DFIG voltage control mode also has the additional effect of reducing the line loading in the 132kV network when compared with both the IG, and DFIG in power factor control mode. While quantifying this benefit and its effect of increasing the possible capacity of a wind farm into a distribution, it does merit some mention.

16.3.3 Conclusion

In summary, it seems that the voltage control mode provides the best network voltage performance when the network is more heavily loaded (eg 100% and 120%). In the 80% network load study case the DFIG voltage and power factor control modes result in a similar network voltage profile.

16.4 DFIG Optimal Control Strategy (I)

In this study, the optimal control strategy to maximise wind farm penetration into a network is assessed for the test network shown in Figure 16.1.1 with a slight modification. To add some alternative flow path for the wind farm generation, and to highlight the OPF results, another 132kV circuit is placed between the RANG C1 and SPEN C4 132kV busbars.

The study is carried out with all the transformers in the network modelled without tap-changers. The coordinated effect of optimising tap positions with the DFIG control schemes will be explored in Section 16.6.

16.4.1 Maximum penetration assessment based on LF method

In this primary assessment, the network performance and maximum possible generation from the wind farm is determined using the standard load flow technique, essentially trial and error until busbar voltage limits and circuit loadings are deemed satisfactory.

In this initial assessment it was found that with this test network, the DFIG based wind farm installation capacity could be greater if the DFIG's employed voltage control in an attempt to boost network voltages by exporting reactive power. It must be noted that in this case when tap changers were not utilised at the wind farm, the network voltage constraint became the wind farm 33kV and 0.69kV voltages being greater than 1.1pu when exporting reactive power in voltage control.

With this in mind and having performed numerous tests on this network with the voltage control option, any realistic voltage control scheme would be required to incorporate busbar voltages at the wind farm 0.69kV, 33kV and 132kV to ensure that limits aren't exceeded. The fact the constraint in this case was the wind farm 0.69kV busbar illustrates this point. This could be easily implemented in the controller with some form of voltage max select function and line drop compensation for each voltage measurement.

With the voltage control option wind farm output could be increased from 130.5MW to 153MW, when compared with the unity power factor control option, an approximate capacity increase of 20%. This is a significant result and is quite a good argument for the implementation of wind farm operators having a more active role in network operation when available to do so.

16.4.2 Maximum penetration assessment based on OPF method – Study Case 1

The OPF was tested for the same network to assess the maximum amount of generation that could be placed at the wind farm before any reinforcement, generation, load shedding or reactive compensation was required.

Once again the wind farm installation voltages were permitted to range between 0.9pu and 1.1pu, the tap-changers were disabled and the network 132kV voltages were permitted to range between 0.95pu and 1.05pu. The costs of installing extra reactive compensation, load shedding, power generation and increasing the capacity of any of the 132kV circuits were all set to be the same. The OPF was then run for differing generation capacities in both control modes until the maximum was obtained.

For the DFIG power factor control case, the cost of reactive compensation at the wind generation 0.69kV busbars was set as high as the rest of the network. For the voltage control case, this cost was set very low. The generation capacity was increased in both cases until the first constraint was attained. These constraints were circuit reinforcement, voltages exceeding 1.1pu at the wind farm and 1.05pu within the 132kV network, voltages lower than 0.9pu at the wind farm and 0.95pu in the 132kV network, load shedding in the network, and any real or reactive power requirements in the network other than at the slack bus PARA C2.

In summary, the maximum generation was determined to be 135MW as opposed to the 130.5MW from the trial and error LF study. Similarly, in the voltage control Case 1 OPF study the maximum generation was found to be approximately 161MW as opposed to the 153MW from the trial and error LF study. With the voltage control option wind farm output could be increased from 135MW to 161MW, when compared with the unity power factor control option, an approximate capacity increase of 20%.

There was very little difference noted for the maximum generation for the range of network loadings (eg 120% 100% and 80%) in this study case so these results are omitted. This result is mainly due to the line ratings and upgrade costings being effectively removed from OPF calculation to isolate the network voltage costs and constraints within the OPF solution.

16.4.3 Maximum penetration assessment based on OPF method – Study Case 2

In this study, the network connection point was modified from RANG C1 to SPEN C3 to see if the results obtained in Section 16.4.2 were similar, e.g. that the voltage control option permitted greater wind farm capacity to be connected into the 132kV network.

In summary to the results, the maximum generation was determined to be 151MW. Similarly, in the voltage control Case 2 OPF study the maximum generation was found to be approximately 189MW.

Similar to the Case 1 results, the voltage control option allowed the wind farm capacity to be increased by almost 20% when compared with the wind farm operated at unity power factor.

16.4.4 Conclusion

This study has assessed the optimal control strategy for a DFIG based wind farm connecting into the 132kV network in order that the penetration capacity can be maximised. The optimal power flow program was utilised to determine this maximum capacity.

The studies was carried out for capacity limits based on N-security thermal constraints with transformer tap-changers, disabled. The wind farm installation voltages were permitted to range between 0.9pu and 1.1pu and the network 132kV voltages were permitted to range between 0.95pu and 1.05pu. The OPF costs of installing extra reactive compensation, load shedding, power generation and increasing the capacity of any of the 132kV circuits were all set to be the same. For the studies the OPF was carried out for increasing wind farm generation capacities in both control modes until a network constraint was attained. These constraints were determined as either of a circuit reinforcement, a busbar voltage exceeding 1.1pu at the wind farm and 1.05pu within the 132kV network, a busbar voltage lower than 0.9pu at the wind farm and 0.95pu in the 132kV network, load shedding in the network, and any real or reactive power requirements in the network other than at the slack bus PARA C2.

The two control strategies assessed were i) unity power factor control and ii) voltage control. The OPF study results indicated that, for this test system at least, when the wind farm is operated in the voltage control mode, a 20% increase in wind farm capacity may be possible when compared with a wind farm operated in unity power factor mode.

This is a significant result and is quite a good argument for the implementation of wind farm operators having a more active role in network operation when available to do so.

16.5 On-shore Reactive Compensation vs DFIG

In this study, the benefits of placing on-shore reactive compensation within the Case 1 132kV test network is assessed for an off-shore wind farm containing IG machines. Once again the wind farm installation power factor correction has been designed to approximately set the power factor at 0.95 lagging for 50% wind farm output.

16.5.1 Study Results

The study was carried out using the OPF and basic LF programs to determine the maximum wind farm penetration capacity using the Case 1 study case, in conjunction with placement of reactive support throughout the network.

The studies was carried out for capacity limits based on N-security thermal constraints with transformer tap-changers, disabled. The wind farm installation voltages were permitted to range between 0.9pu and 1.1pu and the network 132kV voltages were permitted to range between 0.95pu and 1.05pu.

Initial studies suggested that the optimal placement of the reactive support for the wind farm connection would be at the RANG C1 132kV busbar due to the significant reactive power demand from the wind farm. With this in mind and to reduce the number of reactive compensation sites, the OPF costs of installing extra reactive compensation at this bus were set to be significantly less than that of the remaining 132kV busbars, but greater than the slack bus PARA C2.

Further costs such as load shedding, power generation and increasing the capacity of any of the 132kV circuits were all set to be the same. For the studies the OPF was carried out until a network constraint was attained. These constraints were determined as either of a circuit reinforcement, a busbar voltage exceeding 1.1pu at the wind farm and 1.05pu within the 132kV network, a busbar voltage lower than 0.9pu at the wind farm and 0.95pu in the 132kV network, load shedding in the network, and any real power requirements in the network other than at the slack bus PARA C2. The OPF allowed as much reactive compensation as was necessary at the RANG C1 busbar.

Three different capacity wind farms were tested to illustrate that even with significant permissible reactive support throughout the 132kV network (with the exception being the OFSW132 busbar), the maximum generation capacity of the wind farm would be 120MW. The OPF solution then indicated that further capacity increases would require that power factor correction was necessary at the wind farm, even with reactive compensation cost weightings being significantly greater there than elsewhere in the network.

The OPF results indicate that the wind farm capacity limit has been reached at approximately 120MW and the OPF solution requires extra reactive compensation at the wind farm.

For the 90MW installation, 38MVAR of reactive compensation is required at RANG C1, which increase to 139MVAR for a 105MW installation. At 120MW capacity the reactive compensation rises to approximately 180MVAR but requires some additional compensation at the wind farm. One aspect of the large reactive compensation capacities required for these large IG installations is the possible voltage rises in the 132kV network should the wind farm trip off-line. This was in fact tested for all study cases and while the network voltages exceeded 1.05pu after the tripping, they did not exceed 1.1pu.

16.5.2 Conclusions

This study has assessed the benefits of placing on-shore reactive compensation within the Case 1 132kV test network for an off-shore wind farm containing IG machines.

The study determined that 132kV networks will have much reduced penetration capacities when compared with DFIG based wind farms. Additionally the study found that significant reactive compensation would be necessary, to supply the reactive power consumed by higher capacity wind

farms, in this case capacities exceeding 100MW. What should be additionally noted is that reactive compensation of the magnitude studied here will more than likely have significant transient switching implications, and this surely complicates the design and possibly the capacity.

Finally, the assumptions made in this study regarding the wind farm power factor correction will be a constraint with respect to the possible wind farm penetration capacity. If it was permitted to design the power factor correction for 100% wind farm output and coordinate some form of capacitor inter-trip arrangement if the wind farm was tripped, then penetration capacities may be significantly increased when compared to standard installations. However whether all DNO's in the UK would accept such arrangements is presently unknown.

16.6 DFIG Optimal Control Strategy (II)

In this study an optimal control strategy for the coordinated area based voltage control, using both OLTCs at the wind farm and controlling the active/reactive outputs of the wind farm doubly-fed induction machines, is investigated. The previous studies in Section 16.4 were performed with arbitrary fixed tap position transformers with the DFIG based wind farm penetration capacity maximised for both voltage and power factor control.

It was previously found that if DFIG machines were operated in voltage control mode, then in general there may be an approximate 20% increase in wind farm penetration capacity than if power factor control alone (in this case unity power factor) were to be the control method of choice.

In this study, the effect of the strength of the AC system is additionally investigated as this will quite possibly be the main determining factor regarding a generalised voltage control approach for offshore wind farms. The circuit capacity constraints are also ignored and the OPF solved for the two Study cases used previously and for two network load cases, namely 100% and 33%.

In the first study, the slack busbar voltage at PARA C2 was constrained to a maximum of 1.05pu, and the network impedances remained the same as in the previous studies. In the second study in which a weakened AC system is modelled, the slack busbar voltage at PARA C2 was constrained to a maximum of 1.0pu, and the line connection impedance between the PARA C1 and DERV C1 132kV nodes significantly increased. Additionally, in both study cases, the generator connected at HUMB C1 132kV busbar was removed and modelled as a negative load.

This range of wind farm network connections, network loadings and system strengths should sufficiently test whether it is possible to have a general combined DFIG and OLTC voltage control strategy for offshore wind generation.

16.6.1 Scenario 1 – Stronger AC network

In this study the coordinated control strategy using both the wind farm OLTC's and the DFIG control is assessed for maximum wind farm penetration for both Study Cases 1 and 2, and for two network loading cases, namely 100% and 33%.

Study 1 - 100% network load (Case 1)

In the first study (100% network load – Case 1), it was found that wind farm capacity could be increased to 270MW before any voltage constraints are attained when coordinated DFIG voltage control and OLTC's are utilised. The OPF determined that to maximise the wind farm penetration, the transformer taps and DFIG voltage controller would be set to control the wind farm 33/0.69kV

transformer 33kV busbar voltage to 1.1pu, while the 132/33kV transformer 33kV voltage would be set to 0.9pu.

Study 2 - 33% network load (Case 1)

In the second study (33% network load – Case 1), it was found that wind farm capacity could be increased to 277.5MW before any voltage constraints are attained when coordinated DFIG voltage control and OLTC's are utilised. The OPF determined that to maximise the wind farm penetration, the transformer taps and DFIG voltage controller would again be set to control the wind farm 33/0.69kV transformer 33kV busbar voltage to 1.1pu, while the 132/33kV transformer 33kV voltage would be set to 0.9pu.

Study 3 - 100% network load (Case 2)

In the third study (100% network load – Case 2), it was found that wind farm capacity could be increased to 270MW before any voltage constraints are attained when coordinated DFIG voltage control and OLTC's are utilised. The OPF determined that to maximise the wind farm penetration, the transformer taps and DFIG voltage controller would again be set to control the wind farm 33/0.69kV transformer 33kV busbar voltage to 1.1pu, while the 132/33kV transformer 33kV voltage would be set to 0.9pu.

Study 4 - 33% network load (Case 2)

In the fourth study (33% network load – Case 2), it was found that wind farm capacity could be increased to 270MW before any voltage constraints are attained when coordinated DFIG voltage control and OLTC's are utilised.

The OPF determined that to maximise the wind farm penetration, the transformer taps and DFIG voltage controller would again be set to control the wind farm 33/0.69kV transformer 33kV busbar voltage to 1.1pu, while the 132/33kV transformer 33kV voltage would be set to 0.9pu.

The study results indicated that in both network examples (Cases 1 and 2), the optimal DFIG and transformer tap control strategy identified by the OPF for the maximisation of wind farm penetration remained the same.

This strategy was to control the wind farm 33/0.69kV transformer 33kV busbar voltage to 1.1pu, while the 132/33kV transformer 33kV voltage would be controlled to 0.9pu. This results was also the case for the high and low network loading scenarios, albeit with a slight capacity difference noted in Study 2.

The next step is to identify if this voltage control strategy is independent of the relative strength of the AC system. It is known that AC system strength will significantly impact on the possible penetration capacity of the wind farm from previous publications.

16.6.2 Optimal Control Strategy – Weakened AC system

In this study the optimal voltage control strategy determined in Section 4.5.2 is applied when the network connection is considered weaker than in Section 4.5.2. In the study, the slack busbar voltage at PARA C2 was constrained to a maximum of 1.0pu, and the line connection impedance between the PARA C1 and DERV C1 132kV nodes significantly increased.

Study 5 - 100% network load (Case 1 – slack constrained to 1.05pu)

In Study 5 the slack busbar voltage at PARA C2 was constrained to 1.05pu in the weakened AC system. It was found that the wind farm capacity could be increased to a maximum of 187.5MW before any constraints were reached, however the constraints in this case were the reactive power export limits of the wind farm itself. The results illustrate that the optimal tap settings determined in Section 16.6.1 – Study 1 are no longer the same which means that a general results cannot be obtained. The following studies then further test this by reducing the voltage range of the slack bus in the OPF solution.

Study 6 - 100% network load (Case 1 – slack constrained to 1.025pu)

In Study 6 the slack busbar voltage at PARA C2 was constrained to 1.025pu in the weakened AC system. In this case it was found that the wind farm capacity could be increased to a maximum of 142.5MW before any constraints were reached, with the constraints again being the reactive power export limits of the wind farm itself. The results illustrate that the optimal tap settings determined in Section 16.6.1 are no longer the same.

Study 7 - 100% network load (Case 1 – slack constrained to 1.0pu)

In Study 7 the slack busbar voltage at PARA C2 was constrained to 1.0pu in the weakened AC system. In this case it was found that the wind farm capacity could be increased to a maximum of 135MW before any constraints were reached, with the constraints again being the reactive power export limits of the wind farm itself. The study results show that the optimal tap settings determined in Section 16.6.1 are no longer the same.

Study 8 - 100% network load (Case 1 – slack constrained to 0.975pu)

In Study 8 the slack busbar voltage at PARA C2 was constrained to 0.975pu in the weakened AC system. In this case it was found that for the voltage constraints placed on the network, there was no optimal solution for any wind farm capacity.

In summary, this study has indicated that the optimal voltage control strategy will be highly dependent on the strength of the AC system. This means that each wind farm connection will need to be assessed on a case by case basis.

16.6.3 Conclusions

In this study an optimal control strategy for a coordinated area based voltage control, using both OLTCs at the wind farm and controlling the active/reactive outputs of the wind farm doubly-fed induction machines, has been investigated.

The network was tested for different wind farm connection points, network loadings, various system strengths and constrained voltages to see if a general co-ordinated DFIG and OLTC voltage control strategy could be determined.

It was found in the case where the system slack bus was constrained to 1.05pu and for the stronger AC system case, that a general voltage control strategy could be applied. This was tested for two wind farm connection points and for the full range of network loadings (100% and 33%). In these cases the OPF determined that to maximise the wind farm penetration, the transformer taps and DFIG voltage controller would again be set to control the wind farm 33/0.69kV transformer 33kV busbar voltage to 1.1pu, while the 132/33kV transformer 33kV voltage would be set to 0.9pu.

In the second set of simulations, the OPF results were inconclusive regarding an optimal voltage control strategy. These results suggested that the optimal voltage control strategy for a given wind farm is going to be highly dependent on the strength of the AC system it is connected to. It means that each connection must be tested individually for the optimal control strategy, in order that the wind farm capacity may be maximised within an existing network.

16.7 Conclusions for Voltage Control Analysis Using OPF Program

In this study, the Optimal Power Flow program has been utilised to investigate the ability of different wind farm generation technologies to perform some measure of network voltage control.

In the first study (Section 16.4.2) the performance of two types of wind farms were compared using the standard LF program. In the first case a wind farm with approximately 100MW capacity, connected at the OFSW132 busbar using standard IG machines, was compared with a similar capacity wind farm using DFIG machines. In this case, the effect of two DFIG control strategies was investigated, namely voltage and power factor control. The study investigated varying levels of wind farm output (100MW, 66MW and 33MW) and network loading (120%, 100% and 80%). The first study results indicated that using DFIG's in the voltage control mode resulted in better network voltage performance when the network is more heavily loaded (eg 100% and 120%).

In the second study (Section 16.4.3) the optimal control strategy of doubly-fed induction generators to maximise penetration of wind generation on the existing 132kV network, considering the full spectrum of network loading conditions, was investigated. The two control strategies assessed were i) unity power factor control and ii) voltage control. The OPF study results indicated that, for this test system at least, when the wind farm is operated in the voltage control mode, a 20% increase in wind farm capacity may be possible when compared with a wind farm operated in unity power factor mode. This is a significant result and is quite a good argument for wind farm operators having a more active role in network operation when available to do so.

In third study (Section 16.5), the benefits of placing on-shore reactive compensation within the Case 1 132kV test network was assessed for an off-shore wind farm containing IG machines. The study determined that 132kV networks will have much reduced penetration capacities when compared with DFIG based wind farms. Additionally the study found that significant reactive compensation would be necessary, to supply the reactive power consumed by higher capacity IG based wind farms, in this case capacities exceeding 100MW. What should be additionally noted is that reactive compensation of the magnitude studied here will more than likely have significant transient switching implications, and this surely complicates the design and possibly the wind farm capacity.

Additionally, the assumptions made in this study regarding the wind farm power factor correction will be a constraint with respect to the possible wind farm penetration capacity. If it was permitted to design the power factor correction for 100% wind farm output and coordinate some form of capacitor inter-trip arrangement if the wind farm was tripped, then IG based penetration capacities may be significantly increased when compared to standard IG installations. However whether all DNO's in the UK would accept such arrangements is presently unknown.

In the fourth and final study (Section 16.6) an optimal control strategy for the coordinated area based voltage control, using both OLTCs at the wind farm and controlling the active/reactive outputs of the wind farm doubly-fed induction machines, was investigated. The network was tested for different wind farm connection points, network loadings, various system strengths and

constrained voltages to see if a general co-ordinated DFIG and OLTC voltage control strategy could be determined.

It was found in the case where the system slack bus was constrained to 1.05pu and for the stronger AC system case, that a general voltage control strategy could be applied. This was tested for two wind farm connection points and for the full range of network loadings (100% and 33%). In these cases the OPF determined that to maximise the wind farm penetration, the transformer taps and DFIG voltage controller would be set to control the wind farm 33/0.69kV transformer 33kV busbar voltage to 1.1pu, while the 132/33kV transformer 33kV voltage would be set to 0.9pu.

In the second set of simulations, the OPF results were inconclusive regarding an optimal voltage control strategy. These results suggested that the optimal voltage control strategy for a given wind farm is going to be highly dependent on the strength of the AC system it is connected to. It means that each connection must be tested individually for the optimal control strategy, in order that the wind farm capacity may be maximised.

In summary, the OPF program has proved highly useful in determining the solution to a whole range of issues when it comes to connecting new generation into an existing network. It permits the user to firstly maximise the generation capacity, and also to compare how different generation technologies compare when trying to maximise this capacity. The study has also highlighted the benefits of using DFIG machines in voltage control mode, as it has the effect of improving the network voltage performance while eliminating the need for a substantial amount of reactive compensation in the 132kV network for similarly rated IG wind farm connections.

17 Conclusions

Steady state and dynamic models for the Doubly-fed Induction Generators have been developed for the widely used IPSA software. The model details, equivalent circuit, references for the publications and the implementation in the software are presented in sections 2 and 3. The models were used for the studies carried out in this project and the results are presented in this report.

From the load flow and fault level analysis the impact of the variable speed synchronous generator connected via back-to-back static converters is not creating a major thermal overloads or fault level problem with the simplified modelling of the converter contributions. Transient analysis calculations are needed to simulate the behaviour of the converter controllers and its effects on the converter contribution. However the cost and operational complexity of the converters controllers of this size for delivering a special operating conditions often prohibits the developers of using this configuration.

It is also important to consider the issue of power quality. The harmonics introduced by these converters and whether there is any resonance in the local network need investigation.

The advantages and disadvantages of the fixed speed offshore induction generator are clear. In the positive side it is simple, reliable and will known technology. However, it presents the worst reactive power consumption, it is also lack smooth voltage and power control. As a result of the increased reactive power compensation and flows in the local network, switchgear upgrading and protection current and time resetting are needed in the local 132 kV substations. Fixed speed generation has mechanical problems from the wind turbine side with extraction of power of variable wind speed. Various schemes usually used to overcome this problem such as multiples gearbox ratios but they add extra cost and complexities and they are outside the scope of this work.

The doubly fed induction generators technology provides solution for two major shortfalls in the induction generators. The first is the reactive power consumption by controlling power factor of these generators. Setting the power factor to unity provide better alternative compared with capacitive VAR compensation. It also can provide active speed/power control through the back-to-back converters in the rotor windings. There is no harmonics source in the stator connection and the expectation that the power quality is not a problematic issue. However, connection of generation increases the connectivity of the network and fault level flows specially for the initial peak values.

From the transient stability analysis the impact of the variable speed synchronous generator connected via back-to-back static converters is not seem to create a major thermal overloads or fault level problem with the dynamic modelling of the converter contributions. Transient simulation of the behaviour of the converter controllers and their effects on the converter contribution shows that the converter protection is able to disconnect the windfarm very fast for high fault current contribution. However, the fault ride through capability is a problem for the network transmission operator. If the wind farm disconnects itself when a fault occurs on the transmission system then the integrity of the transmission system can be undermined as the lost generation can exceed the amount of spinning reserve.

Section 7 of G75/1 discusses the importance of maintaining system stability of generation within limits of Generating Plant capability during network disturbances and the need to disconnect reliably for true “loss of mains” situations. Some forms of loss of mains protection may not achieve the required level of discrimination.

The cost and operational complexity of converter controllers of this size for delivering special operating conditions often prohibits the developers from using this configuration. It is also important to consider the issue of power quality. The harmonics introduced by these converters and any undesirable effects, needs investigation.

From the transient stability results the fault contribution from doubly fed induction machine proved to be slower to decay and has a higher initial value than a fixed speed induction generator.

Governor and turbine controller characteristics and their time delay play a significant part in the stability of the system and the controllers need to react to change the power input to the turbine with a maximum time delay of 200ms to keep the doubly fed induction generators relatively stable on reconnection to the system. This is more critical in DFIGs, as they may operate at super synchronous speed at a typical –12% slip.

More work needed to put modelling of AVR, governors and turbines for induction generators and DFIGs of windfarm in the full dynamic analysis of the distribution network.

To continue to comply with P2/5 and G75/1 may need some security and contingency studies with the new system loading conditions, and this may introduce further constraints in the operation or maximum generation of the wind farms under certain operating conditions or configurations. These studies are not included within the scope of this report.

The Optimal Power Flow software has been successfully integrated into the IPSA power system analysis program. The same final answers were obtained from the software running under IPSA as when the software was run under console mode. The same intermediary results were obtained while the calculations were in progress.

Facilities for adding Static VAR compensator OPF data will be added to IPSA. This information is currently within the program but it is not yet visible to the user. The conversion of IPSA induction generators to OPF induction generators will be improved. The IPSA user interface will be extended to display OPF data on individual item property pages, and to provide HTML reports on the results of OPF analysis.

Testing needs to be carried out on more complicated networks to ensure the same results are obtained between the OPF in console mode and in IPSA. It is not anticipated that this will pose any significant problems.

The OPF program has proved highly useful in determining the solution to a whole range of issues when it comes to connecting new generation into an existing network. It permits the user to firstly maximise the generation capacity, and also to compare how different generation technologies compare when trying to maximise this capacity. The study has also highlighted the benefits of using DFIG machines in voltage control mode, as it has the effect of improving the network voltage performance while eliminating the need for a substantial amount of reactive compensation in the 132kV network for similarly rated IG wind farm connections.

References:

1. A. E Efthymiadis, "Report in the Status of Steady State and transient Modelling of full Variable Speed Wind Turbine" An IPSA Power Engineering CAD Report submitted to the British Isles Wind Technical Panel, November 2001.
2. J. Hindmarsh "Electrical Machines and their Application" Pergamon Press, 1991.
3. J Arrillaga and C. P. Arnold, "Computer Modelling of Power Systems"; John Wiley 1990.
4. A E Efthymiadis and R D Youssef, "IPSA User Manual" Release 1.7 , May 2000.
5. I. Cadirci and M. Ermis, "Double-output Induction generator operating at subsynchronous and supersynchronous speeds: Steady-state performance optimisation and wind-energy recovery" IEE proceedings-B, Vol-139, No. 5, Sept. 1992, pp 429-442.
6. T Burton, D Sharpe, N Jenkins and E Bossanyi, " Wind Energy Handbook"; (book) John Wiley & Son Ltd, 2001.
7. Ekanayake J B, Holdsworth L, Wu X G, Jenkins N, "Dynamic Modelling of Doubly Fed Induction Generator Wind Turbines", IEEE Transactions on Power Systems, May 2003, Vol. 18, No2, pp 803-809.
8. Ekanayake, J.B., Holdsworth, L., Jenkins, N. "Control of Doubly Fed Induction Generator (DFIG) Wind Turbines", IEE Power Engineer, February 2003, pp 28-32.
9. Holdsworth, L, Wu, X.G., Ekanayake, J.B., Jenkins, N., "Comparison of fixed speed and doubly fed induction wind turbines during power system disturbances" IEE Proceedings Generation Transmission and Distribution, Vol. 150, No 3 May 2003 pp 343-352.
10. Holdsworth, L, Wu, X.G., Ekanayake, J.B., Jenkins, N., "Direct solution method for initialising doubly fed induction wind turbines in power system dynamic models" IEE Proceedings Generation Transmission and Distribution, Vol. 150, No 3 May 2003 pp 353-359.
11. Ekanayake J B, Holdsworth L, Jenkins N, "Comparison of 5th order and 3rd order machine models for Doubly Fed Induction Generator Wind Turbines", Electric Power Systems Research, accepted for publication April 2003.
12. Andre's E Feijó'o and Jos Cidra's, " Modelling of Wind Farm in Load Flow Analysis", IEEE Trans. On Power Systems, Vol. 15, No 1, Feb 2000, pp110-115.
13. M. Machmoum, R. LeDoeuff, F. M. Sargos and M Cherkaoui, "Steady-state analysis of a doubly fed asynchronous machine supplied by a current-controlled cycloconverter in the rotor" IEE Proceeding-B, Vol. 139, No 2, March 1992, pp114-122.
14. V Akhmator, "Modelling of Variable-Speed Wind Turbines with Doubly-fed Induction Generators in Short-term stability investigations" 3rd Int. Workshop on Transmission Networks for Offshore Wind Farms, April 11-12, 2002, Stockholm, Sweden.